Geof. Int. Vol. 24-4, 1985, pp. 477-575.

GEOLOGICAL AND GEOCHEMICAL INVESTIGATIONS ON THE EASTERN TRANS MEXICAN VOLCANIC BELT

J. F. W. NEGENDANK*
R. EMMERMANN**
R. KRAWCZYK**
F. MOOSER***
H. TOBSCHALL****
D. WERLE*

RESUMEN

Este trabajo informa sobre investigaciones geoquímicas y geológicas de la sección este del Cinturón Volcánico Transmexicano (TMVB).

Como resultado de nuestro trabajo, nosotros preferimos considerar que el eje neovolcánico termina en la costa del Golfo de México y no en el área del Altiplano (Robin, 1981), por lo que respecta a la actividad volcánica durante el Plioceno-Quaternario.

Durante esa época el volcanismo presenta un carácter calcalcalino-alcalino.

El volcanismo en el Mioceno produjo rocas ígneas alcalinas-calcalcalinas en el macizo de Palma Sola y rocas ígneas calcalcalinas en la sección occidental de México, debido a la migración este-oeste de la "subducción" de la placa paleopacífica (Robin, 1976).

Nuestros resultados geoquímicos no niegan ni favorecen un modelo geológico único y tampoco excluyen la versión de una microplaca de Shurbet and Cebull (1984).

Sin embargo, los resultados geoquímicos no pueden explicarse por derivación directa del volcanismo de la "litosfera oceánica" (p.e., Robin, 1981, 1982).

Independientemente de esto, el volcanismo del eje neovolcánico parece haber sido causado o inducido por la "subducción" de las placas Rivera y Cocos.

ABSTRACT

This paper reports upon geological and geochemical investigations of the easternmost extension of the Trans Mexican Volcanic Belt (TMVB). As a result of our work we prefer to consider that the TMVB terminates at the Gulf coast and not in the Altiplano area (e.g. Robin, 1981), with respect to a Pliocene-Quaternary volcanic activity. During that time the volcanism is of calcalkaline and alkaline character.

* *Abteilung Geologie der Universität Trier, Trier-Tarforst, D-5500 Trier, Germany.*
** *Mineralogisch-Petrologisches Institut der Universität, Senckenbergstr. 3, D-6300 Giessen, Germany.*
*** *Comisión Federal de Electricidad, Ciudad de México, Atoyac 110, México.*
**** *Institut für Geowissenschaften der Johannes Gutenberg Universität Mainz, Postfach, D-6500 Mainz, Germany.*

The older volcanic activity, e.g. of Miocene times, produced alkaline-calcalkaline igneous rocks in the Massif de Palma Sola and calcalkaline igneous rocks in the western part of Mexico due to the eastwest migration of the subduction of the Palaeopacific plate (Robin, 1976).

Our geochemical results neither deny nor favour one single geological model and do not even exclude the microplate version of Shurbet and Cebull (1984). However, the geochemical data cannot be explained by direct derivation of the volcanics from the oceanic lithosphere (e.g. Robin, 1981, 1982).

Irrespective of this fact, the volcanism of the TMVB suggests to be caused or induced by the subduction of the Rivera and Cocos plate association.

INTRODUCTION

This investigation of volcanic rocks of the Eastern Trans Mexican Volcanic Belt (TMVB) provides information about the evolution of its Cenozoic volcanic history.

According to Robin (1976) and Demant (1978) two different volcanic provinces, the calcalkaline association of the E-W traversing TMVB and the N-S oriented alkaline province which parallels the eastern coast are overlapping in the area under study.

Robin (1976, 1981) provides further evidence supporting different tectonic patterns assuming compression in the area of the TMVB and graben-like tension in the coastal plain area. Thorpe (1977), and Pichler and Weyl (1976) favour the hypothesis that the volcanics of the TMVB including the coast parallel alkaline rocks, e.g. Massif Tuxtlas, are produced exclusively by the influence of the downdipping Cocos plate.

Nixon (1982) recently summarized previous studies of the geological evolution of the TMVB and accentuated the missing time sequence of volcanic activities which has been and is one of the main problems of confusion today.

The TMVB as defined by Demant (1981) is less than 1 m.y. old. It resulted from a new tectonic regime beginning in the Upper Miocene by rotation (pivoting subduction) (10 m.y. B.P.) as the Cocos-NorthAmerica subduction system and was placed in its present day position since the Pliocene.

Robin (1981), however, places the beginning of the TMVB between 3(2.6) - 2(1.6) m.y. B.P. and its evolution as a volcanic axis between 2 (1.6) and 1 m.y. B.P. From that time to the present it is thought to have developed to a mature state. After this author, the TMVB overlays a previous province (Pre-Pliocene).

In our paper, the geological setting of the study area is described followed by a presentation of the geochemistry. The results are discussed with respect to the regional volcano-tectonic evolutionary pattern and the plate tectonic models mentioned above. This interpretation defines the TMVB and its easternmost extension, the so-called Palma Sola Massif, as a cogenetic Pliocene-Quaternary structure (Fig. 1).

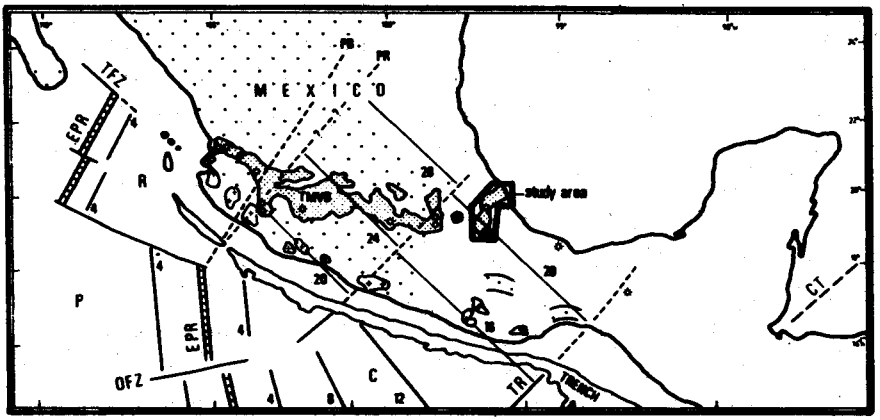

Fig. 1. Study area in context to the Trans Mexican Volcanic Belt (TMVB), old volcanic products and granites south of it and the plate tectonic pattern modified after Nixon, 1982.
LEGEND:
C = Cocos plate, CT = Cayman trough, EPR = East Pacific Rise, P = Pacific plate, R = Rivera plate, PB = transform boundary between Rivera and Cocos plates (predicted), PR = trend of a proto-Rivera fracture zone if one was indeed present in the subducted plate, TMVB = Trans Mexican Volcanic Belt, TFZ = Tamayo fracture zone, TR = Tehuantepec ridge, Trench contour = 2 200 fathoms (4 km)
Crosses: major granite complexes
Points: old volcanic belts
Dense points: Trans Mexican Volcanic Belt and major volcanoes

However, the restricted number of age determinations available does not allow an exact lower time limit as yet established.

The older igneous rocks in the area of the TMVB still need further investigation. Their origin is possibly related to the E-W migration of the Palaeopacific plate as described by numerous authors before 1982 (e.g. Robin, 1976, 1981; Demant, 1978; Urrutia-Fucugauchi, 1978) and recently summarized by Clark *et al.* (1982).

GEOLOGY

We elaborated two petrographic geological overview maps (Figs. 2, 3) out of 8 geological maps 1:50 000 using all available data. The field studies were based on a photogeological interpretation of Band 7 LANDSAT (imagery at scale 1:200 000 and aereal photographs at scale 1:50 000).

Fig. 2 covers from W to E the Altiplano Basin of Oriental, the N-S trending chain between Cofre de Perote and Pico de Orizaba and its easternmost declivity to the Plain of Veracruz. Fig. 3 is the NE continuation and shows large volcanic deposits of the Cofre-Pico range in the S, the SW part of the Chiconquiaco complex in the N and the Massif de Palma Sola in the E along the Gulf of Mexico coast.

These maps were evolved to show primarily the petrographic, i.e. the alkaline and calcalkaline character of the volcanic products. The time sequence of Fig. 4 a, b, c, d, e is based on our geological field dates, photogeological interpretation (Werle, 1984), the radiometric dates of Cantagrel and Robin (1979), the geological and radiometric informations of Mooser and Soto (1980), Banzer-Bussmann (1981), Müller (1979), the geological and radiometric dates of Yáñez García and García Durán (1982), Ferriz and Mahood (1984), and palaeomagnetic dates from Böhnel and Negendank (1981) and Böhnel (1985).

Figs. 2, 3, and 4 have to be used together to give the full information on the evolution of the volcanism in time and space, the sample location indicated with numbers NH, NT, U, R, etc. The classified igneous rocks were printed into the maps. Tab. I and II give the chemical analyses, CIPW-Norm and the trace element sets. A summary of the chemical data is given in Table III.

The ages of the cones and lavas were investigated by the method of Bloomfield (1973) based on C-14 data, used by Martin (1982) for Sierra de Chichinautzin lavas and evolved in Fig. 4 c, by Werle (1984) for our region. A similar additional detailed classification of cone shape evolution (Werle, 1984) was used for dating the volcanoes.

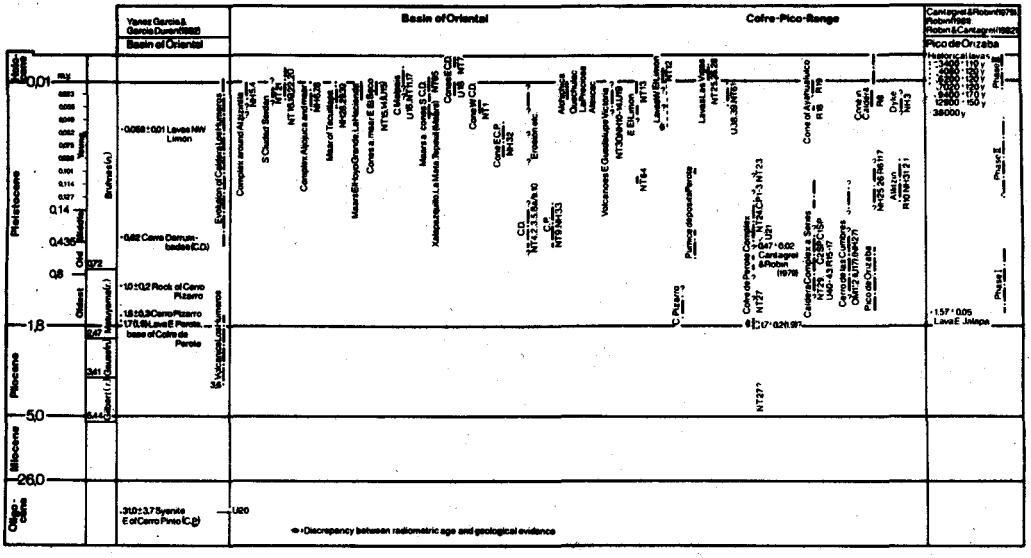

Fig. 4. Stratigraphic table of the volcanic complexes. 4a Region Basin of Oriental - Cofre-Pico range

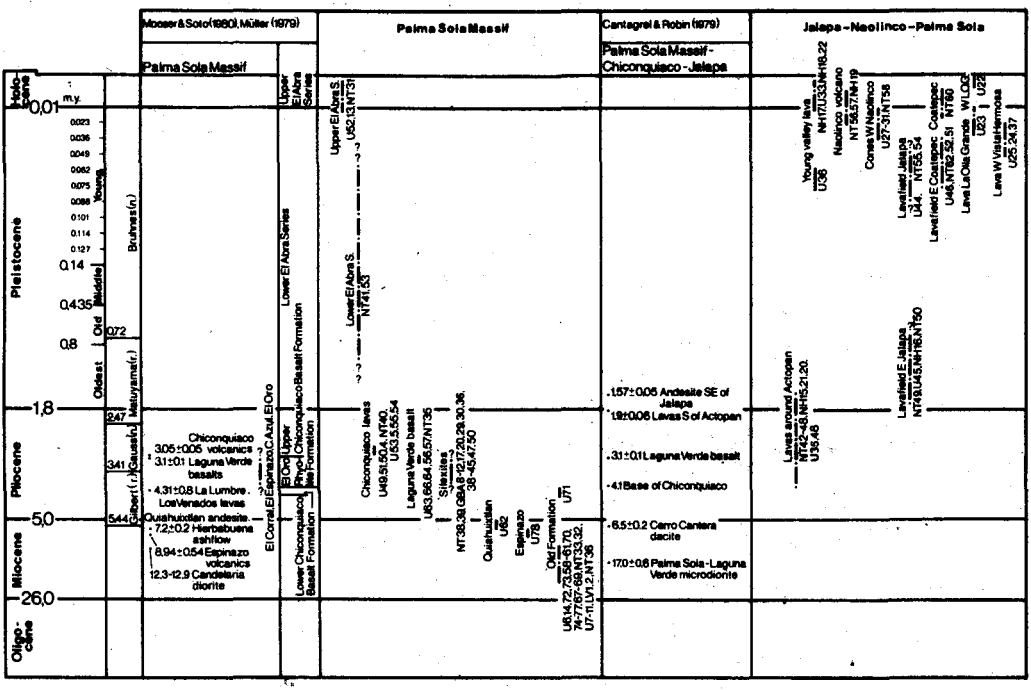

4b Region Palma Sola - Naolinco-Jalapa

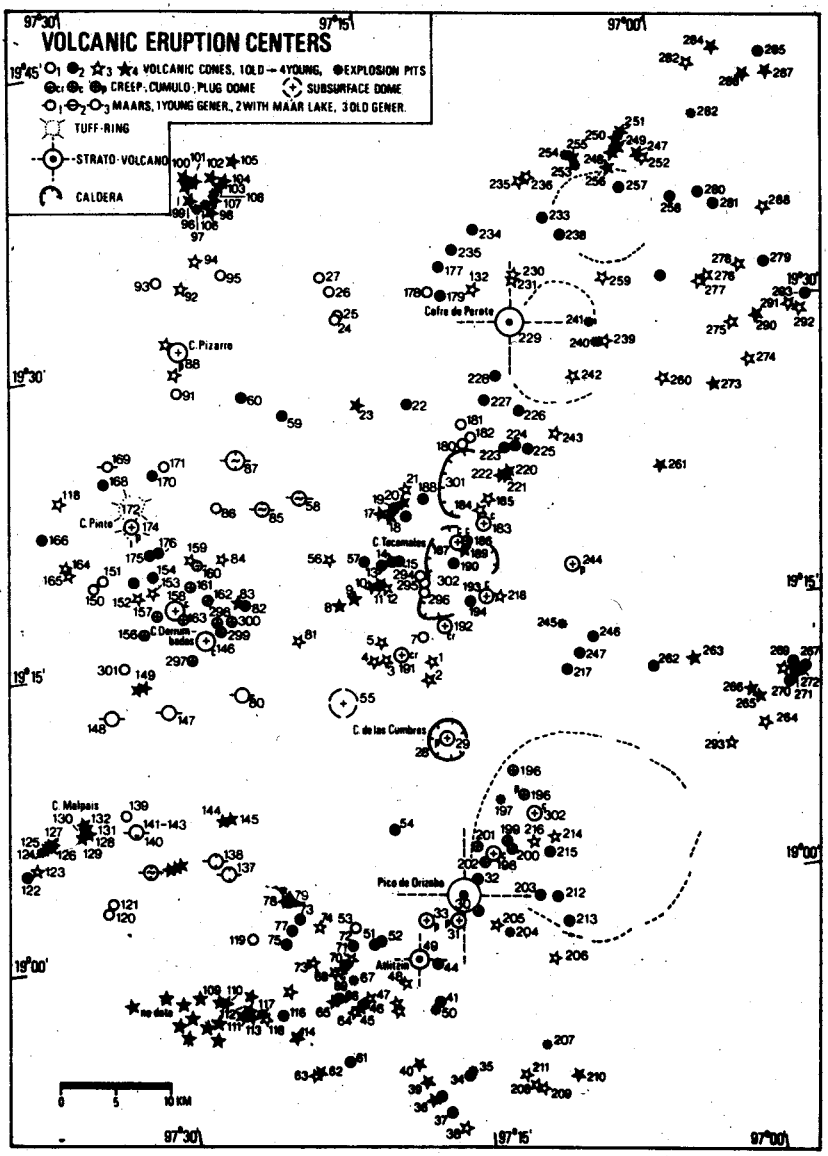

4c Young Pleistocene-Holocene volcanic cones (after Werle, 1984)
4. Young Pleistocene-Holocene: ~0 - 20 000 y. B. P.
2./3. " " ~20 000 - 30 000 y. B. P.
1. " " ~30 000 - 35 000 y. B. P.

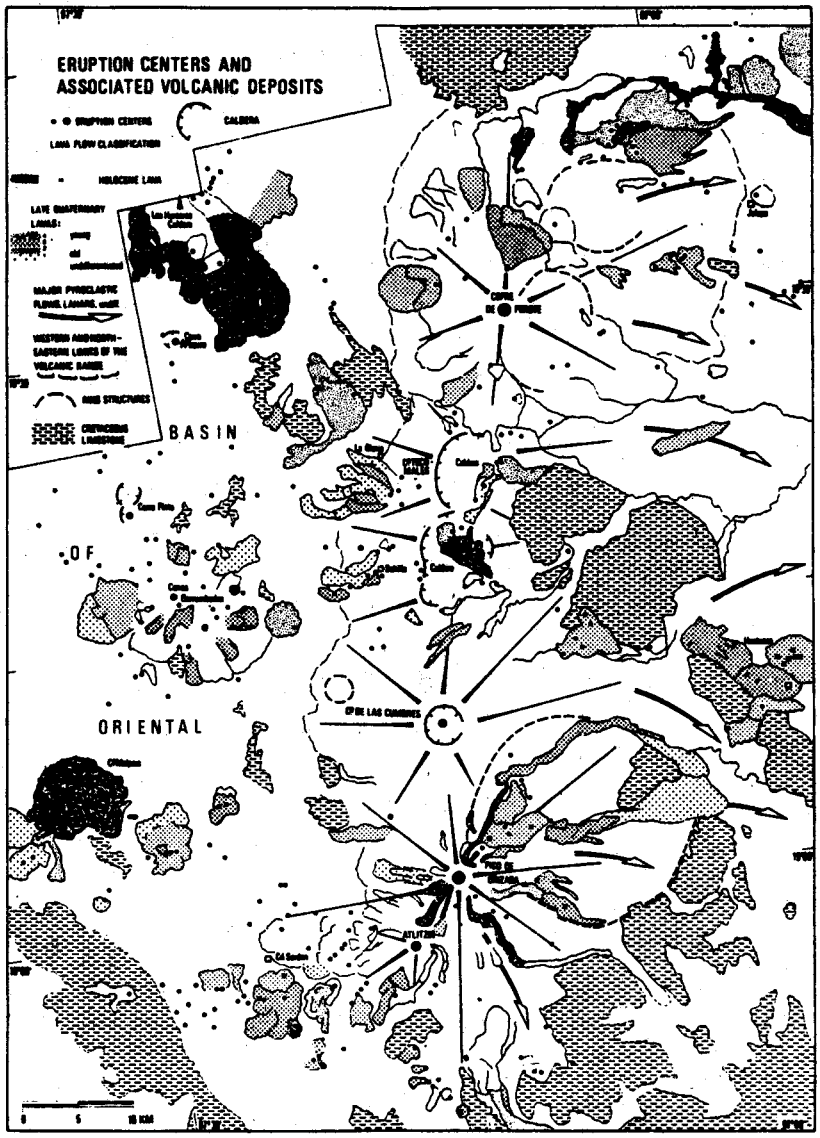

4d Young Pleistocene-Holocene lava stratigraphy inclusive the stratigraphy of the pyroclastic deposits, lahars, etc. of Cerro Derrumbadas indicated with the same time labels as for the lavas (after Werle, 1984)

5. Holocene lavas: 0 - 10 000 y. B. P.
4. Young Pleistocene: 10 000 - 20 000 y. B. P.
2./3. " " ~20 000 - 30 000 y. B. P.
1. " " ~30 000 - 35 000 y. B. P.

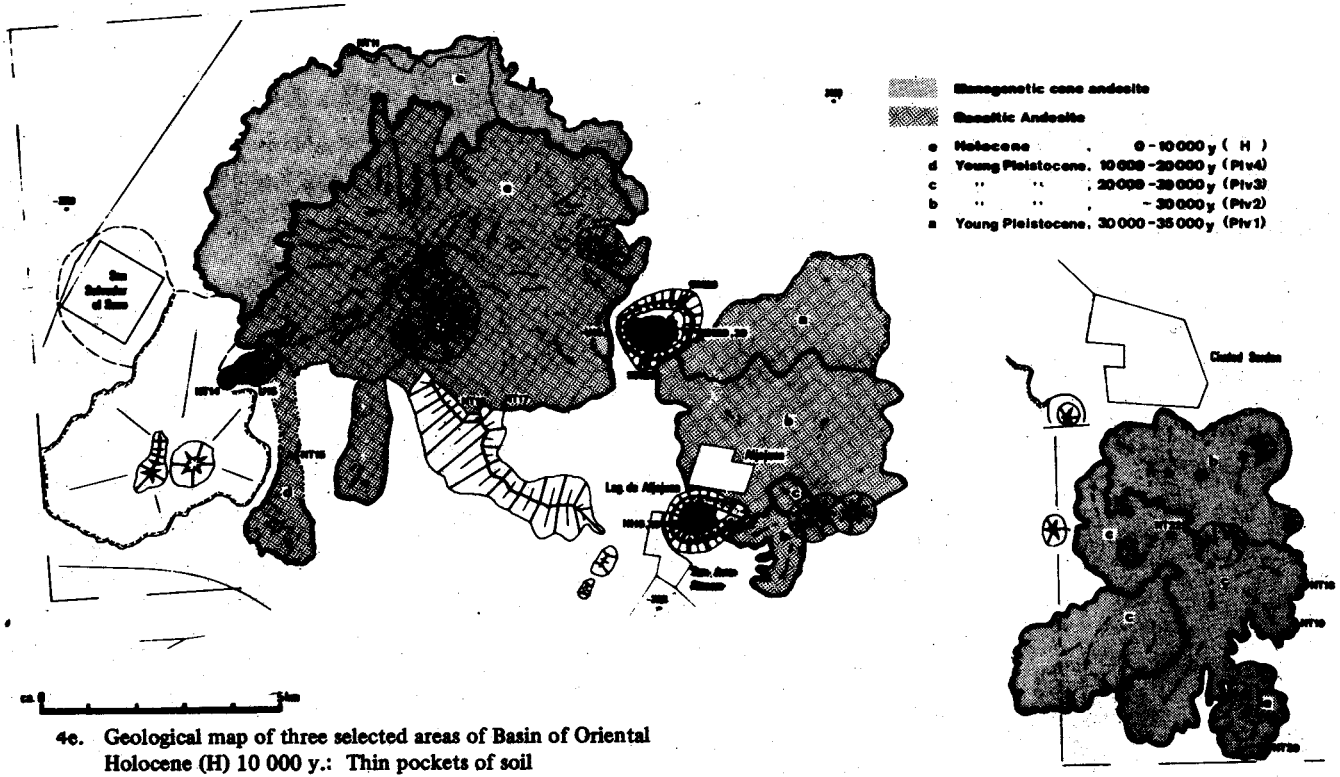

4c. Geological map of three selected areas of Basin of Oriental

Holocene (H) 10 000 y.: Thin pockets of soil
Uniform cover of short trees and shrubs
All flow structures perfectly preserved
Individual flow units mappable
Not cultivated

Pleistocene (Plv 4) 20 000 y.: Individual flow units have marked levees with thin tree cover
Center of flows have thin soil cover

(Plv 3) : Thin persistent soil cover
Outlines of flows very marked
Little erosion of terminal cliffs.

(Plv 2) 30 000 y.: Very distinct flow margins and terminal cliffs
Surface of flow covered with soil
Rare pressure ridges protrude and indicate flow direction

(Plv 1) 35 000 y.: Rounded and lobate flow margins only
Rounded, eroded and subdued terminal cliffs
No internal flow features
Thick soil cover and intensively cultivated

Table I : Bulk and trace element chemistry, CIPW-Norm of the investigated igneous rocks.

Rhyolites	NT 8	NT 5	NE 33	NT 9	NE 33	NT 9b	NT 4	NT 10
SiO_2	70.8	71.6	73.9	74.1	74.7	74.8	75.0	75.2
TiO_2	0.14	0.15	0.03	0.04	0.04	0.04	0.07	0.07
Al_2O_3	15.5	15.7	14.0	14.0	14.1	14.2	14.3	14.3
Fe_2O_3	0.61	1.45	0.20	0.13	0.03	0.32	0.47	0.59
FeO	1.66	0.92	0.49	0.54	0.64	0.36	0.77	0.64
MnO	0.04	0.04	0.14	0.14	0.15	0.14	0.05	0.05
MgO	0.27	0.28	0.09	0.07	0.08	0.09	0.16	0.12
CaO	1.78	1.81	0.49	0.49	0.51	0.48	0.92	0.92
Na_2O	4.56	4.62	4.47	4.49	4.46	4.55	4.49	4.51
K_2O	3.40	3.44	4.09	4.09	4.15	4.16	3.87	3.86
P_2O_5	0.08	0.08	0.04	0.05	0.05	0.04	0.06	0.06
H_2O^+	0.88	0.07	2.00	2.23	1.09	0.99	0.07	0.07
CO_2	0.05	0.08	0.03	0.05	0.05	0.02	0.06	0.05
Σ	99.80	100.20	100.00	100.40	100.10	100.20	100.30	100.40
Q	26.38	27.50	30.84	30.83	31.31	31.09	31.65	31.91
C	1.39	1.46	1.49	1.53	1.58	1.48	1.33	1.28
OR	20.14	20.28	24.18	24.07	24.51	24.54	22.80	22.71
AB	38.67	39.00	37.84	37.83	37.72	38.43	37.88	38.00
AN	8.01	7.93	1.98	1.78	1.89	1.99	3.78	3.84
NE	-	-	-	-	-	-	-	-
MT	0.89	2.10	0.29	0.19	0.04	0.46	0.68	0.85
HM	-	-	-	-	-	-	-	-
IL	0.27	0.28	0.06	0.08	0.08	0.08	0.13	0.13
AP	0.19	0.19	0.10	0.12	0.12	0.10	0.14	0.14
CC	0.11	0.18	0.07	0.11	0.11	0.05	0.14	0.11
DI	-	-	-	-	-	-	-	-
HY	3.07	1.01	1.17	1.25	1.56	0.81	1.40	0.96
OL	-	-	-	-	-	-	-	-
Salic.	94.60	96.17	96.32	96.04	97.00	97.52	97.45	97.74
Femic.	4.52	3.77	1.68	1.74	1.91	1.49	2.49	2.20
Diff.-I.	85.20	86.78	92.85	92.74	93.54	94.05	92.33	92.61
Cr	4	4	4	4	4	2	2	4
Co	2	3	<1	<1	<1	<1	1	1
Ni	4	4	5	5	4	4	3	4
Cu	2	2	<1	<1	<1	<1	1	<1
Zn	68	68	46	46	47	45	56	52
Rb	100	100	192	189	194	188	115	111
Sr	270	275	22	21	22	21	141	138
Y	9	9	24	23	25	24	10	10
Zr	157	150	67	68	68	68	81	81
Nb	14	14	23	23	23	23	16	15
Ba	878	898	<50	30	<50	35	770	896
La	27	25	-	<N	-	<N	16	13
Ce	70	75	10	16	10	12	42	40
Pb	18	17	19	18	18	19	17	18
Th	11	10	7	7	7	7	5	5
K_2O/Na_2O	0.75	0.74	0.91	0.91	0.93	0.91	0.86	0.86
$FeO+Fe_2O_3/MgO$	8.41	8.46	7.67	9.57	8.37	7.56	7.75	10.25
K/Rb	282	286	177	180	178	184	279	288
K/Sr	104	104	1545	1619	1568	1643	228	232
K/Ba	32	32	>680	1133	>690	986	42	36
Ca/Sr	47	47	159	167	164	162	47	48
Rb/Sr	0.37	0.36	8.73	9.00	8.82	8.95	0.82	0.80
Ba/Sr	3.25	3.26	<2.27	1.43	<2.27	1.67	5.46	6.49
Ba/Rb	8.78	8.98	<0.26	0.16	<0.26	0.19	6.70	8.07
Ni/Co	2.00	1.33	<5.00	<5.00	<4.00	<4.00	3.00	4.00

Tab. I 2

Dacites	MT 1	R 6	OM 1	CP 2	U 58
SiO_2	63.1	63.2	63.2	64.0	64.2
TiO_2	0.72	0.64	0.55	0.80	0.55
Al_2O_3	17.1	17.0	16.9	15.7	16.1
Fe_2O_3	4.47	2.66	2.34	1.56	5.46
FeO	0.19	1.56	1.96	2.90	0.31
MnO	0.08	0.08	0.09	0.08	0.09
MgO	2.42	2.39	2.55	2.23	0.78
CaO	5.86	5.46	4.84	4.15	5.48
Na_2O	4.13	4.51	3.95	3.51	3.82
K_2O	1.30	1.82	2.26	3.08	1.69
P_2O_5	0.25	0.24	0.20	0.22	0.18
H_2O^+	0.25	0.30	0.78	1.42	0.69
CO_2	0.24	0.06	0.03	0.06	0.51
Σ	100.10	99.90	99.70	99.70	99.90
Q	19.13	16.07	17.54	19.29	23.30
C	-	-	-	-	-
OR	7.69	10.77	13.41	18.25	9.90
AB	34.99	38.21	33.55	29.79	32.04
AN	24.31	20.79	21.79	18.04	21.60
NE	-	-	-	-	-
MT	3.22	3.11	2.98	2.27	4.90
HM	-	-	-	-	-
IL	1.37	1.22	1.05	1.52	1.04
AP	0.59	0.57	0.48	0.52	0.42
CC	0.55	0.14	0.07	0.14	1.15
DI	1.30	3.47	0.65	0.64	0.82
HY	6.62	5.37	7.72	8.13	4.16
OL	-	-	-	-	-
Salic	86.11	85.84	86.29	85.37	86.84
Femic.	13.65	13.87	12.94	13.22	12.49
Diff.-I.	61.80	65.05	64.50	67.33	65.24
Cr	15	23	65	31	20
Co	9	10	11	11	12
Ni	10	16	27	17	16
Cu	13	13	18	18	24
Zn	57	58	58	55	44
Rb	16	23	48	94	39
Sr	1125	924	601	363	470
Y	20	17	18	23	19
Zr	54	92	141	224	104
Nb	4	4	7	16	6
Ba	409	481	651	593	929
La	16	-	21	30	14
Ce	36	-	57	66	30
Pb	6	8	9	13	4
Th	2	3	8	13	5
K_2O/Na_2O	0.31	0.40	0.57	0.88	0.44
$FeO+Fe_2O_3/MgO$	1.83	1.74	1.67	2.00	8.72
K/Rb	675	657	392	272	359
K/Sr	10	16	31	71	30
K/Ba	26	31	29	43	15
Ca/Sr	37	42	58	82	83
Rb/Sr	0.01	0.03	0.08	0.26	0.08
Ba/Sr	0.36	0.52	1.08	1.63	1.98
Ba/Rb	25.60	20.90	13.60	6.31	23.80
Ni/Co	1.11	1.60	2.46	1.55	1.33

Tab. I 3

Dacites (Shoshonitic Series)	R 11	U 62	U 28	U 21
SiO_2	64.5	65.0	63.7	67.5
TiO_2	0.60	0.40	1.02	0.77
Al_2O_3	16.8	16.8	17.6	15.5
Fe_2O_3	1.81	2.54	3.03	1.39
FeO	1.98	0.66	0.89	2.10
MnO	0.06	0.07	0.12	0.08
MgO	2.34	1.60	0.56	0.71
CaO	4.96	3.74	2.45	1.67
Na_2O	4.72	5.49	4.86	3.95
K_2O	1.76	2.32	5.07	5.56
P_2O_5	0.19	0.23	0.28	0.17
H_2O^+	0.25	0.36	0.60	0.60
CO_2	0.06	0.08	0.06	0.07
Σ	100.00	99.30	100.20	100.10
Q	17.08	14.88	10.88	18.55
C	-	-	0.47	0.52
OR	10.40	13.99	29.90	32.83
AB	39.93	47.42	41.04	33.40
AN	19.45	14.64	9.93	6.73
NE	-	-	-	-
MT	2.62	0.95	1.82	2.01
HM	-	-	1.26	-
IL	1.14	0.78	1.93	1.46
AP	0.45	0.56	0.66	0.40
CC	0.14	0.19	0.14	0.16
DI	2.80	1.80	-	-
HY	5.76	4.45	1.39	3.35
OL	-	-	-	-
Salic	86.85	90.93	92.22	92.02
Femic.	12.91	8.71	7.20	7.39
Diff.-I.	67.40	76.29	81.82	84.78
Cr	17	19	6	6
Co	9	7	6	7
Ni	16	11	5	5
Cu	19	13	8	10
Zn	51	55	71	62
Rb	24	68	128	192
Sr	756	855	414	168
Y	16	11	37	61
Zr	87	69	591	631
Nb	5	23	62	28
Ba	424	1641	1101	708
La	-	4	55	70
Ce	-	50	145	116
Pb	6	21	13	22
Th	1	6	22	28
K_2O/Na_2O	0.37	0.42	1.04	1.41
$FeO+Fe_2O_3/MgO$	1.62	1.17	6.93	4.92
K/Rb	608	284	329	241
K/Sr	19	23	102	275
K/Ba	34	12	38	65
Ca/Sr	47	31	42	71
Rb/Sr	0.03	0.08	0.31	1.14
Ba/Sr	0.56	1.92	2.66	4.21
Ba/Rb	17.70	24.10	8.60	3.69
Ni/Co	1.78	1.57	0.83	0.71

Tab. I 4 Andesites (Monogenetic cone-Andesites)

	U 36	U 16	NT 22	NT 51	NT 54	NT 19
SiO_2	55.8	55.9	56.2	56.3	56.3	56.4
TiO_2	1.14	1.35	0.97	1.04	1.06	0.94
Al_2O_3	16.7	16.9	15.8	16.8	16.5	15.7
Fe_2O_3	1.91	1.39	2.46	4.83	3.69	2.45
FeO	5.01	5.84	4.31	2.40	3.07	4.16
MnO	0.12	0.12	0.11	0.12	0.11	0.11
MgO	5.54	4.72	5.84	4.74	5.88	5.64
CaO	7.68	7.15	8.41	7.66	7.04	8.11
Na_2O	3.54	3.55	3.35	3.62	3.74	3.51
K_2O	1.46	1.60	1.73	1.69	1.53	1.68
P_2O_5	0.38	0.35	0.29	0.26	0.27	0.27
H_2O^+	0.42	0.34	0.59	0.63	0.57	0.54
CO_2	0.04	0.05	0.06	0.25	0.04	0.06
Σ	99.70	99.30	100.10	100.30	99.80	99.60
Q	5.57	6.12	5.86	6.80	5.96	6.22
C	-	-	-	-	-	-
OR	8.69	9.56	10.21	9.98	9.07	9.97
AB	30.16	30.37	28.31	30.60	31.75	29.83
AN	25.54	25.73	22.94	24.57	23.79	22.22
NE	-	-	-	-	-	-
MT	2.79	2.04	3.56	3.68	3.72	3.55
HM	-	-	-	-	-	-
IL	2.18	2.59	1.84	1.97	2.02	1.79
AP	0.91	0.84	0.69	0.62	0.64	0.64
CC	0.09	0.12	0.14	0.57	0.09	0.14
DI	8.12	6.12	13.17	8.13	7.35	12.83
HY	15.98	16.55	12.71	12.47	15.05	12.29
OL	-	-	-	-	-	-
Salic.	69.96	71.77	67.32	71.95	70.57	68.23
Femic.	30.07	28.25	32.11	27.44	28.88	31.24
Diff.-I.	44.42	46.04	44.38	47.37	46.78	46.01
Cr	130	94	110	104	161	105
Co	22	25	21	25	23	21
Ni	53	47	24	33	93	25
Cu	35	26	42	39	29	40
Zn	80	82	71	76	72	70
Rb	32	36	23	46	34	26
Sr	582	501	869	528	497	857
Y	24	27	23	48	21	22
Zr	168	185	93	164	156	91
Nb	14	13	4	4	13	4
Ba	456	458	409	481	459	459
La	25	19	12	23	16	13
Ce	59	59	41	56	50	40
Pb	5	7	8	8	8	10
Th	1	3	6	5	3	7
K_2O/Na_2O	0.41	0.45	0.52	0.47	0.41	0.48
$FeO+Fe_2O_3/MgO$	1.25	1.53	1.16	1.48	1.13	1.17
K/Rb	378	369	626	304	374	535
K/Sr	21	27	17	27	26	16
K/Ba	27	29	35	29	28	30
Ca/Sr	94	102	69	104	101	68
Rb/Sr	0.06	0.07	0.03	0.09	0.07	0.03
Ba/Sr	0.78	0.91	0.47	0.91	0.92	0.54
Ba/Rb	14.30	12.70	17.80	10.50	13.50	17.70
Ni/Co	2.41	1.88	1.14	1.32	4.04	1.19

Tab. I 4

U 15	NE 16	U 41.2	NT 20	NE 31	NT 18
56.6	56.7	56.7	56.8	56.9	56.9
0.97	1.03	1.03	0.84	0.84	0.95
16.7	16.9	16.7	16.0	16.1	15.8
1.75	2.20	3.08	2.07	2.19	2.63
5.12	4.80	4.10	4.52	4.17	4.03
0.12	0.12	0.12	0.11	0.10	0.11
6.09	4.76	4.87	6.14	6.19	5.64
6.74	6.95	7.13	7.84	7.19	8.28
4.09	3.60	3.74	3.70	3.98	3.44
1.62	1.73	1.69	1.37	1.58	1.77
0.24	0.27	0.27	0.19	0.25	0.27
0.31	0.76	0.20	0.48	0.42	0.51
0.05	0.07	0.03	0.05	0.06	0.05
100.30	99.90	99.70	100.10	100.00	100.40
2.87	7.20	6.04	5.38	4.47	6.46
-	-	-	-	-	-
9.54	10.23	10.23	8.09	9.34	10.42
34.47	30.50	32.42	31.27	33.69	29.00
22.34	24.87	24.37	22.98	21.41	22.36
-	-	-	-	-	-
2.53	3.19	0.82	3.00	3.18	3.54
-	-	-	-	-	-
1.84	1.96	2.00	1.59	1.60	1.80
0.57	0.64	0.66	0.45	0.59	0.64
0.11	0.16	0.07	0.11	0.14	0.11
7.33	6.01	8.00	11.49	9.80	13.19
18.12	14.49	15.21	15.17	15.39	11.98
-	-	-	-	-	-
69.21	72.81	73.05	67.72	68.90	68.25
30.50	26.45	26.76	31.81	30.69	31.26
46.87	47.93	48.68	44.74	47.50	45.88
234	112	115	177	130	102
25	22	21	23	22	22
106	32	36	66	90	24
31	41	34	37	36	36
75	72	71	67	63	71
41	47	41	27	23	26
428	492	496	567	644	861
25	43	26	20	21	22
204	172	170	102	107	92
8	6	9	5	5	4
658	516	553	390	554	464
23	45	22	8	18	13
72	57	62	34	48	40
4	14	9	6	7	8
2	8	5	1	2	4
0.40	0.48	0.45	0.37	0.40	0.51
1.13	1.47	1.06	1.07	1.03	1.18
327	306	341	422	670	565
31	29	28	20	20	17
20	28	25	29	24	32
113	101	103	99	80	69
0.10	0.10	0.08	0.05	0.04	0.03
1.54	1.05	1.12	0.69	0.86	0.54
16.10	11.00	13.50	14.40	24.10	17.90
4.24	1.46	1.71	2.87	4.09	1.09

Tab. I 4

NT 49	NT 50	U 41.1	NT 11	U 44	NT 55	NT 21
57.0	57.1	57.1	57.2	57.2	57.3	57.4
1.03	1.08	0.97	1.13	0.97	0.99	0.85
16.9	17.0	16.3	16.6	16.5	16.4	17.5
4.81	4.73	4.65	1.34	1.59	3.40	3.45
2.30	2.50	2.71	5.36	4.76	3.10	3.14
0.12	0.12	0.11	0.11	0.10	0.11	0.11
4.42	4.36	4.92	5.00	5.52	5.66	4.39
7.32	7.04	7.69	6.57	6.90	6.90	7.18
3.79	3.73	3.52	3.87	3.90	3.84	3.88
1.74	1.80	1.52	1.76	1.61	1.60	1.41
0.27	0.29	0.20	0.37	0.27	0.26	0.22
0.42	0.59	0.60	0.38	0.56	0.65	0.69
0.06	0.05	0.05	0.15	0.07	0.04	0.06
100.20	100.40	100.30	99.80	100.00	100.20	100.30
7.97	7.65	7.93	6.07	5.56	6.81	7.90
-	-	-	-	-	-	-
10.38	10.62	9.00	10.42	9.52	9.44	8.32
32.38	31.51	29.84	32.80	33.02	32.44	32.78
24.19	24.28	24.23	22.76	22.77	22.75	26.13
-	-	-	-	-	-	-
3.70	3.73	3.17	1.95	2.31	3.60	3.40
-	-	-	-	-	-	-
1.98	2.05	1.85	2.15	1.84	1.88	1.61
0.65	0.69	0.48	0.88	0.64	0.62	0.52
0.14	0.11	0.12	0.34	0.16	0.09	0.14
8.21	6.74	9.97	5.29	7.48	7.56	6.14
10.00	12.05	12.85	16.99	16.16	14.18	12.40
-	-	-	-	-	-	-
74.92	74.06	70.99	72.05	70.87	71.44	75.12
24.67	25.37	28.42	27.59	28.59	27.92	24.20
50.73	49.78	46.76	49.29	48.10	48.69	49.00
92	86	62	119	148	149	57
21	20	24	25	21	22	20
30	30	28	67	85	86	28
33	33	34	26	35	32	29
68	74	76	70	74	72	70
42	47	33	39	36	36	20
535	527	551	484	484	485	573
33	48	27	25	21	21	21
175	185	139	190	148	147	111
8	8	5	12	12	11	6
500	526	417	548	524	464	325
31	43	25	16	20	14	10
65	76	50	48	47	45	31
9	9	8	6	11	8	6
7	8	5	<1.00	4	4	1
0.46	0.48	0.43	0.45	0.41	0.42	0.36
1.35	1.61	1.39	1.34	1.15	1.13	1.48
343	317	382	374	372	369	585
27	28	23	30	28	27	20
29	28	30	27	26	29	36
98	95	100	97	102	102	90
0.08	0.09	0.06	0.08	0.07	0.07	0.04
0.94	1.00	0.76	1.13	1.08	0.96	0.57
11.90	11.20	12.60	14.10	14.60	12.90	16.30
1.43	1.50	1.17	2.68	4.05	3.91	1.40

Tab. I 4

	R 10	U 42	R 17	MT 27
SiO_2	57.6	57.7	57.7	58.1
TiO_2	0.84	0.94	0.95	1.03
Al_2O_3	17.1	16.2	16.5	16.5
Fe_2O_3	2.39	2.39	3.44	2.68
FeO	3.81	4.54	3.90	3.67
MnO	0.09	0.11	0.12	0.10
MgO	5.01	5.05	4.91	3.96
CaO	7.05	7.43	7.65	6.68
Na_2O	4.25	3.65	3.33	3.82
K_2O	1.58	1.68	1.49	2.40
P_2O_5	0.25	0.20	0.20	0.27
H_2O^+	0.14	0.24	0.32	0.38
CO_2	0.07	0.05	0.04	0.26
Σ	100.20	100.20	100.30	99.90
Q	5.52	7.67	9.21	8.35
C	-	-	-	-
OR	9.32	9.91	8.78	14.21
AB	35.90	30.83	28.11	32.38
An	22.88	22.82	25.61	20.82
NE	-	-	-	-
MT	3.39	3.46	3.54	3.67
HM	-	-	-	-
IL	1.59	1.78	1.80	1.96
AP	0.59	0.47	0.47	0.64
CC	0.16	0.11	0.09	0.59
DI	7.98	9.95	8.63	7.19
HY	12.55	12.78	13.45	9.83
OL	-	-	-	-
Salic.	73.62	71.23	71.71	75.75
Femic.	26.26	28.55	27.98	23.88
Diff.-I.	50.74	48.41	46.10	54.93
Cr	87	66	62	86
Co	21	21	23	18
Ni	60	31	26	21
Cu	25	25	18	23
Zn	63	68	73	65
Rb	22	38	33	74
Sr	668	529	556	503
Y	20	25	25	25
Zr	100	157	136	207
Nb	5	7	6	13
Ba	390	437	-	598
La	-	17	-	20
Ce	-	44	-	67
Pb	7	8	8	12
Th	<1	7	5	14
K_2O/Na_2O	0.37	0.46	0.45	0.63
$FeO+Fe_2O_3/MgO$	1.24	1.37	1.47	1.60
K/Rb	595	366	378	269
K/Sr	20	26	22	40
K/Ba	34	32	98	33
Ca/Sr	75	100	98	95
Rb/Sr	0.03	0.07	0.06	0.15
Ba/Sr	0.58	0.83	-	1.19
Ba/Rb	17.70	11.50	-	8.08
Ni/Co	2.86	1.48	1.13	1.17

Tab. I 4

Stratovolcanoe-Andesites

	U 40.1	U 40.2	R 15	R 16	U 18b	CIBP
SiO_2	59.0	59.1	59.4	59.4	59.8	59.9
TiO_2	1.04	1.04	1.02	1.03	0.76	0.78
Al_2O_3	16.3	16.6	16.1	16.2	17.8	17.4
Fe_2O_3	3.26	3.38	2.04	3.11	1.94	2.68
FeO	3.27	3.18	3.97	3.07	4.33	3.21
MnO	0.10	0.11	0.10	0.10	0.13	0.11
MgO	3.50	3.56	3.61	3.31	1.84	3.64
CaO	6.03	6.15	6.10	5.94	4.89	6.75
Na_2O	3.87	3.88	3.87	3.97	5.21	3.46
K_2O	2.56	2.51	2.71	2.66	2.20	1.37
P_2O_5	0.30	0.28	0.24	0.24	0.53	0.22
H_2O^+	0.61	0.20	0.81	0.51	0.27	0.20
CO_2	0.12	0.05	0.04	0.04	0.06	0.04
Σ	100.00	100.00	100.00	99.60	99.80	99.80
Q	9.25	8.90	9.12	9.91	7.48	14.62
C	-	-	-	-	-	-
OR	15.43	15.10	16.01	15.79	13.03	8.12
AB	33.39	33.42	32.74	33.76	44.19	29.36
AN	19.93	20.83	18.55	18.62	18.73	27.98
NE	-	-	-	-	-	-
MT	1.06	1.24	2.96	3.69	2.82	3.32
HM	-	-	-	-	-	-
IL	2.01	2.01	1.94	1.97	1.45	1.49
AP	0.73	0.60	0.57	0.57	1.26	0.52
CC	0.28	0.12	0.09	0.09	0.14	0.09
DI	6.35	6.70	7.98	7.36	1.44	3.14
HY	10.97	10.89	9.24	7.75	9.22	11.18
OL	-	-	-	-	-	-
Salic.	78.00	78.26	76.43	78.08	83.43	80.08
Femic.	21.40	21.56	22.78	21.43	16.33	19.74
Diff.-I.	58.07	57.42	57.87	59.46	64.70	52.10
Cr	66	78	59	57		33
Co	18	20	16	17		16
Ni	19	19	19	19		13
Cu	27	28	20	26	64	14
Zn	65	67	63	63	64	63
Rb	80	77	84	84	56	27
Sr	429	429	415	427	505	676
Y	27	26	28	28	27	24
Zr	262	256	279	274	357	107
Nb	15	15	15	15		6
Ba	527	524	-	-		556
La	26	25	-	-		19
Ce	67	57	-	-		47
Pb	10	8	12	12		5
Th	10	9	12	11.		3
K_2O/Na_2O	0.66	0.65	0.70	0.67	0.42	0.40
$FeO+Fe_2O_3/MgO$	1.33	1.34	1.66	1.85	3.41	1.61
K/Rb	266	270	268	263	327	422
K/Sr	50	48	54	52	36	17
K/Ba	40	40			-	21
Ca/Sr	100	102	105	99	69	71
Rb/Sr	0.19	0.18	0.20	0.20	0.11	0.04
Ba/Sr	1.23	1.22	-	-	-	0.82
Ba/Rb	6.58	6.81	-	-	-	20.60
Ni/Co	1.06	0.95	1.19	1.12		0.81

Tab. I 4

	U 18	R 18	R 8	NT 7	NE 1	NE 2
SiO_2	60.1	60.3	60.5	60.6	60.7	61.1
TiO_2	0.77	1.03	0.76	0.85	0,64	0.63
Al_2O_3	18.0	16.3	16.4	18.1	18.2	18.1
Fe_2O_3	1.99	2.89	2.72	1.75	1.89	2.09
FeO	4.26	2.88	2.73	3.57	3.25	2.98
MnO	0.14	0.10	0.09	0.09	0.09	0.09
MgO	1.78	3.18	3.47	2.82	2.72	2.58
CaO	4.81	5.41	5.63	5.90	5.77	5.68
Na_2O	4.53	3.96	4.18	4.23	4.48	4.45
K_2O	2.17	3.04	2.21	1.65	1.66	1.69
P_2O_5	0.52	0.28	0.25	0.22	0.28	0.29
H_2O^+	1.08	0.35	0.37	0.22	0.55	0.70
CO_2	0.06	0.06	0.06	0.04	0.06	0.06
Σ	100.20	99.80	99.40	100.00	100.30	100.40
Q	10.65	10.74	11.56	12.24	11.57	12.67
C	0.84	-	-	-	-	-
OR	12.81	18.01	13.15	9.75	9.78	9.94
AB	38.29	33.60	35.61	35.78	37.80	37.49
AN	20.06	17.77	19.59	25.52	24.58	24.31
NE	-	-	-	-	-	-
MT	1.46	3.68	3.30	2.54	2.73	3.02
HM	-	-	-	-	-	-
IL	1.46	1.96	1.45	1.61	1.21	1.19
AP	1.23	0.67	0.60	0.52	0.66	0.68
CC	0.14	0.14	0.14	0.09	0.14	0 14
DI	-	5.53	5.21	1.67	1.43	1.19
HY	12.01	7.58	9.04	10.08	9.57	8.68
OL	-	-	-	-	-	-
Salic.	82.65	80.12	79.91	83.28	83.73	84.42
Femic.	16.33	19.55	19.73	16.51	15.74	14.90
Diff.-I.	64.70	62.35	60.32	57.76	59.15	60.10
Cr	8	60	70	24	16	15
Co	16	17	16	14	14	12
Ni	5	30	39	9	15	13
Cu	9	28	29	11	16	19
Zn	82	64	64	61	61	60
Rb	57	90	48	39	28	28
Sr	503	485	558	578	686	677
Y	21	31	23	21	20	19
Zr	275	284	150	139	125	124
Nb	10	14	6	4	6	5
Ba	858	-	608	507	684	670
La	30	-	-	7	20	13
Ce	72	-	-	30	39	37
Pb	11	11	10	9	6	6
Th	5	12	6	3	<1	<1
$K2O/Na_2O$	0.48	0.77	0.53	0.39	0.37	0.38
$FeO+Fe_2O_3/MgO$	3.46	1.80	1.56	1.89	1.89	1.97
K/Rb	316	280	381	351	357	500
K/Sr	36	52	33	24	20	21
K/Ba	21		30	27	20	21
Ca/Sr	68	80	72	73	60	60
Rb/Sr	0.11	0.19	0.09	0.07	0.04	0.04
Ba/Sr	1.71	-	1.09	0.88	1.00	0.99
Ba/Rb	15.10	-	12.70	13.00	24.40	23.90
Ni/Co	0.31	1.77	2.44	0.64	1.07	1.08

Tab. I 4

NT 23	OM 2	U 17	NH 25	NH 27	CP 3	NT 29
61.1	61.3	61.4	61.5	61.6	61.9	62.0
1.09	0.63	0.75	0.68	0.68	1.10	0.60
16.4	16.2	17.1	18.1	18.2	16.3	17.4
1.99	2.55	2.41	2.20	2.55	2.07	2.33
3.96	2.42	2.80	2.80	2.40	3.94	2.38
0.10	0.09	0.09	0.08	0.08	0.10	0.09
2.73	3.85	3.37	2.30	2.28	2.76	1.90
5.04	5.53	5.57	5.19	5.32	5.15	4.87
4.05	3.55	4.03	4.60	4.66	3.82	4.30
2.57	2.48	1.70	1.92	1.90	2.34	2.22
0.27	0.30	0.24	0.19	0.17	0.27	0.28
0.89	0.72	0.29	0.37	0.23	0.20	1.58
0.05	0.04	0.09	0.14	0.09	0.04	0.03
100.20	99.70	99.80	99.90	100.20	100.00	100.00
12.73	14.36	14.74	12.78	12.43	15.35	15.31
-	-	-	-	-	-	-
15.15	14.71	10.06	11.34	11.21	13.83	13.12
34.19	30.15	34.16	38.90	39.38	32.33	36.40
18.93	21.02	23.59	23.05	23.10	20.42	21.63
-	-	-	-	-	-	-
2.88	3.10	3.27	3.16	3.13	3.00	3.18
-	-	-	-	-	-	-
2.07	1.20	1.43	1.29	1.29	2.09	1.64
0.64	0.71	0.57	0.45	0.40	0.64	0.66
0.11	0.09	0.21	0.32	0.20	0.09	0.07
3.20	3.42	1.56	0.45	1.27	2.53	0.42
9.23	10.51	10.14	7.91	7.35	9.54	6.51
-	-	-	-	-	-	-
81.00	80.25	82.56	86.07	86.14	81.92	86.46
18.13	19.04	17.17	13.57	13.64	17.89	11.98
62.07	59.23	58.97	63.02	63.03	61.50	64.83
26	108	43	14	10	30	11
16	14	14	12	12	16	11
13	47	28	9	8	15	7
15	24	18	19	16	19	10
70	62	59	62	61	72	61
66	46	32	39	38	62	45
413	796	567	590	609	419	585
25	19	20	18	17	24	20
222	130	149	112	108	214	150
13	7	7	5	5	13	8
685	947	594	693	759	672	733
17	28	10	12	11	24	23
53	81	39	31	26	52	52
11	12	7	10	9	11	9
9	9	2	3	3	10	4
0.63	0.70	0.42	0.42	0	0	0.52
2.18	1.28	1.54	2.17	2	2	2.44
323	448	441	408	416	313	409
52	26	25	27	26	46	31
31	22	24	23	21	29	25
87	50	70	63	62	88	58
0.16	0.06	0.06	0.07	0.06	0.15	0.08
1.66	1.19	1.05	1.18	1.25	1.60	1.25
10.40	20.60	18.60	17.80	20.00	10.80	16.30
0.81	3.36	2.00	0.75	0.67	0.94	0.64

Tab. I 4

MT 24	R 7	MH 26	C28P
62.1	62.4	62.6	62.7
0.92	0.68	0.66	0.64
16.6	16.8	18.1	17.2
2.32	2.90	2.09	2.14
2.73	1.69	2.77	2.65
0.08	0.09	0.08	0.09
3.15	2.55	2.35	2.43
5.38	5.62	4.44	5.17
3.89	4.40	4.63	3.75
2.68	1.93	1.89	1.98
0.23	0.26	0.19	0.20
0.31	0.27	0.26	0.89
0.05	0.04	0.15	0.09
100.40	99.70	100.20	99.90
14.00	14.98	15.23	18.43
-	-	1.17	0.18
15.77	11.46	11.15	11.71
32.77	37.40	39.10	31.75
19.83	20.48	19.80	23.79
-	-	-	-
3.35	3.18	3.02	3.11
-	-	-	-
1.74	1.30	1.25	1.22
0.54	0.62	0.45	0.47
0.11	0.09	0.34	0.21
3.92	4.43	-	-
7.67	5.82	8.25	8.27
-	-	-	-
82.37	84.31	86.43	85.85
17.33	15.43	13.32	13.27
62.54	63.83	65.47	61.89
44	25	14	18
14	10	12	12
30	17	8	9
28	15	19	12
59	60	58	56
74	25	39	40
454	945	598	522
22	18	18	18
209	98	109	126
16	5	5	8
611	577	712	692
25	-	11	19
53	-	29	43
12	8	9	9
12	5	1	5
0.69	0.44	0.41	0.53
1.60	1.77	2.07	1.97
300	640	403	410
49	17	26	31
36	28	22	24
85	43	53	71
0.16	0.03	0.07	0.08
1.35	0.61	1.19	1.33
8.26	23.10	18.30	17.30
2.14	1.70	0.67	0.75

Tab. I 5 Basaltic Andesites

	U 29	U 37	NT 63	U 45	NT 57	NT 41
SiO_2	52.0	52.1	52.5	52.6	52.7	52.8
TiO_2	1.38	1.29	1.22	2.02	1.26	1.92
Al_2O_3	19.1	16.8	16.8	17.9	18.0	17.7
Fe_2O_3	8.01	2.19	6.49	7.43	5.57	6.41
FeO	0.80	7.30	2.41	2.15	2.55	2.72
MnO	0.13	0.15	0.13	0.15	0.13	0.16
MgO	3.25	6.57	6.57	2.60	5.74	2.88
CaO	7.64	8.91	8.26	6.44	8.58	6.64
Na_2O	3.51	3.44	3.49	4.65	3.73	4.64
K_2O	1.94	0.95	1.35	2.46	1.10	2.53
P_2O_5	0.41	0.21	0.24	0.78	0.34	0.77
H_2O^+	1.49	0.38	0.74	0.65	0.50	0.54
CO_2	0.09	0.06	0.07	0.05	0.07	0.05
Σ	99.80	100.30	100.30	99.90	100.10	99.80
Q	0.98	-	-	-	-	-
C	-	-	-	-	-	-
OR	11.75	5.62	8.06	14.74	6.56	15.14
AB	30.43	29.14	29.82	39.89	31.83	39.77
AN	31.38	27.62	26.45	20.99	29.37	20.26
NE	-	-	-	-	-	-
MT	1.99	2.24	2.01	2.16	1.80	2.07
HM	-	-	-	-	-	-
IL	2.69	2.45	2.34	3.89	2.41	3.69
AP	1.00	0.50	0.57	1.87	0.81	1.85
CC	0.21	0.14	0.16	0.12	0.16	0.12
DI	3.43	12.16	10.51	4.96	8.85	6.42
HY	16.18	15.73	16.37	4.73	16.56	3.07
OL	-	4.42	3.72	6.71	1.67	7.65
Salic.	74.54	62.38	64.33	75.62	67.75	75.17
Femic.	25.49	37.64	35.69	24.43	32.27	24.87
Diff.-I.	43.15	34.76	37.88	54.63	38.38	54.92
Cr	57	190	222	16	119	13
Co	29	36	31	27	26	24
Ni	30	69	125	9	63	7
Cu	50	40	44	25	33	25
Zn	79	88	76	92	82	87
Rb	29	20	29	66	18	74
Sr	700	331	437	837	584	847
Y	28	29	33	45	27	35
Zr	174	144	181	296	170	290
Nb	19	6	12	34	12	34
Ba	539	273	503	813	465	861
La	31	15	14	66	12	32
Ce	67	35	44	152	49	101
Pb	10	6	10	9	6	8
Th	9	<1	7	9	3	9
K_2O/Na_2O	0.55	0.28	0.39	0.53	0.29	0.55
$FeO+Fe_2O_3/MgO$	2.51	1.43	1.28	3.46	1.31	3.00
K/Rb	555	395	386	309	506	284
K/Sr	23	24	26	24	16	25
K/Ba	30	29	22	25	20	24
Ca/Sr	78	192	135	55	105	56
Rb/Sr	0.04	0.06	0.07	0.08	0.03	0.09
Ba/Sr	0.77	0.83	1.15	0.97	0.80	1.02
Ba/Rb	18.60	13.70	17.40	12.30	25.80	11.60
Ni/Co	1.04	1.92	4.03	0.33	2.42	0.29

Tab. I 5

U 55	NB 4	U 39	NT 12	NT 17	NB 5	NT 15
53.0	53.3	53.3	53.4	53.4	53.7	53.7
2.01	0.97	1.55	1.48	1.37	0.97	1.32
17.6	15.7	17.8	18.1	16.5	15.7	16.7
6.45	2.55	2.52	1.58	1.50	2.39	3.27
2.99	4.99	5.73	6.68	6.50	5.08	4.80
0.13	0.12	0.12	0.13	0.13	0.12	0.13
2.71	9.01	4.67	4.66	7.13	8.69	6.72
6.19	8.81	8.05	8.24	7.77	8.71	7.88
4.50	3.03	3.61	3.96	3.67	3.11	3.76
2.46	1.12	1.41	1.41	1.35	1.14	1.31
0.81	0.25	0.41	0.33	0.36	0.25	0.34
0.91	0.37	0.50	0.33	0.44	0.25	0.40
0.05	0.05	0.06	0.04	0.19	0.05	0.08
99.80	100.30	99.70	100.30	100.30	100.20	100.40
-	0.76	3.14	-	-	1.15	1.17
-	-	-	-	-	-	-
14.77	6.63	8.40	8.33	7.99	6.74	7.74
38.69	25.67	30.78	33.51	31.10	26.34	31.83
20.89	25.96	28.42	27.45	24.59	25.54	24.83
-	-	-	-	-	-	-
2.17	3.70	3.68	2.29	2.18	3.47	4.09
-	-	-	-	-	-	-
3.88	1.84	2.97	2.81	2.61	1.84	2.51
1.95	0.59	0.98	0.78	0.85	0.59	0.81
0.12	0.11	0.14	0.09	0.43	0.11	0.18
3.86	12.62	7.09	9.04	8.45	12.58	9.24
11.40	22.14	14.43	15.18	20.37	21.64	1.62
2.32	-	-	0.55	1.46	-	-
74.36	59.00	70.73	69.28	63.68	59.77	65.57
25.69	41.01	29.29	30.74	36.35	40.24	34.45
53.46	33.05	42.32	41.84	39.08	34.24	40.74
15	341	34	49	213	318	189
27	28	26	27	29	27	28
86	105	33	29	105	91	87
25	31	36	34	35	51	34
88	74	85	83	81	70	77
71	18	30	31	27	18	27
777	673	570	488	515	666	505
47	23	27	29	26	23	26
295	94	184	185	167	93	169
32	5	15	11	11	5	11
839	279	390	395	427	287	376
50	11	22	10	16	10	12
138	31	60	38	48	34	39
11	6	7	6	7	5	7
12	2	4	4	3	1	4
0.55	0.37	0.39	0.36	0.37	0.37	0.35
3.30	0.84	1.77	1.77	1.12	0.86	1.19
287	517	390	377	415	528	404
26	14	21	24	22	14	22
24	33	30	30	26	33	29
57	94	101	121	108	94	111
0.09	0.03	0.05	0.06	0.05	0.03	0.05
1.08	0.42	0.68	0.81	0.83	0.43	0.75
11.80	15.50	13.00	12.70	15.80	15.90	13.90
3.19	3.75	1.27	1.07	3.62	3.37	3.11

Tab. I 5

NT 30	U 31	NT 61	U 30	NE 32	NT 47	NT 14
53.7	53.8	53.9	54.3	54.4	54.4	54.6
1.10	1.22	1.55	1.26	0.79	2.16	1.07
16.7	17.5	17.8	17.2	15.6	15.9	16.9
2.40	2.02	6.02	3.44	7.43	6.56	2.65
5.20	5.39	2.54	4.13	0.55	3.19	4.80
0.13	0.13	0.13	0.12	0.13	0.13	0.12
6.42	5.59	4.40	5.47	7.00	3.15	6.78
8.74	8.39	7.73	7.98	10.00	6.15	7.48
3.69	3.63	3.93	3.89	3.08	4.05	3.78
1.33	1.26	1.56	1.40	0.80	2.94	1.40
0.33	0.34	0.37	0.35	0.17	1.02	0.23
0.17	0.23	0.35	0.42	0.11	0.32	0.28
0.09	0.13	0.08	0.05	0.21	0.07	0.04
100.00	99.60	100.30	100.00	100.20	100.00	100.10
0.66	2.28	3.02	2.64	4.13	4.42	1.70
-	-	-	-	-	-	-
7.87	7.49	9.24	8.31	4.74	17.49	8.29
31.28	30.90	33.35	33.08	26.15	34.50	32.03
25.12	27.90	26.40	25.46	26.47	16.63	25.05
-	-	-	-	-	-	-
3.49	2.95	4.44	4.02	3.33	5.34	3.73
-	-	-	-	-	-	-
2.09	2.33	2.95	2.41	1.51	4.13	2.04
0.78	0.81	0.88	0.83	0.40	2.43	0.55
0.21	0.30	0.18	0.11	0.48	0.16	0.09
12.52	8.82	7.36	9.38	16.77	5.62	8.29
16.00	16.24	12.20	13.78	16.02	9.34	18.25
-	-	-	-	-	-	-
64.93	68.58	72.01	69.48	61.20	73.04	67.07
35.09	31.44	28.01	30.54	38.51	27.02	32.94
39.81	40.68	45.62	44.02	35.03	56.41	42.02
152	107	29	115	194	24	258
27	23	27	25	27	27	26
53	52	30	55	36	23	115
40	38	34	35	58	96	37
74	81	88	82	71	104	72
35	21	34	29	13	100	33
479	555	546	550	742	403	447
26	27	28	26	20	54	25
131	172	200	174	51	538	173
5	12	15	12	4	31	7
365	520	437	388	279	778	419
8	18	22	17	19	38	19
30	59	54	58	42	110	40
4	8	8	6	5	21	5
1	3	5	3	3	21	2
0.36	0.35	0.40	0.36	0.26	0.73	0.37
1.18	1.33	1.88	1.37	1.07	2.97	1.10
314	500	382	400	508	244	352
23	19	24	21	9	61	26
30	20	30	30	24	31	28
130	108	101	104	96	109	120
0.07	0.04	0.06	0.05	-	0.25	0.07
0.76	0.94	0.80	0.71	0.38	1.93	0.94
10.40	24.80	12.90	13.40	21.50	7.78	12.70
1.96	2.26	1.11	2.20	1.33	0.85	4.42

Tab. I 5

NH 30	NH 28	U 38	NH 29	U 71	NH 6	NT 62
54.9	55.0	55.2	55.3	55.3	55.6	55.6
1.09	1.14	1.42	1.10	0.93	0.88	1.13
17.5	17.8	17.1	17.6	18.0	15.2	15.7
2.33	1.91	1.97	3.75	4.96	2.25	5.02
5.01	5.50	5.62	3.82	3.37	5.33	2.45
0.12	0.12	0.12	0.12	0.15	0.13	0.11
5.76	5.22	4.58	5.69	3.22	7.51	6.69
7.04	7.01	7.50	7.00	8.00	9.03	7.15
4.08	4.20	3.92	4.01	3.46	3.00	3.34
1.54	1.62	1.90	1.54	1.86	1.14	1.97
0.31	0.37	0.43	0.31	0.23	0.18	0.31
0.17	0.22	0.41	0.07	0.39	0.09	0.82
0.06	0.14	0.06	0.06	0.04	0.11	0.05
99.90	100.20	100.20	100.40	99.90	100.40	100.30
1.70	1.28	2.90	2.72	5.83	4.92	4.68
-	-	-	-	-	-	-
9.12	9.57	11.25	9.08	11.06	6.71	11.73
34.61	35.53	33.23	33.86	29.46	25.29	28.47
24.95	24.92	23.49	25.42	28.27	24.55	22.19
-	-	-	-	-	-	-
3.39	2.77	2.86	3.76	3.69	3.25	3.84
-	-	-	-	-	-	-
2.08	2.16	2.70	2.09	1.78	1.67	2.16
0.74	0.88	1.02	0.73	0.55	0.43	0.74
0.14	0.32	0.14	0.14	0.09	0.25	0.12
6.16	5.30	8.61	5.61	8.16	14.63	8.93
17.13	17.28	13.82	16.62	11.12	18.31	17.17
-	-	-	-	-	-	-
70.39	71.31	70.87	71.08	74.63	61.48	67.06
29.63	28.72	29.15	28.94	25.39	38.53	32.95
45.44	46.38	47.38	45.66	46.36	36.93	44.88
160	127	55	162	20		245
25	23	25	27	24		26
76	60	37	75	11		117
29	39	34	23	67		26
77	75	82	77	74		75
38	39	44	36	53		52
514	539	502	520	595		475
25	25	27	24	30		30
179	176	202	175	106		193
8	9	15	8	6		12
494	557	397	464	672	307	524
20	23	22	24	24	9	21
62	58	57	55	51	25	53
7	6	9	5	9		10
3	2	6	2	4		10
0.38	0.39	0.48	0.38	0.54	0.38	0.59
1.27	1.42	1.66	1.31	2.54	1.01	1.08
405	344	359	356	291	-	315
25	25	31	25	26	-	35
26	24	40	28	23	31	31
98	93	107	96	96	-	108
0.07	0.07	0.09	0.07	0.09	-	0.11
0.96	1.03	0.79	0.89	1.13	-	1.10
13.00	14.30	9.02	12.90	12.70		10.10
3.04	2.61	1.48	2.78	0.46	0.51	4.50

Basalts *Tab.I 6*

	U 8	U 5.12	U 7	U 5.11	U 53	MT 32
SiO_2	46.3	47.5	47.6	48.1	48.1	48.5
TiO_2	1.05	2.27	2.45	2.28	2.15	1.09
Al_2O_3	15.9	16.1	17.0	16.3	16.5	18.1
Fe_2O_3	5.78	4.53	7.80	3.73	5.73	5.37
FeO	5.15	6.72	3.87	7.62	5.55	3.65
MnO	0.17	0.17	0.16	0.17	0.14	0.13
MgO	6.54	6.73	5.17	6.73	6.37	3.81
CaO	13.10	10.40	9.89	9.78	10.50	11.40
Na_2O	2.26	3.14	2.78	3.09	3.11	3.05
K_2O	0.99	1.06	0.76	1.07	0.88	1.41
P_2O_5	0.22	0.45	0.91	0.45	0.39	0.32
H_2O^+	1.46	0.39	1.80	0.22	0.85	1.27
CO_2	1.38	0.60	0.07	0.06	0.06	1.85
Σ	100.30	100.10	100.30	99.60	100.20	100.00
Q	-	-	-	-	-	-
C	-	-	-	-	-	-
OR	5.94	6.30	4.59	6.38	5.25	8.48
AB	19.43	26.73	24.04	26.36	26.56	26.26
AN	30.80	26.87	32.36	27.67	28.72	32.08
NE	-	-	-	-	-	-
MT	2.53	2.61	2.68	2.68	2.61	2.08
HM	-	-	-	-	-	-
IL	2.03	4.34	4.76	4.37	4.12	2.11
AP	0.53	1.07	2.20	1.08	0.93	0.77
CC	3.19	1.37	0.16	0.14	0.14	4.28
DI	20.47	14.95	9.28	14.66	17.13	9.49
HY	1.61	0.10	18.29	2.39	0.64	11.14
OL	13.49	15.68	1.69	14.32	13.93	3.93
Salic.	56.17	59.90	60.98	60.41	60.53	66.82
Femic.	43.84	40.12	39.07	39.62	39.49	33.20
Diff.-I.	25.37	33.04	28.63	32.73	31.81	34.73
Cr	98	189	78	176	150	27
Co	40	41	39	42	41	31
Ni	50	78	41	84	71	18
Cu	130	54	35	42	59	140
Sn	74	91	90	93	87	82
Rb	23	24	17	24	17	32
Sr	678	623	1333	638	617	761
Y	21	31	32	39	34	25
Zr	54	163	114	167	152	98
Nb	5	12	32	11	9	9
Ba	298	474	1975	580	410	344
La	14	14	42	13	10	15
Ce	37	49	82	54	34	47
Pb	5	4	<1	4	4	11
Th	3	2	<1	2	1	7
K_2O/Na_2O	0.44	0.34	0.27	0.35	0.28	0.46
$FeO+Fe_2O_3/MgO$	1.61	1.63	2.14	1.66	1.71	2.27
K/Rb	430	367	371	371	429	366
K/Sr	12	14	5	14	12	15
K/Ba	28	19	3	15	18	34
Ca/Sr	138	119	53	110	122	107
Rb/Sr	0.03	0.04	0.01	0.04	0.03	0.04
Ba/Sr	0.44	0.76	1.48	0.91	0.67	0.45
Ba/Rb	13.00	19.80	116.20	24.20	24.10	10.80
Ni/Co	1.25	1.90	1.05	2.00	1.73	0.58

Tab. I 6

U 6	NN 18	U 22	U 31b	R 4	NN 19
48.6	49.5	49.5	49.5	51.4	51.9
0.92	1.52	1.58	1.54	1.54	1.31
15.0	16.9	16.8	16.7	17.9	17.3
5.22	1.83	2.51	2.12	3.31	2.51
3.84	8.25	7.46	7.90	5.26	5.96
0.24	0.16	0.16	0.16	0.13	0.13
6.04	8.06	7.82	8.16	6.52	6.62
11.10	9.81	9.94	9.87	8.96	9.24
2.79	3.30	3.09	3.29	3.46	3.42
1.09	0.64	0.58	0.67	0.85	0.88
0.25	0.25	0.26	0.26	0.29	0.25
3.28	0.15	0.10	0.29	0.21	0.40
1.49	0.07	0.04	0.04	0.17	0.15
99.90	100.40	99.80	100.40	100.00	100.10
-	-	-	-	-	-
-	-	-	-	-	-
6.70	3.77	3.44	3.95	5.04	5.22
24.54	27.85	26.24	27.80	29.40	29.05
26.18	29.33	30.36	28.78	30.92	29.37
-	-	-	-	-	-
2.14	2.39	2.36	2.36	1.99	2.01
-	-	-	-	-	-
1.82	2.88	3.01	2.92	2.94	2.50
0.62	0.59	0.62	0.62	0.69	0.59
3.52	0.16	0.09	0.09	0.39	0.34
16.03	13.94	13.96	14.77	8.72	11.44
16.22	3.21	8.27	2.58	15.63	15.79
2.25	15.90	11.67	16.16	4.30	3.70
57.42	60.95	60.04	60.52	65.36	63.64
42.60	39.06	39.97	39.49	34.66	36.38
31.24	31.62	29.68	31.75	34.44	34.27
181	276	238	276	75	187
34	42	40	41	30	33
67	99	86	104	25	75
97	54	55	55	18	46
83	87	83	89	84	86
13	11	11	13	13	17
606	376	386	376	462	430
22	28	29	28	27	28
63	136	140	140	160	141
9	7	8	8	11	7
369	159	154	184	202	358
11	10	5	16	-	10
38	30	26	34	-	33
4	4	3	4	3	5
3	1	<1	2	<1	1
0.39	0.19	0.19	0.20	0.25	0.26
1.44	1.25	1.26	1.22	1.29	1.27
692	482	436	431	546	429
15	14	12	15	15	17
24	33	31	30	35	20
131	186	184	188	139	153
0.02	-	0.03	0.04	0.03	0.04
0.61	0.42	0.40	0.49	0.44	0.83
28.40	14.50	14.00	14.20	15.50	21.10
1.97	2.36	2.15	2.54	0.83	2.27

Tab. I 7 Alkali-Basalts

	NT 44R	NT 44	U 57	U 72	U 56	U 10
SiO_2	43.4	43.5	44.0	44.6	44.8	45.3
TiO_2	1.49	1.50	2.84	1.24	2.62	1.09
Al_2O_3	13.6	13.6	12.6	14.5	13.4	14.3
Fe_2O_3	4.56	4.57	6.75	6.20	9.12	5.21
FeO	4.88	4.89	6.53	4.40	4.12	4.94
MnO	0.17	0.17	0.17	0.18	0.18	0.18
MgO	10.60	10.50	9.08	11.50	7.96	13.40
CaO	14.30	14.30	10.10	11.90	10.60	11.00
Na_2O	2.91	2.88	4.06	2.71	3.80	2.37
K_2O	0.60	0.57	0.99	0.94	0.81	0.81
P_2O_5	0.87	0.87	0.99	0.34	0.78	0.33
$H2O^+$	2.20	2.20	1.81	0.77	1.80	1.27
CO_2	0.11	0.10	0.04	0.59	0.05	0.14
Σ	99.70	99.70	100.00	99.90	100.00	100.30
Q	-	-	-	-	-	-
C	-	-	-	-	-	-
OR	3.65	3.47	5.99	5.63	4.91	4.85
AB	4.08	4.76	15.62	9.89	18.30	11.78
AN	22.92	23.16	13.54	24.96	17.55	26.33
NE	11.52	11.01	10.59	7.24	7.95	4.62
MT	2.22	2.24	3.12	2.44	3.05	2.35
HM	-	-	-	-	-	-
IL	2.91	2.93	5.52	2.39	5.10	2.10
AP	2.12	2.12	2.40	0.82	1.89	0.79
CC	0.26	0.23	0.09	1.36	0.12	0.32
DI	35.03	34.92	25.12	23.27	25.19	20.78
HY	-	-	-	-	-	-
OL	15.34	15.20	18.06	22.04	16.00	26.09
Salic.	42.16	42.40	45.74	47.71	48.70	47.58
Femic.	57.89	57.65	54.32	52.31	51.35	52.44
Diff.-I.	19.24	19.24	32.19	22.75	31.15	21.25
Cr	341.00	303	389	654	447	717
Co	28.00	39	58	44	56	43
Ni		143	264	254	237	271
Cu	80.00	18	68	103	87	102
Zn		78	1	84	120	84
Rb		27	24	22	81	19
Sr		1071	163	665	931	662
Y		29	32	23	26	20
Zr		125	332	66	297	63
Nb		65	46	8	39	8
Ba	880.00	1045	609	1048	461	416
La	40.00	49	31	22	23	26
Ce	133.00	141	98	40	73	54
Pb		8	6	5	7	7
Th		14	7	3	8	5
K_2O/Na_2O	0.21	0.20	0.24	0.35	0.21	0.34
$FeO+Fe_2O3/MgO$	0.86	0.87	1.41	0.88	1.58	0.73
K/Rb		174	342	355	83	353
K/Sr		4	7	12	7	10
K/Ba		4	13	7	15	16
Ca/Sr		95	62	128	81	119
Rb/Sr		0.03	0.02	0.03	0.09	0.03
Ba/Sr		0.98	0.52	1.58	0.50	0.63
Ba/Rb		38.70	25.40	47.60	5.69	21.90
Ni/Co	5.71	3.67	4.55	5.77	4.23	6.30

Tab. I 7

U 50	NT 43	U 67	U 74	U 52	ClCo(U 4)	NT 35	U 7b
45.9	46.0	46.1	46.2	46.3	46.7	46.9	46.9
2.37	2.46	2.80	2.79	2.40	2.39	2.45	2.70
15.5	17.2	15.5	15.6	16.7	15.4	17.1	16.5
6.26	9.20	4.50	5.75	4.53	8.54	5.88	6.10
5.44	2.79	7.39	6.26	6.36	3.03	5.42	5.95
0.17	0.17	0.17	0.18	0.17	0.17	0.16	0.16
6.56	4.30	7.82	7.18	7.56	5.85	6.21	5.78
11.00	9.91	9.53	9.60	9.65	10.30	9.86	9.17
3.25	3.20	3.36	2.97	2.80	3.33	3.40	3.79
1.25	2.33	1.40	1.37	1.43	1.27	1.48	1.41
0.61	0.82	0.66	0.65	0.52	0.72	0.51	0.63
0.91	0.97	1.00	1.35	1.57	0.96	0.53	0.63
0.92	0.37	0.11	0.26	0.15	0.58	0.07	0.03
100.10	99.70	100.30	100.20	100.10	99.20	100.00	99.70
-	-	-	-	-	-	-	-
-	-	-	-	-	-	-	-
7.48	14.05	8.35	8.23	8.60	7.69	8.83	8.44
22.21	19.44	20.89	24.10	22.20	26.87	21.70	24.70
24.31	26.21	23.29	25.59	29.27	23.89	27.29	24.16
3.05	4.44	4.23	0.78	1.03	1.09	3.98	4.22
2.70	2.72	2.78	2.80	2.57	2.66	2.61	2.79
-	-	-	-	-	-	-	-
4.56	4.77	5.37	5.38	4.64	4.65	4.70	5.20
1.46	1.98	1.58	1.56	1.25	1.75	1.22	1.51
2.12	0.86	0.25	0.60	0.35	1.35	0.16	0.07
17.22	13.37	15.78	13.73	12.21	16.33	14.99	14.46
-	-	-	-	-	-	-	-
14.94	12.21	17.52	17.27	17.91	13.77	14.56	14.48
57.04	64.13	56.76	58.69	61.10	59.53	61.80	61.53
42.99	35.91	43.28	41.35	38.93	40.51	38.23	38.51
32.74	37.92	33.47	33.10	31.83	35.64	34.51	37.37
287	67	262	244	132	244	144	99
44	40	49	47	42	42	42	44
131	29	105	111	62	120	61	66
50	40	57	57	40	49	44	47
93	90	96	94	84	87	82	94
23	53	20	19	30	26	33	18
767	979	767	798	756	934	740	771
31	35	30	29	32	29	32	33
167	202	194	193	174	167	181	198
26	34	37	37	19	28	18	34
481	1003	387	461	462	538	600	412
19	29	15	27	20	26	18	28
70	96	67	72	70	80	61	75
1	8	5	4	5	4	5	3
2	9	5	5	6	4	7	2
0.38	0.73	0.42	0.46	0.51	0.38	0.44	0.37
1.72	2.62	1.49	1.62	1.40	1.86	1.76	2.01
452	364	580	600	397	404	373	650
14	20	15	14	18	11	17	15
22	19	30	25	26	20	21	3
102	72	89	86	91	79	95	85
0.03	0.05	0.03	0.02	0.04	0.03	0.05	0.02
0.63	1.03	0.51	0.58	0.61	0.58	0.81	0.53
20.90	18.90	19.40	24.30	15.40	20.70	18.20	22.90
2.98	0.73	2.14	2.36	1.48	2.86	1.45	1.50

Tab. I 7

NH 21	U 75	NH 15	NT 64	NT 40	U 51	U 63	U 49
47.0	47.0	47.1	47.2	47.4	47.6	47.6	47.9
2.49	2.74	1.69	2.65	2.39	2.20	2.37	2.21
16.9	16.7	15.6	17.0	16.2	16.8	16.8	17.1
3.97	10.06	7.01	14.06	6.66	6.22	7.16	9.29
7.23	1.78	3.50	0.10	4.72	4.66	4.17	1.99
0,17	0.20	0.17	0.20	0.16	0.17	0.17	0.25
6.42	5.10	7.41	4.72	6.25	5.20	5.74	4.83
9.67	9.15	10.90	8.14	9.76	9.95	9.80	9.35
3.47	4.08	3.84	4.13	3.72	4.14	3.43	3.47
1.47	1.43	0.59	0.91	1.36	1.35	1.48	1.45
0.57	0.67	0.71	0.53	0.81	0.71	0.57	0.75
0.49	0.53	1.05	0.10	0.46	0.73	0.67	0.97
0.23	0.05	0.12	0.09	0.05	0.05	0.04	0.05
100.10	100.00	99.70	100.30	99.90	99.80	100.00	99.70
-	-	-	-	-	-	-	-
-	-	-	-	-	-	-	-
8.74	8.57	3.55	5.43	8.12	8.09	8.85	8.75
23.13	25.26	24.33	31.53	24.85	24.48	24.53	29.33
26.36	23.35	24.04	25.40	23.73	23.60	26.39	27.38
3.48	5.28	4.76	2.03	3.77	5.98	2.62	0.36
2.63	2.78	2.41	3.22	2.61	2.52	2.60	2.55
-	-	-	-	-	-	-	-
4.76	5.28	3.27	5.08	4.59	4.24	4.56	4.29
1.36	1.61	1.71	1.27	1.94	1.71	1.37	1.82
0.53	0.12	0.28	0.21	0.12	0.12	0.09	0.12
13.68	14.79	20.84	9.42	16.00	17.66	15.44	12.13
-	-	-	-	-	-	-	-
15.37	13.02	14.84	16.43	14.35	11.65	13.58	13.33
61.71	62.45	56.68	64.40	60.45	62.16	62.40	65.82
38.32	37.59	43.36	35.63	39.59	37.88	37.63	34.22
35.35	39.10	32.64	39.00	36.73	38.56	36.01	38.44
121	107	326	35	217	114	155	100
40	49	38	54	41	37	40	43
64	75	125	36	96	51	68	51
40	38	66	36	43	45	41	43
85	98	83	133	88	87	78	89
35	18	95	11	29	27	32	30
815	774	867	494	983	812	785	828
31	30	31	41	31	34	32	49
187	196	178	242	179	180	179	183
19	35	19	12	29	25	17	23
385	359	1045	292	686	524	554	739
16	28	25	13	21	20	21	46
61	69	83	48	66	82	62	109
3	3	9	2	5	5	5	4
<1	3	5	<1	4	2	6	4
0.42	0.35	0.15	0.22	0.37	0.33	0.43	0.42
1.71	2.26	1.35	2.85	1.74	2.01	1.88	2.18
349	661	52	691	390	415	384	400
15	15	6	15	11	14	16	14
32	33	5	26	16	23	22	16
85	84	90	118	71	88	89	81
0.04	0.02	0.11	0.02	0.03	0.03	0.04	0.04
0.47	0,46	1.21	0.59	0.70	0.65	0.71	0.89
11.00	19.90	11.00	26.60	23.70	19.40	17.70	24.60
1.60	1.53	3.29	0.67	2.34	1.38	1.70	1.19

Tab. I 7

NT 33	U 24	NT 48	U 48	NT 45	NT 25	U 35	U 25	U 9
48.5	48.5	48.7	48.7	49.0	49.1	49.4	50.0	50.2
1.23	1.50	1.85	1.54	2.07	1.85	1.65	1.55	1.10
17.5	16.8	17.2	16.4	17.0	16.0	14.0	16.4	18.4
4.91	3.24	8.84	1.86	6.19	4.89	2.73	5.87	4.74
5.30	5.32	1.49	8.77	4.06	5.68	6.50	3.81	4.28
0.15	0.14	0.15	0.16	0.17	0.16	0.17	0.15	0.19
4.97	8.26	5.68	8.78	5.26	8.32	10.20	5.68	3.27
9.61	9.96	9.75	9.67	9.56	8.25	7.89	10.20	8.08
3.60	2.85	3.22	3.46	3.30	3.61	3.65	3.52	4.03
1.62	1.64	1.66	0.60	1.88	1.18	1.53	1.75	2.46
0.40	0.42	0.64	0.22	0.66	0.43	0.54	0.46	0.58
2.02	1.43	0.39	0.10	0.59	0.14	0.98	0.42	2.08
0.10	0.05	0.07	0.04	0.06	0.07	0.13	0.07	0.33
99.90	100.10	99.70	100.30	99.80	99.70	99.40	99.90	99.70
-	-	-	-	-	-	-	-	-
-	-	-	-	-	-	-	-	-
9.81	9.84	9.86	3.54	11.25	7.03	9.20	10.44	14.94
25.90	22.86	27.21	26.85	27.44	30.68	29.69	26.37	32.13
27.48	28.64	27.99	27.40	26.35	24.16	17.60	24.01	25.53
2.89	0.88	0.24	1.29	0.46	0.06	0.94	2.01	1.58
2.41	2.02	2.31	2.52	2.35	2.46	2.20	2.21	2.12
-	-	-	-	-	-	-	-	-
2.39	2.89	3.57	2.92	3.98	3.54	3.19	2.97	2.15
0.97	1.01	1.54	0.52	1.58	1.03	1.30	1.10	1.41
0.23	0.12	0.16	0.09	0.14	0.16	0.30	0.16	0.77
14.93	14.89	13.45	15.29	13.91	11.22	14.34	19.35	8.03
-	-	-	-	-	-	-	-	-
13.01	16.89	13.61	19.61	12.59	19.70	21.27	11.40	11.39
66.07	62.22	65.39	59.07	65.49	61.92	57.43	62.84	74.17
33.95	37.81	34.64	40.94	34.55	38.10	42.60	37.19	25.86
38.60	33.58	37.41	31.67	39.14	37.77	39.83	38.82	48.64
65	260	110	306	103	293	446	115	18
34	32	36	45	35	40	39	35	28
33	125	38	146	49	145	282	51	12
150	46	37	67	48	50	56	58	187
86	77	92	87	85	88	100	87	94
43	63	50	11	56	21	36	52	56
657	639	823	346	822	513	653	588	703
28	27	32	27	30	30	28	31	36
119	165	214	124	215	190	252	216	165
11	17	18	8	21	14	51	24	17
423	335	803	141	856	304	583	569	527
10	17	23	6	20	12	50	24	27
51	46	68	25	66	38	102	72	76
8	4	7	2	4	6	7	5	12
5	3	6	<1	2	<1	12	6	8
0.45	0.58	0.52	0.17	0.57	0.33	0.42	0.50	0.61
1.98	1.01	1.69	1.21	1.86	1.23	0.89	1.63	2.66
312	216	276	55	279	466	353	279	364
20	21	17	14	19	19	19	25	29
32	41	17	35	18	32	22	25	39
105	143	85	200	83	115	86	124	82
0.07	0.10	0.06	0.03	0.07	0.04	0.04	0.09	0.08
0.64	0.52	0.98	0.41	1.04	0.59	0.89	0.97	0.75
9.84	5.32	16.10	12.80	15.30	14.50	16.20	10.90	9.41
0.97	3.91	1.06	3.24	1.40	3.63	7.23	1.46	0.43

Hawaiites

Tab. I 8

	NT 52	NT 46	NH 22	NT 60	U 46	R 19
SiO_2	48.6	49.4	49.6	49.8	50.0	50.2
TiO_2	2.09	2.09	1.60	1.89	1.85	1.38
Al_2O_3	16.6	17.4	16.6	16.4	16.3	16.3
Fe_2O_3	7.00	9.42	1.80	7.73	3.69	6.55
FeO	4.95	1.16	8.37	3.75	6.76	2.76
MnO	0.17	0.16	0.16	0.17	0.17	0.15
MgO	6.77	3.94	7.82	6.87	6.39	8.58
CaO	8.30	9.13	9.67	8.45	9.76	9.32
Na_2O	3.71	3.32	3.45	3.34	3.22	3.34
K_2O	0.95	1.90	0.71	0.93	1.16	0.92
P_2O_5	0.47	0.73	0.27	0.39	0.39	0.31
H_2O^+	0.60	0.97	0.18	0.68	0.41	0.29
CO_2	0.09	0.06	0.08	0.04	0.05	0.03
Σ	100.30	99.70	100.30	100.40	100.20	100.10
Q	-	-	-	-	-	-
C	-	-	-	-	-	-
OR	5.66	11.47	4.19	5.54	6.89	5.47
AB	31.65	28.69	29.16	28.50	27.37	28.45
AN	26.05	27.53	27.68	27.24	26.72	26.95
NE	-	-	-	-	-	-
MT	2.73	2.38	2.40	2.60	2.45	2.10
HM	-	-	-	-	-	-
IL	4.00	4.05	3.04	3.62	3.53	2.64
AP	1.12	1.77	0.64	0.93	0.93	0.74
CC	0.21	0.14	0.18	0.09	0.11	0.07
DI	9.68	11.17	14.64	10.00	15.60	14.05
HY	1.70	6.08	1.78	12.25	6.70	4.94
OL	17.23	6.77	16.31	9.26	9.73	14.60
Salic.	63.36	67.69	61.03	61.28	60.98	60.87
Femic.	36.67	32.36	38.98	38.75	39.04	39.15
Diff.-I.	37.31	40.15	33.35	34.04	34.26	33.93
Cr	186	81	255	229	170	359
Co	44	34	41	45	38	35
Ni	103	34	95	118	66	110
Cu	34	41	55	46	68	37
Zn	102	96	87	109	99	77
Rb	12	47	14	15	29	17
Sr	467	854	381	455	499	454
Y	35	31	29	33	33	26
Zr	196	234	144	181	166	142
Nb	12	23	9	11	15	10
Ba	294	740	189	283	324	260
La	12	16	5	11	18	-
Ce	47	76	25	34	50	-
Pb	5	5	2	4	5	2
Th	<1	4	<1	<1	3	<1
K_2O/Na_2O	0.26	0.57	0.21	0.28	0.36	0.28
$FeO+Fe_2O_3/MgO$	1.69	2.49	1.30	1.59	1.60	1.03
K/Rb	658	336	421	513	331	447
K/Sr	17	19	15	17	19	17
K/Ba	27	21	32	27	30	29
Ca/Sr	127	79	181	133	140	147
Rb/Sr	0.03	0.06	0.04	0.03	0.06	0.04
Ba/Sr	0.63	0.87	0.50	0.62	0.65	0.57
Ba/Rb	24.50	15.80	13.50	18.90	11.20	15.30
Ni/Co	2.34	1.00	2.32	2.62	1.74	3.14

Tab. I 8

NH 11	NH 12	NT 28	NT 42	NH 10	NH 17	NH 14	U 33
50.6	50.6	50.6	50.6	50.7	50.7	50.8	50.8
1.46	1.49	1.64	1.80	1.49	1.58	1.50	1.57
16.2	15.9	15.7	15.4	16.3	16.4	16.0	16.2
2.70	3.16	2.99	6.11	2.18	5.24	3.16	3.29
6.55	6.13	6.76	3.18	7.04	3.85	5.95	5.66
0.15	0.15	0.16	0.16	0.15	0.15	0.15	0.14
8.03	8.38	8.52	5.65	8.01	7.33	8.34	7.30
9.57	9.20	8.16	9.31	9.66	9.21	8.95	9.30
3.31	3.41	3.50	3.21	3.38	3.53	3.43	3.58
1.02	1.09	1.25	2.08	1.01	1.12	1.16	1.17
0.28	0.35	0.38	0.65	0.29	0.41	0.33	0.42
0.14	0.13	0.41	1.49	0.07	0.49	0.41	0.48
0.06	0.15	0.11	0.25	0.05	0.10	0.05	0.07
100.10	100.10	100.20	99.90	1oo.30	100.10	100.20	100.00
-	-	-	-	-	-	-	-
-	-	-	-	-	-	-	-
6.04	6.45	7.41	12.55	5.96	6.67	6.88	6.96
28.06	28.90	29.73	27.74	28.55	30.10	29.30	30.50
26.38	24.90	23.52	21.92	26.27	25.79	24.92	24.85
-	-	-	-	-	-	-	-
2.18	2.16	2.29	2.13	2.17	2.09	2.12	2.10
-	-	-	-	-	-	-	-
2.78	2.83	3.13	3.49	2.82	3.02	2.86	3.00
0.66	0.83	0.90	1.57	0.69	0.98	0.78	1.00
0.14	0.34	0.25	0.58	0.11	0.23	0.11	0.16
15.39	14.24	11.28	15.77	15.70	13.72	13.89	14.93
5.58	5.51	7.22	8.16	4.13	6.18	5.74	4.49
12.81	13.85	14.29	6.12	13.62	11.24	13.58	12.02
60.48	60.25	60.66	62.21	60.78	62.56	60.93	62.32
39.53	39.77	39.36	37.83	39.24	37.46	39.09	37.71
34.10	35.35	37.14	40.29	34.50	36.77	36.00	37.47
293	327	361	348	286	253	341	242
35	34	37	34	35	33	35	34
106	128	156	161	99	74	126	75
50	47	49	56	45	35	49	34
78	76	87	82	77	88	83	88
20	21	27	60	19	23	22	24
470	500	471	1278	468	523	507	527
26	26	27	29	26	29	24	30
139	146	161	229	140	194	150	195
9	10	13	17	10	12	12	12
302	302	304	1338	284	322	330	277
9	10	11	16	12	12	15	17
33	37	37	62	34	47	44	47
5	4	6	2	4	5	3	7
1	2	1	<1	<1	3	<1	3
0.31	0.32	0.36	0.65	0.30	0.32	0.34	0.33
1.14	1.09	1.13	1.56	1.14	1.19	1.07	1.20
425	429	385	288	526	404	436	404
18	18	22	14	18	18	19	18
28	30	34	13	30	29	29	35
146	132	124	52	147	126	126	126
0.04	0.04	0.06	0.05	0.04	0.04	0.04	0.05
0.64	0.60	0.65	1.05	0.61	0.62	0.65	0.53
15.10	14.40	11.30	22.30	15.00	14.00	15.00	11.50
3.03	3.77	4.22	4.74	2.83	2.24	3.60	2.21

Tab. I 8

NT 58	U 19	NT 65	U 23	NT 53	NE 20	NE 3	NT 13
51.0	51.4	51.6	51.7	52.1	52.2	52.4	52.8
1.48	1.27	1.30	1.21	1.41	1.36	0.90	1.09
16.4	15.7	16.0	16.8	16.9	16.5	16.1	16.2
5.24	2.30	2.04	3.13	5.38	3.58	2.90	1.48
3.82	6.20	6.29	5.91	23.17	4.01	5.02	5.94
0.15	0.14	0.15	0.15	0.14	0.14	0.13	0.13
7.98	8.29	8.48	7.55	6.59	6.03	8.94	8.58
9.00	9.43	8.57	8.81	8.45	7.80	8.96	8.45
3.55	3.08	3.47	3.40	3.68	3.41	3.39	3.10
1.09	1.21	1.45	0.93	1.25	3.24	1.10	1.65
0.38	0.40	0.38	0.21	0.39	0.58	0.20	0.40
0.16	0.20	0.37	0.42	0.37	0.77	0.29	0.33
0.10	0.05	0.04	0.04	0.06	0.08	0.05	0.19
100.30	99.70	100.10	100.30	100.30	99.70	100.30	100.30
-	-	-	-	-	-	-	-
-	-	-	-	-	-	-	-
6.45	7.19	8.59	5.56	7.42	19.40	6.50	9.75
30.10	26.22	29.45	29.12	31.29	29.24	28.69	26.24
25.64	25.60	23.87	28.17	26.03	20.41	25.47	25.42
-	-	-	-	-	-	-	-
2.06	2.01	1.96	1.92	2.04	1.76	1.84	1.76
-	-	-	-	-	-	-	-
2.82	2.43	2.48	2.33	2.69	2.62	1.71	2.07
0.90	0.95	0.90	0.50	0.93	1.39	0.47	0.95
0.23	0.11	0.09	0.09	0.14	0.18	0.11	0.43
12.93	14.98	12.95	11.68	10.75	11.73	14.00	10.22
6.32	12.60	6.82	14.49	12.22	0.96	10.70	17.85
12.56	7.92	12.91	6.15	6.57	12.34	10.51	5.33
62.19	59.01	61.92	62.85	64.73	69.05	60.66	61.41
37.83	41.01	38.11	37.16	35.29	30.98	39.36	38.61
36.55	33.42	38.04	34.68	38.71	48.64	35.19	35.99
240	325	347	220	150	242	309	378
35	33	30	33	32	24	32	29
110	113	209	85	82	102	142	163
36	54	62	30	39	46	56	55
82	79		83	92	85	74	73
20	27		20	22	96	18	35
508	566		372	577	906	521	595
27	24		27	30	34	21	25
171	138		137	171	325	89	177
14	11		137	9	38	4	10
341	387		269	384	1384	438	598
13	24		11	16	48	9	25
43	56		36	51	126	29	70
4	6		3	7	12	7	8
1	3		1	4	15	2	9
0.31	0.39	0.42	0.27	0.34	0.95	0.32	0.53
1.09	1.02	0.97	1.06	1.30	1.22	0.87	0.86
488	370		385	473	280	506	391
18	18		21	18	30	17	23
26	26		29	27	19	21	23
127	119		169	105	61	123	102
0.04	0.05		0.05	0.04	0.11	0.04	0.06
0.67	0.68		0.72	0.67	1.53	0.84	1.01
17.10	14.30		13.50	17.50	14.40	24.30	17.10
3.14	3.42	6.97	2.58	2.56	4.25	4.44	5.62

Tab. I 9

Tholeiites

	NT 31	U 13	U 78
SiO_2	52.2	52.3	53.5
TiO_2	1.37	1.37	0.84
Al_2O_3	16.9	16.8	13.1
Fe_2O_3	3.75	4.77	9.48
FeO	4.47	4.05	1.45
MnO	0.14	0.14	0.19
MgO	5.33	6.35	5.32
CaO	9.56	8.66	6.42
Na_2O	3.60	3.27	3.93
K_2O	1.17	1.15	0.30
P_2O_5	0.33	0.36	0.19
H_2O^+	0.37	0.60	2.82
CO_2	0.98	0.08	2.94
Σ	100.20	99.90	100.30
Q	0.51	2.26	12.72
C	-	-	1.87
OR	6.94	6.87	1.74
AB	30.60	27.86	32.68
AN	26.62	28.06	11.82
NE	-	-	-
MT	1.91	2.04	10.17
HM	-	-	-
IL	2.61	2.63	1.57
AP	0.79	0.86	0.44
CC	2.24	0.18	6.57
DI	10.33	10.16	-
HY	17.49	21.02	20.43
OL	-	-	-
Salic.	64.66	63.13	60.83
Femic.	35.36	36.89	39.19
Diff.-I.	38.05	35.08	47.14
Cr	86	158	235
Co	26	31	40
Ni	44	81	112
Cu	35	37	150
Zn	82	90	77
Rb	21	20	6
Sr	593	559	577
Y	27	29	17
Zr	160	163	47
Nb	8	9	10
Ba	444	325	113
La	13	21	7
Ce	43	53	23
Pb	4	6	8
Th	<1	2	2
K_2O/Na_2O	0.32	0.35	0.08
$FeO+Fe_2O_3/MgO$	1.50	1.34	2.82
K/Rb	462	475	313
K/Sr	16	17	4
K/Ba	22	29	22
Ca/Sr	115	111	80
Rb/Sr	0.04	0.04	0.01
Ba/Sr	0.75	0.58	0.20
Ba/Rb	21.10	16.30	18.80
Ni/Co	1.69	2.61	2.80

Differentiate

Tab. I 10

	LV 2	U 11	U 64	U 61	LV 1
SiO_2	47.9	48.5	48.5	49.3	50.6
TiO_2	1.05	1.08	1.13	1.04	1.24
Al_2O_3	16.6	15.3	18.6	18.4	17.0
Fe_2O_3	2.56	7.69	5.45	6.89	4.56
FeO	5.92	1.18	3.73	1.85	4.50
MnO	0.21	0.28	0.15	0.16	0.19
MgO	2.73	1.45	2.83	2.16	2.77
CaO	8.87	9.39	9.28	11.50	7.27
Na_2O	2.93	3.85	3.13	3.44	3.56
K_2O	2.37	1.65	2.44	0.75	2.75
P_2O_5	0.55	0.63	0.61	0.32	0.64
H_2O^+	3.12	2.03	2.30	0.98	1.30
CO_2	4.28	6.70	1.39	3.05	2.68
Σ	99.10	99.70	99.50	99.80	99.10
Q	7.55	13.29	-	3.98	4.08
C	4.51	7.35	-	-	2.76
OR	14.61	10.05	14.89	4.51	16.68
AB	25.87	33.56	27.35	29.61	30.91
AN	13.93	0.12	30.46	33.11	15.34
NE	-	-	-	-	-
MT	2.07	2.02	2.16	1.98	2.13
HM	-	-	-	-	-
IL	2.08	2.11	2.22	2.01	2.42
AP	1.36	1.54	1.49	0.77	1.56
CC	10.16	15.70	3.26	7.06	6.25
DI	-	-	3.27	2.69	-
HY	17.90	14.31	9.87	14.34	17.92
OL	-	-	5.07	-	-
Salic.	66.46	64.37	72.70	71.18	69.76
Femic.	33.57	35.67	27.34	28.84	30.28
Diff.-I.	48.02	56.90	42.24	38.07	51.66
Cr	19	11	19	26	13
Co	26	25	30	32	28
Ni	10	6	12	18	5
Cu	173	44	194	28	116
Zn	105	100	107	101	120
Rb	52	44	68	10	72
Sr	691	367	660	754	623
Y	34	37	38	27	38
Zr	156	234	187	78	218
Nb	16	18	19	11	19
Ba	675	78	620	404	746
La	27	23	22	9	37
Ce	71	78	84	41	95
Pb	13	9	14	10	22
Th	10	8	11	3	11
K_2O/Na_2O	0.81	0.43	0.78	0.22	0.77
$FeO+Fe_2O_3/Mg$	3.06	5.68	3.10	3.79	3.16
K/Rb	379	311	299	620	317
K/Sr	29	37	31	8	37
K/Ba	29	176	33	15	31
Ca/Sr	92	183	100	109	83
Rb/Sr	0.08	0.12	0.10	0.01	0.12
Ba/Sr	0.98	0.21	0.94	0.54	1.20
Ba/Rb	13.00	1.77	9.12	40.40	10.40
Ni/Co	0.39	0.24	0.40	0.56	0.18

Table II: Bulk and trace element chemistry of the superacid rocks ("Silexite" Miller, 1919).

	GBA8A	GBA8B	GBA9	GBA10	GBA11	GBA12A	GBA12B	GBA17	GBA20
SiO_2	96.87	97.46	95.98	96.51	96.34	96.93	94.65	93.99	96.78
TiO_2	1.06	1.18	1.73	1.89	1.11	1.90	1.85	1.28	1.27
Al_2O_3	0.38	0.41	0.19	0.25	0.22	0.17	0.17	1.36	0.13
Fe_2O_3(T)	0.03	0.03	0.86	0.05	0.08	0.05	0.05	2.03	0.04
MnO	<0.01	<0.01	<0.01	<0.01	<0.01		0.01		
MgO	0.36	0.26	0.40	0.29	0.36	0.43	0.23	0.23	0.45
CaO	0.03	0.03	0.02	0.04	0.03	0.03	0.02	0.04	0.02
Na_2O	<0.01	<0.01	0.01	0.02	<0.01	<0.01	0.02	0.02	<0.01
K_2O	<0.01	0.02	<0.01	0.01	0.01	<0.01	<0.01	0.02	0.01
P_2O_5	0.02	0.02	<0.01	<0.01		<0.01	<0.01	0.08	<0.01
Cr_2O_3	0.02	0.02	0.04	0.01	0.02	<0.01	0.03	0.03	
NiO	<0.01	0.02	0.02	<0.01	0.01	0.02	0.02	0.02	0.02
L.O.I.	0.30	0.31	0.34	0.32	0.27	0.40	0.33	1.20	0.49
H_2O^-	0.03	0.03	0.06	0.04	0.03	0.04	0.09	0.10	0.05
Summe	99.14	99.81	99.68	99.46	98.50	100.01	97.49	100.40	99.28

	GBA29	GBA30	GBA31	GBA33A	GBA33B	GBA36	GBA38	GBA39	GBA40
SiO_2	97.67	96.16	97.32	97.03	96.52	96.81	95.81	94.93	96.30
TiO_2	1.06	2.15	0.78	0.87	1.45	1.15	1.34	1.12	1.15
Al_2O_3	0.22	0.22	0.26	0.08	0.10	0.23	0.29	0.56	0.30
Fe_2O_3(T)	0.05	0.20	0.11	0.47	0.61	0.10	0.23	0.28	0.25
MnO		<0.01	<0.01		<0.01	<0.01			
MgO	0.39	0.44	0.41	0.31	0.28	0.30	0.29	0.17	0.28
CaO	0.03	0.05	0.04	0.01	0.02	0.02	0.02	<0.01	0.02
Na_2O	<0.01	<0.01	<0.01	0.01	<0.01	<0.01	<0.01	<0.01	<0.01
K_2O	0.02	0.02	0.02	0.01	0.01	0.01	0.01	<0.01	0.02
P_2O_5		<0.01	0.03	<0.01	<0.01	0.01	0.01	<0.01	<0.01
Cr_2O_3	0.03	0.06	0.01		0.01	0.04	0.01		<0.01
NiO	0.02	0.02	0.02	0.02	<0.01	0.01	<0.01	0.02	0.02
L.O.I.	0.36	0.34	0.36	0.35	0.26	0.51	0.29	0.26	0.21
H_2O^-	0.03	0.04	0.05	0.05	0.03	0.05	0.02	0.05	0.03
Summe	99.89	99.73	99.43	99.22	99.33	99.26	98.34	97.43	98.61

Tab. II (contd.)

	GBA41	GBA42	GBA43	GBA44	GB45	GBA47	GBA50
SiO_2	91.34	95.18	97.11	97.63	96.28	95.94	96.56
TiO_2	1.69	1.01	1.03	1.26	1.25	1.22	1.06
Al_2O_3	0.19	0.17	0.08	0.22	0.19	0.62	0.32
Fe_2O_3(T)	5.16	0.52	0.19	0.08	0.33	0.13	0.10
MnO	0.02			<0.01			
MgO	0.27	0.22	0.37	0.25	0.24	0.31	0.32
CaO	0.03	0.02	0.02	0.02	<0.01	0.02	0.01
Na_2O	<0.01	0.01	<0.01	0.01	0.01	0.02	<0.01
K_2O	0.01	0.02	<0.01	<0.01	0.01	0.01	0.02
P_2O_5	<0.01	<0.01	<0.01			0.03	
Cr_2O_3	0.04			0.03	0.03	<0.01	0.01
NiO	0.02	<0.01	0.02	0.02	0.01	<0.01	0.02
L.O.I.	0.77	0.41	0.31	0.23	0.18	0.57	0.47
H_2O^-	0.06	0.07	0.04	0.05	0.04	0.05	0.03
Summe	99.62	97.65	99.20	99.82	98.58	98.94	98.93

GBA	8A	8B	9	10	11	12A	12B	17	20	29	30	31	33A	33B	36	38	39	40	41	42	43	44	45	47	50
Co			3					1					1	4	1				7					1	
Cr			3					4			20			7		5			8			1	2	4	
V	15	16	19	11	7	8	9	70	15	18	21		5	10	27	43	36	28	25	25	14	5	4	29	12
La	1	1					2	13				1	1		1						1.	1			
Ce		2						18			1	1						1							
Nd		1						4		1															

Table III: Geochemical characteristics of some rock types and their distribution in time and space. Tab. III 1

	Rhyolites		Dacites	Dacites Shoshonitic trend
	Cerro Derrumbadas (n=4)	Cerro Pinto (n=4)	(n=7)	(n=2)
SiO_2	70.8 - 75.2 (73.2)	73.9 - 74.8 (74.4)	63.1 - 65.0 (63.9)	63.7 - 67.5 (65.6)
Al_2O_3	14.3 - 15.7 (15.0)	14.0 - 14.2 (14.1)	15.7 - 17.1 (16.6)	15.5 - 17.6 (16.6)
TiO_2	0.07 - 0.15 (0.11)	0.03 - 0.04 (0.04)	0.40 - 0.80 (0.61)	0.77 - 1.02 (0.90)
MgO	0.12 - 0.28 (0.21)	0.07 - 0.09 (0.08)	0.78 - 2.25 (2.04)	0.56 - 0.71 (0.64)
CaO	0.92 - 1.81 (1.36)	0.48 - 0.51 (0.49)	3.74 - 5.86 (4.93)	1.67 - 2.45 (2.06)
K_2O	3.40 - 3.87 (3.64)	4.09 - 4.16 (4.12)	1.3 - 3.08 (2.03)	5.07 - 5.56 (5.32)
Rb	100 - 115 (107)	188 - 194 (191)	16 - 94 (45)	128 - 192 (160)
Sr	138 - 275 (206)	21 - 22 (22)	363 - 1125 (728)	168 - 414 (291)
	270 - 275+ (273) (n=2)			
Zr	81 - 157 (117)	67 - 68 (68)	54 - 224 (110)	591 - 631 (611)
	150 - 157+ (154)			
Ba	770 - 898 (861)	30 - 50 (41)	409 - 1641 (733)	708 - 1101 (905)
Ce	40 - 75 (57)	10 - 16 (12)	30 - 66 (48) (n=5)	116 - 145 (131)
K/Rb	279 - 288 (284)	177 - 184 (180)	272 - 675 (464)	241 - 329 (285)
K/Sr	104 - 228 (167)	1545 -1643 (1594)	10 - 71 (29)	102 - 275 (189)
Rb/Sr	0.36 - 0.82 (0.59)	8.37 - 9.00 (8.88)	0.01 - 0.26 (0.08)	0.31 - 1.14 (0.73)

+) pyroclastic deposits

Tab. III 2

	Monogenetic cone andesites		
	Basin of Oriental (n=8)	Cofre-Pico range (n=7)	Naolinco-Jalapa (n=8)
SiO_2	55.9 - 57.4 (56.7)	56.7 - 58.1 (57.4)	55.8 - 57.3 (56.7)
Al_2O_3	15.7 - 17.5 (16.4)	16.1 - 17.1 (16.5)	16.4 - 17.0 (16.7)
TiO_2	0.84 - 1.35 (1.00)	0.84 - 1.03 (0.94)	0.97 - 1.14 (1.04)
MgO	4.39 - 6.14 (5.43)	3.96 - 6.19 (4.99)	4.36 - 5.88 (5.11)
CaO	6.57 - 8.41 (7.54)	6.68 - 7.69 (7.26)	6.90 - 7.68 (7.19)
K_2O	1.37 - 1.77 (1.62)	1.49 - 2.40 (1.71)	1.46 - 1.80 (1.65)
Rb	20 - 41 (30)	22 - 74 (38)	32 - 47 (40)
Sr	428 - 869 (643)	496 - 668 (564)	484 - 582 (516)
Zr	91 - 204 (134)	100 - 207 (145)	147 - 185 (164)
Ba	325 - 658 (464)	390 - 598 (492) (n=6)	456 - 526 (491)
Ce	31 - 72 (46)	44 - 67 (54) (n=5)	45 - 76 (57)
K/Rb	327 - 626 (475)	269 - 670 (429)	304 - 378 (345)
K/Sr	16 - 31 (22)	20 - 40 (26)	21 - 29 (27)
Rb/Sr	0.03 - 0.10 (0.05)	0.03 - 0.15 (0.07)	0.06 - 0.10 (0.08)

Tab. III 3

Basaltic andesites

	Basin of Oriental Mean MgO (n=10)	High MgO (n=2)	Naolinco-Jalapa (n=10)	Palma Sola Low MgO (n=4)
SiO_2	53.4 - 55.6 (54.4)	53.3 - 53.7 (53.5)	52.0 - 55.6 (53.5)	52.6 - 54.4 (53.2)
Al_2O_3	15.2 - 18.1 (16.9)	15.7 (15.7)	15.7 - 19.1 (17.4)	15.9 - 17.9 (17.3)
TiO_2	0.79 - 1.48 (1.13)	0.97 (0.97)	1.13 - 1.55 (1.33)	1.92 - 2.16 (2.03)
MgO	4.66 - 7.51 (6.29)	8.69 - 9.01 (8.85)	3.25 - 6.69 (4.89)	2.60 - 3.15 (2.84)
CaO	7.01 - 10.00 (8.02)	8.71 - 8.81 (8.76)	7.15 - 8.91 (8.02)	6.15 - 6.64 (6.36)
K_2O	0.80 - 1.62 (1.34)	1.12 - 1.14 (1.13)	0.95 - 1.97 (1.48)	2.46 - 2.94 (2.60)
Rb	13 - 39 (31) (n=9)	18 (18)	18 - 52 (31)	66 - 100 (78)
Sr	447 - 742 (528) (n=9)	666 - 673 (670)	331 - 700 (525)	403 - 847 (716)
Zr	51 - 185 (156) (n=9)	93 - 94 (94)	144 - 202 (179)	290 - 538 (355)
Ba	279 - 557 (408)	279 - 287 (283)	273 - 529 (444)	778 - 861 (823)
Ce	25 - 62 (44)	31 - 34 (33)	35 - 67 (54)	101 - 152 (125)
K/Rb	314 - 508 (386) (n=9)	517 - 528 (523)	315 - 555 (419)	244 - 309 (281)
K/Sr	9 - 26 (22) (n=9)	14 (14)	16 - 35 (24)	24 - 61 (34)
Rb/Sr	0.05 - 0.07 (0.06) (n=8)	0.03 (0.03)	0.03 - 0.11 (0.06)	0.08 - 0.25 (0.13)

Tab. III 4

	Stratovolcano andesites	
	Basin of Oriental (n=3)	Cofre-Pico range (n=20)
SiO_2	59.8 - 60.6 (60.2)	59.0 - 62.7 (61.0)
Al_2O_3	17.8 - 18.1 (18.0)	16.1 - 18.2 (17.0)
TiO_2	0.76 - 0.85 (0.79)	0.63 - 1.10 (0.82)
MgO	1.78 - 2.82 (2.15)	1.90 - 3.85 (2.96)
CaO	4.81 - 5.90 (5.20)	4.44 - 6.75 (5.54)
K_2O	1.65 - 2.20 (2.01)	1.37 - 3.04 (2.20)
Rb	39 - 57 (51)	25 - 90 (52.6)
Sr	503 - 578 (529)	413 - 945 (564)
Zr	139 - 357 (257)	98 - 357 (174)
Ba	507 - 858 (683) (n=2)	524 - 947 (661) (n=17)
Ce	30 - 72 (51) (n=2)	26 - 81 (47)
K/Rb	316 - 351 (331)	263 - 640 (376)
K/Sr	24 - 36 (32)	17 - 54 (35)
Rb/Sr	0.07 - 0.11 (0.10)	0.03 - 0.20 (0.11)

Tab. III 5

	Basalts		
	Nzolinco-Jalapa	Palma Sola	
		Pliocene	Miocene
	(n=4)	(n=3)	(n=4)
SiO_2	49.5 - 51.9 (50.1)	47.5 - 48.1 (47.9)	46.3 - 48.6 (47.8)
Al_2O_3	16.7 - 17.3 (16.9)	16.1 - 16.5 (16.3)	15.0 - 18.1 (16.5)
TiO_2	1.31 - 1.58 (1.49)	2.15 - 2.28 (2.23)	0.92 - 2.45 (1.38)
MgO	6.62 - 8.16 (7.67)	6.37 - 6.73 (6.61)	3.81 - 6.54 (5.39)
CaO	9.24 - 9.94 (9.72)	9.78 - 10.50 (10.23)	9.89 - 13.10 (11.37)
K_2O	0.58 - 0.88 (0.69)	0.88 - 1.07 (1.00)	0.76 - 1,41 (1.06)
Rb	11 - 17 (13)	17 - 24 (22)	13 - 32 (21)
Sr	376 - 430 (392)	617 - 638 (626)	606 - 1333 (845)
Zr	136 - 141 (139)	152 - 167 (161)	54 - 114 (82)
Ba	154 - 358 (214)	410 - 580 (488)	298 - 1975 (747)
Ce	26 - 34 (31)	34 - 54 (46)	37 - 82 (51)
K/Rb	429 - 482 (445)	367 - 429 (389)	366 - 692 (465)
K/Sr	12 - 17 (15)	12 - 14 (13)	5 - 15 (12)
Rb/Sr	0.03 - 0.04 (0.04) (n=3)	0.03 - 0.04 (0.04)	0.01 - 0.04 (0.03)

Tab. III 6

	Alkali basalts		
	Basin of Oriental down to Palma Sola	Actopan	
	Holo-/Young Pleistocene (n=5)	Oldest Pleistocene (n=6)	Pliocene (n=3)
SiO_2	46.3 - 50.0 (48.2)	43.4 - 48.7 (46.0)	48.7 - 49.4 (49.0)
Al_2O_3	16.0 - 17.0 (16.6)	13.6 - 17.2 (15.7)	14.0 - 17.0 (15.8)
TiO_2	1.50 - 2.65 (1.99)	1.49 - 2.49 (1.91)	1.54 - 2.07 (1.75)
MgO	4.72 - 8.32 (6.91)	4.30 - 10.60 (7.49)	5.26 - 10.20 (8.08)
CaO	8.25 - 10.20 (9.24)	9.67 - 14.30 (11.47)	7.89 - 9.67 (9.04)
K_2O	0.91 - 1.75 (1.38)	0.57 - 2.33 (1.20)	0.60 - 1.88 (1.34)
Rb	11 - 63 (35)	27 - 95 (52) (n=5)	11 - 56 (34)
Sr	494 - 756 (598)	815 - 1071 (911) (n=5)	346 - 822 (607)
Zr	165 - 242 (197)	125 - 214 (181) (n=5)	124 - 252 (197)
Ba	292 - 569 (392)	385 - 1045 (860)	141 - 856 (527)
Ce	38 - 72 (55)	61 - 141 (97)	25 - 102 (64)
K/Rb	216 - 691 (410)	52 - 364 (243) (n=5)	55 - 353 (229)
K/Sr	15 - 25 (20)	4 - 20 (12) (n=5)	14 - 19 (17)
Rb/Sr	0.02 - 0.10 (0.06)	0.03 - 0.11 (0.06) (n=5)	0.03 - 0.07 (0.05)

Tab. III 7

	Alkali basalts	
	Palma Sola	
	Pliocene (n=9)	Miocene (n=8)
SiO_2	44.0 - 47.9 (46.5)	44.6 - 50.2 (46.9)
Al_2O_3	12.6 - 17.1 (15.7)	14.3 - 18.4 (16.1)
TiO_2	2.20 - 2.84 (2.43)	1.09 - 2.80 (1.96)
MgO	4.83 - 9.08 (6.41)	3.27 - 13.40 (7.38)
CaO	9.35 - 11.00 (10.08)	8.08 - 11.90 (9.76)
K_2O	0.81 - 1.48 (1.27)	0.81 - 2.46 (1.43)
Rb	23 - 81 (34)	18 - 56 (27)
Sr	163 - 983 (771)	657 - 798 (725)
Zr	167 - 332 (207)	63 - 198 (149)
Ba	461 - 686 (577)	359 -1048 (504)
Ce	61 - 109 (78)	40 - 76 (63)
K/Rb	83 - 452 (360)	312 - 661 (484)
K/Sr	7 - 17 (12)	10 - 29 (16)
Rb/Sr	0.02 - 0.09 (0.04)	0.02 - 0.08 (0.04)

Tab. III 8

	"Hawaiites" Basin of Oriental (n=7)	Cofre-Pico range (n=2)	Naolinco-Jalapa (n=9)	Actopan Pliocene (n=3)
SiO_2	50.6 - 52.8 (51.2)	50.2 - 52.4 (51.3)	48.6 - 51.7 (50.3)	49.4 - 52.2 (50.7)
Al_2O_3	15.7 - 16.2 (16.0)	16.1 - 16.3 (16.2)	15.7 - 16.8 (16.4)	15.4 - 17.4 (16.4)
TiO_2	1.09 - 1.50 (1.37)	0.90- 1.38 (1.14)	1.21 - 2.09 (1.66)	1.36 - 2.09 (1.75)
MgO	8.01 - 8.58 (8.30)	8.58- 8.94 (8.76)	6.39 - 8.52 (7.39)	5.65 - 6.77 (6.15)
CaO	8.45 - 9.66 (9.12)	8.96- 9.32 (9.14)	8.16 - 9.76 (8.96)	7.80 - 9.31 (8.75)
K_2O	1.01 - 1.65 (1.23)	0.92- 1.10 (1.01)	0.71 - 1.25 (1.03)	1.90 - 3.24 (2.41)
Rb	19 - 35 (24) (n=6)	17 - 18 (18)	12 - 29 (20)	47 - 96 (68)
Sr	468 - 595 (518) "	454 - 521 (488)	372 - 527 (467)	854 -1278 (1013)
Zr	138 - 177 (148) "	89 - 142 (116)	137 - 196 (172)	229 - 325 (263)
Ba	284 - 598 (367) "	260 - 438 (349)	269 - 341 (289)	384 -1338 (821)
Ce	33 - 70 (46) "	29 (n=1)	25 - 50 (39)	62 - 126 (88)
K/Rb	370 - 526 (430) "	447 - 506 (477)	331 - 658 (453)	280 - 336 (301)
K/Sr	18 - 23 (19) "	17 (17)	15 - 22 (18)	14 - 30 (21)
Rb/Sr	0.04 - 0.06 (0.05) (n=6)	0.04 (0.04)	0.03 - 0.06 (0.04)	0.05 - 0.11 (0.07)

Tab. III 9

	Tholeiites Palma Sola (n=2)
SiO_2	52.2 - 52.3 (52.3)
Al_2O_3	16.8 - 16.9 (16.9)
TiO_2	1.37 (1.37)
MgO	5.33 - 6.35 (5.84)
CaO	8.66 - 9.56 (9.11)
K_2O	1.15 - 1.17 (1.16)
Rb	20 - 21 (21)
Sr	559 - 593 (576)
Zr	160 - 163 (162)
Ba	325 - 444 (385)
Ce	43 - 53 (48)
K/Rb	462 - 475 (469)
K/Sr	16 - 17 (17)
Rb/Sr	0.04 (0.04)

This region has been studied recently by numerous authors (Robin, 1976, 1981, 1982; Robin *et al.*, 1982, 1983; Robin and Nicolas, 1978; Robin and Tournon, 1978; Robin and Cantagrel, 1976; Cantagrel and Robin, 1979; Yáñez García and García Durán, 1982; Demant, 1981; Negendank *et al.*, 1982a; Ferriz and Mahood, 1984; Verma and López, 1982; Mooser and Soto, 1980). However, it is the credit of Robin (1981) to have revealed the first model for understanding the history of this complicated region.

Today this region is of economic interest too as geothermal reservoir, therefore a detailed geological history of the caldera "Los Humeros" was written additionally to Demant (1981) and Robin (1981) by Verma and López (1982) and Ferriz and Mahood (1984).

In our study we have excluded this area, investigating only the El Limón lavas.

On the other hand, the evolution of the grand volcano Pico de Orizaba was reported by Robin (1981, 1982), Robin and Cantagrel (1982), Robin *et al.* (1983).

The Altiplano Area and the Pico de Orizaba - Cofre de Perote Massif (Figs. 2, 4).

This area is characterized by basaltic, andesitic and rhyolitic volcanism, stratovolcanoes and domes rising above Cretaceous NW-SE folded mountain ranges and numerous monogenetic cones and maars mostly lying inside flat undrained basins. The Lower and Upper Cretaceous limestones have been subdivided in different "Formaciones" and described by Yáñez García and García Durán (1982).

1) Cofre de Perote-Pico de Orizaba-Range

This mountain range is formed by two major stratovolcanoes, the Pleistocene Cofre de Perote (4 200 m) and the Pleistocene Pico de Orizaba (5 700 m) on its northern and southern extremes, respectively, the northern one being partly eroded. Yáñez García and García Durán (1982) have reported an age of 1.7 (1.9) m.y. for lavas east of the pueblo Perote situated at the base of the W-flank of this volcano, so that the beginning of the volcanic activity may be placed in Pliocene times.

Older Pleistocene volcanic elements are from N to S a central caldera complex including Cerro Desconocido (3 120 m), Cerro Tecomales (3 500 m) and Cerro de las

Cumbres (3 940 m), another caldera however smaller and younger with a central dome structure.

This volcanic range is basically of andesitic-dacitic character. Elevations above 3 600 m seems to be affected by glacial erosion. Most obvious results of glacial activity are cirques and moraines around the summit areas of Cerro de las Cumbres and Cofre de Perote. A SW oriented cirque and U-shaped valley is cut into Cofre de Perote. The summit area of Cofre de Perote is defined by a major escarpment on its eastern flank, forming a caldera-like structure of possible volcano-tectonic origin.

The results of glacial activity are overprinted by volcanic events especially concerning the young history of Pico de Orizaba, reported by Robin (1981), Robin and Cantagrel (1982) and Robin *et al.* (1983) (Fig. 4a).

The base of the volcanic system of Cofre de Perote is dated by Cantagrel and Robin (1979) with 1.57 ± 0.05 m.y. (lavas E of Jalapa) whereas Yáñez García and García Durán (1982) give two dates, 1.7 and 1.9 m.y. for lavas east of pueblo Perote (Fig. 4 a). If we consider the additional radiometric data from Cantagrel and Robin (1979) for samples north of Perote (Fig. 2, possibly sample location around U 21) this may be interpreted as discrepancy. Palaeomagnetic dates from Böhnel and Negendank (1981) and Böhnel (1985) show a normal magnetic character for the rocks of Cofre de Perote erupted during the Bruhnes epoch, that means the volcanism is younger than 0.72 m.y. which is in coincidence with the dates of Cantagrel and Robin (1979). However, in this complex are parts which have been erupted presumably during the Matuyama epoch (or Gilbert epoch?) as evidence by their reversed magnetic character (e.g. Microondas NT 27).

Rocks of Cofre de Perote complex are andesites with dacites (Fig. 2, NT 24, NT 23, CP 2, 3) (Robin 1981, VE 156-161). Location U 21, situated north of Cofre de Perote, shows a lava with High-potassium dacite. Rocks of possibly old Cofre Series, we sampled in locations U 38, 39, NT 61 east of Xico (Figs. 2, 4 a).

South of Cofre de Perote the mountain range is characterized by two large calderas, overtopping andesite-dacite stratovolcanoes. The igneous rocks classify as andesites (Tab. I 4, 5) e.g. N caldera (C1SP), S caldera (C2SP, NT 29, NT 30) (Robin, 1981, p. 91) and caldera series overlying the eastern flank of this range (U 42, U 41, U 40, R 17, R 16, R 15). These rocks seem to be of Old-Middle Pleistocene age (Fig. 4 a)

as the S lying structure of Cerro de las Cumbres (OM 1, OM 2) being dacites and acid andesites. In this region numerous domes are distributed. During Young Pleistocene times the volcanism of this area is characterized by monogenetic cones with small effusive activity (e.g. R 19, lava around Ayahualulco (20 000 - 10 000 years)) or around Guadalupe Victoria (U 19, NH 10, NH 11, NH 12, NH 14) having subalkaline character (hawaiites, Figs. 2, 4a).

Pico de Orizaba and Atlitzin (Sierra Negra, Robin, 1981; Demant, 1981) situated south of the former build up the southern part of this mountain range. Robin (1981), Robin and Cantagrel (1982) and Robin *et al.* (1983) have evolved for the first time a detailed model of the geological history of these two volcanoes.

As it is drawn in Fig. 4 a, Robin (1981) distinguishes three phases of volcanism. The first being contemporaneous with stratovolcanoes mentioned above, the second lasting around 100 000 years and of Young Pleistocene age and the third phase starting around 13 000 years B. P. (Robin and Cantagrel, 1982):

"*1.* The first one, probably discontinuous effusive activity, lasted more than one million years. It is mainly composed of two pyroxenes-andesites with scarce associated basaltic and dacitic lava flows. Amphibole is an accessory mineral in most differentiated lavas. On the eastern flank, numerous massive and autobrecciated lava flows pass outward into thick conglomeratic formations. This effusive phase has built a primitive central volcano and a parasitic cone: the Sierra Negra.

2. The second phase is of short duration - about 100 000 years or less - in comparison with the first period. It seems that this period began with the formation of a caldera followed by the extrusion of amphibole dacite domes and the overflow of viscous silica-rich (andesite to dacite) lava flows on the northern flank. An intense explosive activity develops: pelean nuées ardentes are associated with extrusion of the domes; numerous plinian eruptions leading to widespread dacitic pumiceous air-falls are produced by both the central and the adventive volcanoes. This sequence of events is interpreted as the progressive emptying of a superficial chamber containing differentiated magma. A rhyolite flow erupted during this phase.

3. The age of the recent phase is better defined. It started 13 000 years B.P. with the eruption of a dacitic ash-flow containing pumice and scoria bombs. This was such an intense event that products were found 30 km S.E. of the summit, erasing

the top of the former volcano and creating a large crater (4 -5 km wide). The present cone, of 1 400 - 1 500 m elevation, grew in this crater. During a period of 7 000 to 8 000 years, the new stratovolcano experienced various important pyroclastic eruptions with a cycle of the order of 1 000 to 1 500 years. The pyroclastic flows (ash, pumice, and bombs) associated with airfall deposits are of Saint Vincent type. They present an heterogeneous dacitic and andesitic magma. The dacitic component is similar to previous differentiated materials. On the other hand, the andesitic magma appears somewhat similar to lava flows from morphologically young cones erupted outside the central vent system. This eruptive cycle can be interpreted as the result of reoccurring injections of deep basic magma within the crustal chamber. For the last 5 000 years the activity of the modern Pico de Orizaba has again been essentially effusive (andesites) with periodic plinian eruptions."

For sample locations and their stratigraphic position see Fig. 2 and 4 a. One dyke rock SE of volcano Atlitzin was sampled having a subalkaline composition (NH 3, hawaiite).

The entire mountain range between Cofre de Perote and Pico de Orizaba is covered by pumice strata of varying thickness. They belong to different explosion events. Around Perote this pumice covers the area along two lines N and S Cofre de Perote crossing from W to E the mountain range down to S of Jalapa for instance. In detail studied by Robin (1981), Demant (1981) and Ferriz and Mahood (1984), these pumice layers are caused by the eruption history of Los Humeros Caldera (Fig. 4).

The pumice strata on the western flank of the caldera region are stemming from different sources as it has been shown by Robin (1981, p. 89-106) e.g. Madero, Hidalgo and Tlalnalapa E of Guadalupe Victoria.

The pumice deposits E of Ciudad Serdán belong to the volcanoes Atlitzin and Pico de Orizaba and were traced in detail by Robin (1981), Robin *et al.* (1983).

2). The Altiplano-Area (= Basin of Oriental)

This drainageless basin is characterized by numerous volcanic eruption centers and associated lava flows. It is also structured in small basin areas by a network of occa-

sional outcrops of NW-SE-striking and folded Lower and Upper Cretaceous limestones (Laramide folding system). Various Pleistocene-Holocene volcanic complexes with only minor older volcanic elements can be identified from S to N within the basin.

The Young Pleistocene monogenetic cone of Atzizintla, Fig. 2, 4a, (NH 4, NH 5) is situated south of the volcano Atlitzin, and is a basaltic andesite (Tab. I 5).

The Ciudad Serdán area is characterized by numerous monogenetic cones, in parts with lava flows having an age of Young Pleistocene - Holocene (~35 000 B.P. - Recent). S of Ciudad Serdán the 20 - 40 m thick block lava field consists of several eruption centers and is andesitic in character (Fig. 2, 4 a, NT 22, NT 18, NT 19, NT 20). Fig. 4 e gives a detailed map of this area with the time sequence b, c, e, the last being the Holocene part. The lava fields b and c erupted after each other during 30 000 to 20 000 y. B.P.

Robin (1981) concluded after detailed petrological studies, that the andesites of this complex additional to the lava complex SE of it (Fig. 2, 4a, Tab. I 4, NT 21) have to be selected as primary andesitic magma type rock of the Pico de Orizaba evolution.

The distribution of the numerous cones and their age estimation (Young Pleistocene-Holocene) can be read in Fig. 4 c.

In the NW lies the shield volcano of Cerro Malpaís with a south-western cone succession and the maars of Tecuitlapa and San Juan Atenco, which erupted through the older lava flows of the cone alignment of Aljojuca. The most recent lavas of Cerro Malpaís were dammed in the SW by a succession of NE oriented cones and an associated lava flow, in the E by the maar of Tecuitlapa. Three W-E aligned cinder cones and one additional maar formed inside of this maar.

This group of volcanoes erupted during Young Pleistocene and Holocene times (Fig. 2, 4 a, e). The second lava of Cerro Malpaís is of Holocene age, whereas the other eruptions seem to have the following time relations. In Fig. 4 e we can observe the lava b (NH 6, 7, 8) around Aljojuca erupted around ~30 000 years, later on perforated by the maar eruptions of San Juan Atenco and Tecuitlapa followed by the lavas erupted during the time interval b and c with the three W-E aligned cones

having an age of 20 000 - 30 000 years. During this time the 3 cones inside the maar Tecuitlapa and the small maar formed (NH 27, 28, 29, 30).

In a third phase ~10 000 - 20 000 years B.P. (d) the linear SW-NE directed cone association with one maar in the SW built up with a lava prolongated to the south (Fig. 2, 4 a, e, NT 14, U 15, NT 15). The fourth unit, the shield-like volcano of Cerro Malpaís is of Holocene age (e), changing its composition from andesite to basaltic andesite (Fig. 2, 4 a, e, NT 11, NT 17, U 16).

The central part of the Basin of Oriental is dominated by the Cerro Derrumbadas and Cerro Pinto complexes and surrounding edifices. The area is characterized by rhyolitic volcanism, whereas small monogenetic cinder cones are of basaltic (Fig. 2, 4 a, d), (hawaiitic, NT 65 S of Cerro Derrumbadas), basaltic-andesitic (Fig. 2, 4 a, d, N of Cerro Derrumbadas, NH 32), andesitic (Fig. 2, 4 a, d, NE of Cerro Derrumbadas U 18, NT 7) and dacitic (Fig. 3, 4 a, d, NT 1, W of Cerro Derrumbadas) character.

The most recent evidence of volcanism is a highly viscous andesitic lava flow in the E of Cerro Derrumbadas (Fig. 2, 4 a, d, Tab. I 4, NT 7) having Holocene age.

Demant (1981), Robin (1981) and Yáñez García and García Durán (1982) reported upon this volcanism in context with Los Humeros caldera.

Cerro Derrumbadas is a double peaked rhyolitic dome of possibly Middle to Young Pleistocene age (0.32 m.y., Yáñez García and García Durán, 1982), source of a series of ashflows, lahars including the nuée ardente of Merapi type. In Fig. 4 d the sequence of the events can be read.

Samples of the complex Cerro Derrumbadas are located in Fig. 2 (NT 4, NT 2, NT 3, NT 10, NT 5, NT 8 a/b). All other mentioned volcanoes around Cerro Derrumbadas formed during Young Pleistocene times, the single events are marked in Fig. 4 a.

During the same time Cerro Pinto formed as a twin structure. Its northern tuff-ring is characterized by an inner caldera and composed of pumice and obsidian breccia (Fig. 2, 4 a, NT 9). In the S a glassy rhyolitic dome (NH 33) with local pyrite formation arises on a semicircular fracture zone and forms the present summit of Cerro Pinto.

To the S this complex is accompanied by a succession of three maar eruptions. The westernmost is dated > 35 000 y. B.P. (Ohngemach, 1973; Ohngemach and Straka, 1983) and filled with lake sediments from 35 000 y. B.P. to 7 000 - 8 000 y. B.P.

Therefore these maars must have an age older than 35 000 y. B.P. On basis of the study of Tertiary and Quaternary maars of the Eifel region (Germany), we guess that the dry maars must have a minimum age of around 50 000 to 40 000 y. B.P., whereas those with water and a depth of around 50 - 60 m have an age of around 30 000 - 20 000 y. B.P. (Irion and Negendank, 1984; Negendank *et al.*, 1982b), which can be inferred for Laguna Atexcac, Laguna Preciosa, a trilobed morphological structure, the result of three different explosions, and Laguna Quechulac and Laguna Alchichica.

Two exceptions to this rule calculating the age by waterdepth and sedimentload are the lagunas El Hoyo Grande and La Hacienda, E of El Seco, having an age of around 30 000 - 20 000 years B.P.

Various lava fields dominate the northern part of the basin between the Los Humeros caldera and Guadalupe Victoria, the most extensive of which are basaltic andesite lava flows associated with Holocene and Young Pleistocene eruptions in the SE of Los Humeros caldera (Fig. 2, 4a, d, NT 12, NW of El Limón). A late Pleistocene lava flow SE of El Limón (Fig. 2, 4 a, d, NT 13) and lavas along two scoria cones E of Guadalupe Victoria (Fig. 2, 4 a, d, NH 10-14, U 19), are also of hawaiitic character.

The El Limón lavas and the Guadalupe Victoria occurrences have been described in detail by Robin (1981), in parts by Demant (1981). They belong to the alkaline and calcalkaline series of Robin (1981) and Robin and Tournon (1978).

Additionally to the short description of these single but dominating volcanoes, all volcanic features have been analysed photogeologically. In Fig. 4 c all volcanic cones were classified in 4 evolutionary degradation stages measured by the cone height to cone width ratios, the domes as creep-, cumulo- or plug-domes after Emani and Michel (1982), subsurface domes, stratovolcanoes, calderas, tuffrings and maars. One result is that the huge number of volcanic cones of monogenetic origin is of Young Pleistocene - Holocene age (Fig. 2, 4 c), overtopping the Basin of Oriental and the Cofre-Pico mountain range.

If we consider the evolution of the volcanism in the described areas we can summarize that the volcanic products of Oldest, Old and Middle Pleistocene age have calcalkaline character.

Possibly this volcanism started in late Pliocene times if we include the radiometric data of Yáñez García and García Durán (1982) E of Perote.

During Young Pleistocene and Holocene times a second phase of intensive volcanism starts in the area, however, besides calcalkaline products alkaline-subalkaline rocks were erupted. (Fig. 2, 4 a, Tab. I 7, 8, locations NH 3 (SE Atlitzin), NT 65 (S of Cerro Derrumbadas), NT 64 (NE of El Limón), U 19, NH 10-14 (Guadalupe Victoria), R 19 (Ayahualulco).)

Area east of Cofre-Pico range towards the Massif de Palma Sola
(Fig. 3, 4 b)

Fig. 3 in combination with Fig. 4 b gives the regional distribution of the rocks and its ages. The time sequence and evolution of the volcanism in this area originally was described by Robin and Tournon (1978), Cantagrel and Robin (1979), Robin (1976, 1981, 1982). Further investigations were made by Müller (1979) and Mooser and Soto (1980).

In the Massif de Palma Sola a Miocene volcanism (Old Formation of Mooser and Soto, 1980) underlays a Pliocene phase followed by an Old and Young Pliocene to Holocene phase.

This pattern is different to the sequences which can be observed between Naolinco-Jalapa and Actopan. These lavas formed in Oldest Pliocene times followed by a second phase mostly erupted during Young Pleistocene-Holocene times.

The eastern and northeastern slopes of the Cofre de Perote-Pico de Orizaba range are characterized by extensive lava fields with alternating layers of lavas and lahars. These are well defined W of Jalapa towards Actopan and extend to the S as far as Cosautlan (Fig. 3). Lava series are dissected by deep barrancos and expose ignimbritic layers at the base of the volcanic sequence (e.g. ignimbrites near Jacocomulco, south of the River Cohetero SW of Dos Ríos). Often these lavas and pyroclastic deposits (tuffs, lahars) are strongly weathered, especially in the region between Jalapa

and Huatusco. The reversed magnetic character of these lavas (Matuyama epoch, Böhnel and Negendank, 1981) are in accordance with the results of Cantagrel and Robin (1979), suggesting a Pleistocene age, similar to the alkaline-subalkaline lavas around Alto Lucero.

The sequence from Actopan to Jalapa starts with alkali basalts (Fig. 3, 4 b, Tab. I 7, NT 44, 44 R, NT 43, NH 15, NT 48) and basaltic andesites (Fig. 3, 4 b, Tab. I 5, NT 47) overlain by andesites and basaltic andesites (Fig. 3, 4 b, Tab. I 4, 5, NT 49, U 45, NH 16, NT 50).

The lava field immediately around Jalapa (Fig. 3, 4 b, Tab. I 4, U 44, NT 55, NT 54) is of Young Pleistocene age (Bruhnes normal epoch, Böhnel, 1985).

The lava field E of Coatepec (Fig. 2, 4 b, Tab. I 8, 5, 4, U 46, NT 62, NT 52, NT 51) has to be attributed to a Young Pleistocene volcanism being of alkaline character, overtopped by the late Pleistocene to Holocene hawaiitic cone of Coatepec (Fig. 2, 4 b, Tab. I 8, NT 60).

Layers of volcanic rocks extending from Actopan over Alto Lucero to Chiconquiaco belong to the caldera complex, which was studied in detail by Robin and Tournon (1978), Cantagrel and Robin (1979), Robin (1981). The lava units have been dated radiometrically by the mentioned authors and are marked in Fig. 4 b.

The samples NT 45, 46, U 48, 35, NH 21, 20 (Fig. 3, Tab. I 7, 8) W and SE of Alto Lucero represent alkali basalts and hawaiites and seem to belong to the youngest parts of the Chiconquiaco lava system.

The entire area is dotted by Young Pleistocene to Holocene monogenetic volcanic cones (Fig. 3). In addition to these volcanic cones Young Pleistocene to Holocene lava units occur, e.g. of Holocene age (Fig. 2, 3, 4 d) as Las Vigas (NT 26, NT 28), the valley lava (NH 22) and lava W of La Olla Grande (U 22).

Late Young Pleistocene age (~20 000 y. B.P. (Fig. 2, 4 b, d, Tab. I 8)) formed the La Olla Grande volcano (U 23), hawaiitic in composition as lavas NE of Jalapa (Tab. I 8 NH 17, the volcano Naolinco de Victoria with its lava field (Tab. I 5, 57), however, of calcalkaline character (basaltic andesite), and the basalt NE of Jalapa (Tab. I 6, NH 18). The alkali basalt lava field W of Vista Hermosa (Fig. 2, 4 b, Tab. I 7, U

25, 24) erupted contemporaneously with the cones W of Naolinco (Fig. 2, 3, 4 b, Tab. I 5, U 31, 30, 29) composed of basaltic andesites.

If we include the youngest volcanic activity of the Massif de Palma Sola (Upper El Abra Series of Mooser and Soto, 1980), we can realize we have to add alkali basalts with tholeiites (Yoder and Tilley, 1962) (Fig. 3, 4 b, Tab. I 7, 9, U 13, 52, NT 31). However, 8 km SW of Cerro de la Cruz a basaltic andesite lava with 3 cones is distributed (NT 41) named Lower El Abra Series and of Pleistocene age.

In conclusion we summarize that during the Oldest and Old Pleistocene the volcanism is of mainly alkaline character but with calcalkaline portions. This is repeated during the Young Pleistocene to Holocene time in the area from Las Vigas, through Naolinco to Massif de Palma Sola as described above.

1. Massif de Palma Sola

This massif is a complex volcanic structure with volcanism occurring from Miocene to Recent (Robin and Tournon, 1978). Cantagrel and Robin (1979), Robin (1981) as well as Mooser and Soto (1980) published similar and diverging rock ages (Fig. 3, 4 b). The Miocene "Old Formation" is cut by an erosion surface dipping to the east. It is formed by different volcanics including dykes of mostly alkaline composition.

Besides alkali basalts (Fig. 3, 4 b, Tab. I 7, U 67, 75, 74, 7b, 9, 10) basalts (Tab. I U 8), special dyke rocks named differentiates (Fig. 3, 4 b, Tab. I 10, Punta Delgada, LV 1, LV 2, U 11, U 61, U 64), dacite (Tab. I 2, U 58), plutonic rocks are widespread, e.g. gabbros (Fig. 3, 4 b, U 6, 59, 60) and diorites (U 72, 73, 70, NT 36, U 14). These diorites are of calcalkaline character and the diorite in the outcrop south of Villa Candelaria was dated by Mooser and Soto (1980) as 12.3 - 12.9 m.y.

Cantagrel and Robin (1979) report an age of 17.0 ± 0.6 m.y. in the Laguna Verde region. The volcanic group of Espinazo and Hierbabuena, of Young Miocene age, has for example tholeiitic character (Fig. 3, 4 b, Tab. I 9, U 78).

The calcalkaline dacite of Quiahuixtlan (Fig. 3, 4 b, Tab. I 2, U 62) west of Punta Villa Rica, is a tholoid-like structure and was dated radiometrically by Cantagrel and Robin (1979) as 6.5 ± 0.2 m.y. whereas Mooser and Soto (1980) report an age of 7.2 ± 0.2 m.y.

According to the time sequence presented in Fig. 3, 4 b the next younger unit (Mid Pliocene age) is represented by Cerro Azul, El Oro and Corral volcanics with widespread superacid rocks of "exotic" composition forming three main domes. These superacid rocks (92-98 wt.-% SiO_2) are connected with hydrothermally altered diorites, dacites and rhyolites (NT 39), accompanied by pyrite-containing dykes (NT 37, 38).

Laguna Verde alkali basalt (Fig. 3, 4 b, Tab. I 7, NT 35, U 63, 56, 57), overlying the Cerro El Oro complex to the NE, is of Pliocene age (3.1 ± 0.1 m.y., Cantagrel and Robin, 1979).

The Chiconquiaco lavas, distributed from the coast N of Palma Sola to Cerro del Sombrero, were dated in this region by Mooser and Soto (1980) 3.05 ± 0.05 m.y., therefore they belong to the middle part of the Chiconquiaco lava pile dated by Cantagrel and Robin (1979) between 4.1 and 2 m.y. This sequence of lavas has mainly alkaline character (alkali basalts (Fig. 3, 4 b, Tab. I 7, U 4, NT 40, U 49, 50, 51)) and changes to the west to basalts (Fig. 3, 4 b, Tab. I 6, U 53, 5). However, to the direction of Cerro del Sombrero we found the rocks U 55, 54, which we classified as basaltic andesites with calcalkaline trends.

The Pleistocene Lower El Abra Series (Mooser and Soto, 1980) produced similar transitional rocks distributed in the same region (Fig. 3, 4 b, Tab. I 5, NT 41).

A late Pleistocene to Holocene lava and ashfield (Upper El Abra Series of Mooser and Soto, 1980), erupted from the volcanic cones of Cerro de la Cruz and El Abra, extends towards the coast and is composed of alkali basaltic and mainly tholeiitic rock material.

In conclusion, during the Miocene the volcanic products of the Massif de Palma Sola have mainly alkaline character, although calcalkaline dacites and diorites also occur.

During the Pliocene the same pattern is observable, the basaltic andesites show calcalkaline affinities and calcalkaline products were erupted within the "El Oro Rhyolite" formation (Mooser and Soto, 1980). Within the last volcanic phase (Pleistocene-Holocene) the mentioned alkaline character is dominating with calcalkaline trends within basaltic andesites.

LANDSAT-1 Linear and Circular Features in the Study Area (Fig. 5)

The investigation of lineaments of satellite image analysis is in part trying to answer the question if a pattern of lineaments, circular features or possible fracture systems is present within the study area and this being the case if it implies any consequences or apparent control over the occurrence of volcanic eruption centers. Lineaments as defined by O'Leary *et al.* (1976) were classified according to their morphological characteristics (after Isachsen *et al.*, 1973).

Some 300 lineaments, with a total length of 750 km including three circular features were analysed in greater detail by Werle (1984). LANDSAT linear anomaly data determined at 5-degree-intervals and cross checked with aerial photography are plotted in a radial diagram showing accumulated length and direction. Five prominent maxima each one 80 to 100 km in length occur in distinctly different directions: N 280 W, N 340 W, N 025 E, N 055 E, N 070 E (Fig. 5).

Major alignments of monogenetic cinder cones are noticeable only locally along 025° trending lineaments in the central part of the study area (e.g. central caldera complex (Fig. 2)). Only few eruption centers can readily be associated with 340° trending lineaments. These represent outcrop lines of overthrusted Cretaceous limestone sediments of the Laramide folding system, while trends oriented normal (070°) to the folding axis (340°) represent transverse vertical faults as previously recognized by Mossmann and Viniegra (1976) south of the study area.

There is evidence that the setting of Pico de Orizaba is affected by 340°-trends in combination with both 55° and 70° trending lineaments. Holocene to subrecent eruptions are noticeable on the SW and NE slopes of this stratovolcano (Fig. 2, 5) and continue a directional trend that was also dominant during Late Pleistocene times. Aside from these local coincidence of near surface volcanic activities developing along lineaments there is no clear evidence on a regional scale that would support the idea of volcanic eruption centers in combination with lineaments being strictly associated with deeper volcano-tectonic and magmatic activity. There is no indication in LANDSAT imagery analysis for graben-tectonics and N-S faulting as postulated by Mooser and Soto (1980) and Cantagrel and Robin (1979), respectively.

Several discontinuous circular features of different size and age as a result of differential fluvial erosion along circular stress fields are noticeable on low sun angle

space imagery. Most obvious is a ring structure ENE of Pico de Orizaba, 18 km in diameter. A similar , but less clear and apparently older feature, 12 km in diameter, can be detected ESE of Cofre de Perote, as well as a set of curvilinear features approximately 10 km NE of this summit. So far, there is no plausible explanation for these circular features. However, the close geographic association of the two major volcanoes of the area and the circular structures supports the speculation that they are of volcano-tectonic origin.

It should be recognized that the overall distribution of Pleistocene-Holocene volcanic eruption centers in the eastern part of the TMVB shows a continuous northeastern trend towards the Gulf of Mexico (Fig. 5). This can be regarded as a surface expression and coincidence with the direction of the subducted slab (segments of

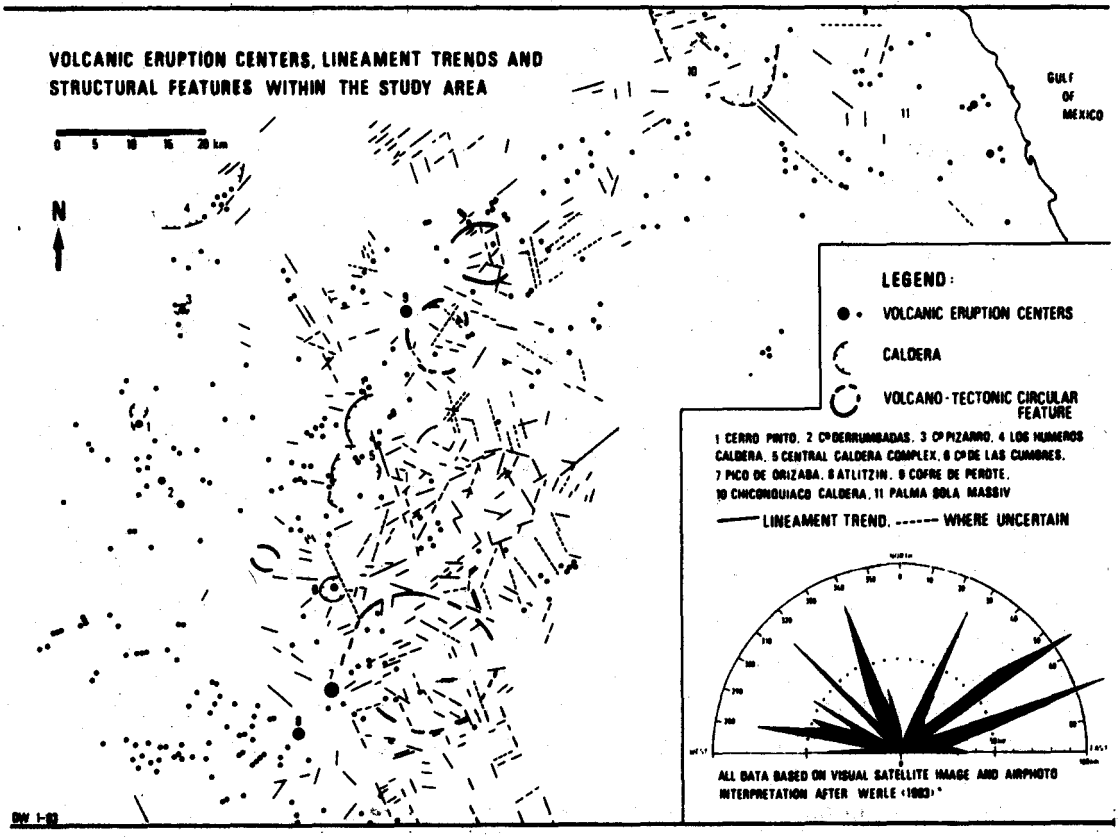

Fig. 5. Structural features within the study area.

the Cocos plate) as previous observations by Nixon (1982) for other parts of the TMVB have shown. Holocene to subrecent lava eruptions as part of SW-NE oriented alignments of volcanic eruption centers (e.g.: Pico de Orizaba-Atlitzin complex, central caldera complex, Los Humeros caldera fissure eruptions) document young volcanic activities along this directional trend.

PETROGRAPHY AND GEOCHEMISTRY OF THE IGNEOUS ROCKS

Analytical techniques

All specimens were split in a crusher fitted with cast iron jaws to pass a 30 mesh sieve and ground in an automatic agate mortar to pass a 120 mesh screen. Perspex sieves fitted with nylon screens were used throughout to avoid contamination of particularly Cu, Ni and Zn from the usual metal screens.

Analyses were carried out on air-dried powders, X-ray fluorescence spectrometry was used to determine all major and trace elements. Two sample preparation techniques were employed. For Na and all trace elements 5 g of rock powder was briquetted under a pressure of 15 ton/sq. inch for 1 min with a backing of bakelite powder-boric acid (1:1 by weight). For the remaining major elements either fusion discs of 1 g of sample powder and 4 g of lithium tetraborate were prepared (Giessen laboratory) or the method of Norrish and Chappell (1967) was used (Mainz laboratory) involving fusion of 0.56 g of rock powder with 0.04 g of sodium nitrate and 3 g of a premelted mixture of lithium tetraborate and lanthanum oxide as heavy absorber. In Giessen the ALPHA correction program of Philips was used to convert the spectrometric data to element concentrations; in Mainz the correction programs written mainly by R. V. Danchin and J. P. Willis, University of Cape Town, Department of Geochemistry, were employed.

An attempt has been made to produce data which are generally correct to within 5% of their true values, and this applies specially to the elemental ratios involved. The international standard rocks BR, BM, BHVO-1, DR-N, BCR-1, AGV-1, GSP-1, G-2, GA, GM and GR were run both for the evaluation of working curves and as unknowns for checking accuracy and precision of the data. Further analytical details are given e.g. in Tobschall (1975). In all samples Cr, Ni, Cu, Co, Na and partly Zn was determined with atomic absorption spectroscopy (Philips AAS, SP9 with graphite tube) (Trier laboratory). The rock material was decomposed with a mixture of

hydrofluoric, nitric and hydrochloric acid ($HF/HNO_3/HCl$) in a pressure decomposition vessel (pressure digestion bomb, PTFE-lined) and boric acid added to dissolve any precipitated fluorides. The international standard rocks GA, GR, GR-N, GS-N, BR, DR-N, SY-2 were run for evaluation of accuracy and precision of the data.

A comparison of the produced data by these different methods revealed a good correspondence. Carbon dioxide was determined using the apparatus Coulomat 701 SO (Ströhlein), for Fe^{2+} a titrimetric determination was used.

H_2O^+ was either determined by the Penfield method or according to the Karl Fischer method using the apparatus E 547 METROHM.

Classification of the Rocks

The investigated igneous rocks were classified as rhyolites, dacites, dacites with shoshonitic trend, andesites, basaltic andesites, basalts, alkali basalts, hawaiites, tholeiites and differentiates. In some rocks a real shoshonitic trend is given by the ratio $K_2O/Na_2O \cong 1$ or > 1. The discrimination of the "basalt"-clan (<53 wt.-% SiO_2) was arranged as follows: Ne-normative as "alkali"-basalts, Q-normative as tholeiites, hawaiites with normative An/Ab-ratio of andesine, basalts with normative labradorite.

Major oxide abundances, trace element concentrations, and CIPW-norms are given in Tables I and II for each specimen with increasing SiO_2 wt.-%.

CIPW-norms were calculated water-free up to 56 wt.-% SiO_2 and with the following correction for the ratio FeO/Fe_2O_3. For the volcanic rocks with SiO_2-concentrations smaller than 53 wt.-% this ratio was fixed at 85 wt.-% FeO/15 wt.-% Fe_2O_3, for those having a SiO_2-content higher than 53 wt.-%, we used the formula % Fe_2O_3 = % TiO_2 + 1.5. The analyses given in Tab. 1 show the analysed values of FeO and Fe_2O_3. The analyses were normalized to 100% and then classified.

Oxide-plots were used to characterize the investigated rocks. It appears appropriate to give an overview by means of the diagram K_2O/SiO_2 after Peccerillo and Taylor (1976). This graph which represents more a chemical rather than a mineralogical system, has been the basic tool for the classification of the rocks of this investigation. Different trends can be observed (Fig. 6). With one exception, tholeiitic,

the igneous rocks plot within the calcalkaline, high-K-calcalkaline and shoshonitic fields. Total alkalies versus SiO_2 reveals the well established weak to normal alkaline character of 1/3 of the investigated rocks. The regional distribution seems to support the observation that the alkaline and subordinate shoshonitic trend starts with a few examples in the Altiplano area and increases down to the Massif de Palma Sola.

For comparison the igneous rocks of Los Humeros caldera (Verma and López,

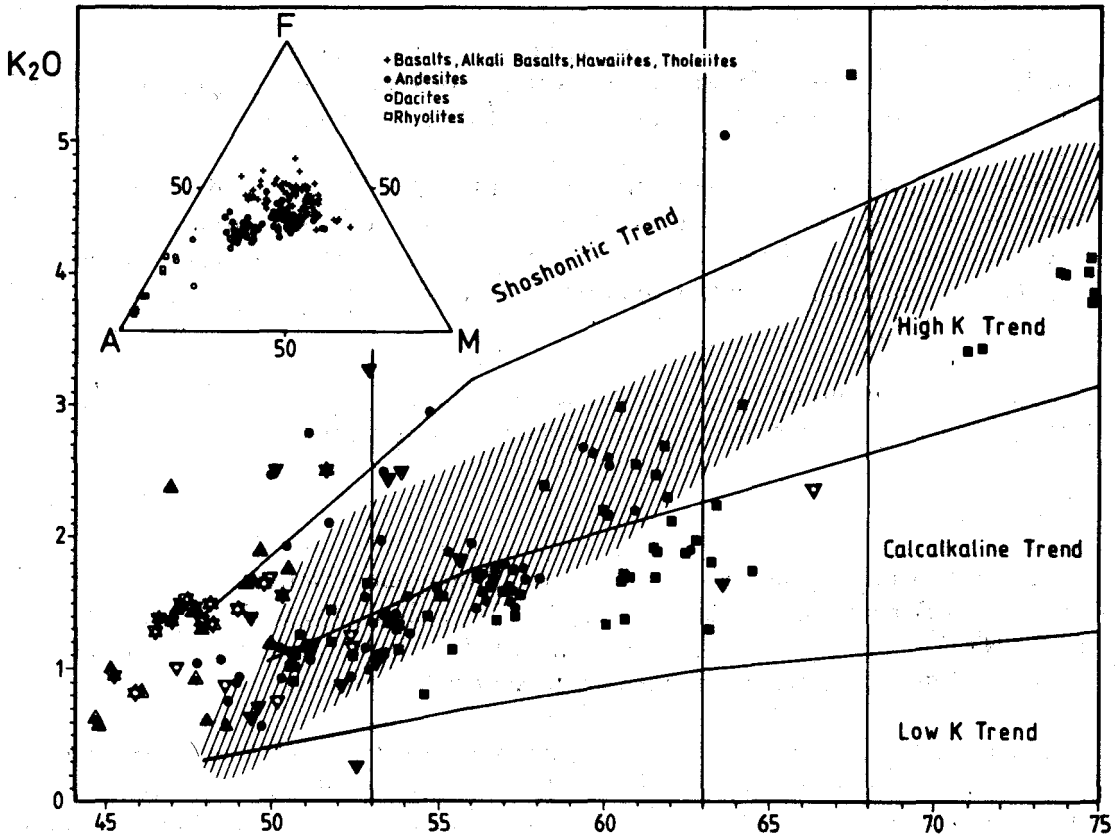

Fig. 6. Classification of the investigated rocks by the K_2O/SiO_2-diagram (with AFM-diagram of the investigated rocks).
Shadow area: Volcanics of the Los Humeros Caldera
Black squares: Volcanics of the Altiplano Area inclusive Cofre de Perote - Pico de Orizaba range
Black circles: Volcanics of the Area east of Cofre-Pico range down to Massif de Palma Sola
Triangles apex down: volcanics of the Massif de Palma Sola
Triangles apex up: Ne-normative rocks

1982) were plotted into the K_2O/SiO_2-diagram (Fig. 6). It demonstrates a similar geochemical evolution along a narrow band but without the extremely calcalkaline and alkaline trend of our study area.

No important iron-enrichment can be observed in the conventional AFM-diagram (Fig. 6), but an insignificant enrichment is obvious within the alkaline rocks of the Altiplano down to the coastal plain.

Negendank *et al.* (1982a) published binary plots of several oxides against the D.I. (Differentiation Index of Thornton and Tuttle, 1960), showing the dispersion caused by the divergent geochemical evolution from alkaline to calcalkaline.

SiO_2- and K_2O-contents increase with differentiation. The two oxides show covariance in both the alkaline and the calcalkaline trends. The concentrations of CaO, MgO decrease with differentiation, whereas Al_2O_3 and Na_2O first show an increase and then a decrease with differentiation, each time with two different regression lines.

The concentrations of TiO_2 and P_2O_5 scatter decreasing with differentiation, however giving two regression lines in each diagram for both trends.

1. Rhyolites

These rocks belong to the well established rhyolitic dome structures of the Altiplano area, Cerro Derrumbadas (C.D.: NT 4, 5, 8, 10) (~320 000 y. B.P.) and Cerro Pinto (C.P.: NT 9 a, b, NH 33 (1/2)). In both cases felsic to glassy rocks with a few phenocrysts of feldspar, biotite and in one case garnet can be observed.

The chemical analyses show differences between the two complexes. Cerro Pinto (C.P.) volcanic rocks have a range of 73.90-74.80 wt.-% SiO_2, Cerro Derrumbadas (C.D.) 70.80-75.20 wt.-% SiO_2. The following oxides differ systematically in both complexes: MgO: Cerro Pinto: 0.07-0.09, Cerro Derrumbadas: 0.12-0.28; CaO: Cerro Pinto: 0.48-0.51, Cerro Derrumbadas 0.92-1.81; K_2O: Cerro Pinto: 4.09-4.16, Cerro Derrumbadas: 3.40-3.87. This divergence becomes even more pronounced, when trace element contents are discussed. Rb-contents in C.P. rhyolites are between 188 - 194 ppm, those of the C.D. rhyolites between 100 - 115 ppm. Also the Sr-contents are very different: in the C.P.-massif they are constant (21 - 22 ppm),

whereas they range between 138 - 275 ppm in the C.D.-massif. Samples from the ashflows of the Cerro Derrumbadas massif have Rb-contents between 270 - 275 ppm.

The Y-contents in the samples of C.P. are approximately twice those from C.D. (Tab. I 1). Samples from C.P. have an average Zr-content of 68 ppm, those of the C.D. (NT 4, 10) of M7 ppm, whereas in the pyroclastics it is 154 ppm (Tab. 0 1).

The contrasts between both complexes are also significantly expressed by the Ba-contents (C.P. vs. C.D.: 30 - 50 ppm vs. 770 - 898 ppm) and those of Ce (10 - 16 ppm vs. 40 - 75 ppm). The ratios K/Rb, K/Sr and Rb/Sr are extremely different (177 - 184 vs. 279 - 288, 1545 - 1643 vs. 104 - 228, 8.37 - 9.00 vs. 0.36 - 0.82).

2. Dacites

Dacites from different areas were analysed. NT 1 (Fig. 2, 4 a, Tab. I 2) young Pleistocene) is located south-west of Cerro Pinto in the Altiplano, R 6, OM 1, CP 2, R 11 in the Cofre de Perote - Pico de Orizaba range (Fig. 2, 4 a, Tab I 2), and U 58, 62 (Miocene) in the Palma Sola Massif, U 62 from the dacite tholoid west of Punta Villa Rica (Fig. 3).

Results of the chemical analyses are given in Tab. I 2. As shown by their plots in the K_2O/SiO_2-diagram, the dacites cluster and form one group together with acid andesites which have SiO_2-contents higher than 59 wt.-%. The textures of the rocks R 6 and R 11 are very similar, however, petrographically R 11 bearing clinopyroxene instead of hornblende (R 6); both are characterized by small plagioclase phenocrysts.

Samples CP 2, OM 1, U 58 and U 62 (Tab. I 2) are varieties of porphyric dacites containing phenocrysts with diameters between 1 and 6 mm i.e., plagioclase, hornblende, ortho- and clinopyroxene in changing ratios within felsitic to glassy groundmasses. The Quiahuixtlan dacite additionally bears clinopyroxene agglomerates. NT 1 is a nonporphyric, nearly felsic rock.

Two dacites (U 21, W Las Vigas, U 28 SW Naolinco (Fig. 2, 4 a, b, Tab. I 3)) have High potassium contents (5.07 and 5.56 wt.-%) therefore they belong to the shoshonitic trend.

Dacites: Distribution in time and space

	Basin of Oriental	Cofre-Pico range	Palma Sola
Pleistocene	NT 1, U 21, U 28	0M 1, CP 2, R 6, R 11	
Pliocene			"El Oro Rhyolite" - Formation
Miocene			U 58, U 62

Robin(1981) has published analyses of the dacite from Palma Sola (VE 15), the dacites from Cofre-Pico range and possibly from a location near U 21. All these rocks are of calcalkaline character.

3. Andesites

According to the classification of Peccerillo and Taylor (1976) we can distinguish between andesites and basaltic andesites. In the K_2O/SiO_2-diagram (Fig. 6) our samples plot in three separate data fields. The andesites and basaltic andesites are forming three clusters, the first from 59 to 63 wt.-% SiO_2 which includes the dacites, the second from 56 to 58 wt.- % SiO_2 and a third which lies mostly in the basaltic andesite field with an overlap into the basaltic field, with the exception of some High-potassium rocks. To the first group (stratovolcano andesites) belong the samples in Tab. I 4 (Fig. 2, 3, 4) and as follows.

Stratovolcano andesites: Distribution in time and space

	Basin of Oriental	Cofre-Pico range
Holocene	NT7	
Young Pleistocene 20 000	+U18, U18b	
30 000		+R8
35 000		R18
		NH1, NH2
		NH25, NH26, (NH27), R7
Middle Pleistocene		C1SP, NT23, NT24, C2SP, CP3
Old		U40. 1, U40. 2, R15, R16, OM2, U17.
Oldest Pliocene		NT29

+ trachyandesitic trend

Samples marked with crosses have high Na_2O+K_2O-contents and indicate trachy-andesitic trends.

Samples NT 7 and U 18, 18b belong to the stratovolcano andesite group (Tab. I 4), but are stemming from small monogenetic cones of the Altiplano area.

The Rb/Sr-ratios of these "acid" andesites have a range between 0.03 and 0.20 (9 of 24 are higher than 0.10).

The second group of andesites (monogenetic cone andesites) (Fig. 6, 7, Tab I 4) forms a dense cluster between 56 and 58 wt.-% SiO_2. The D.I-index varies from 44-49 with three exceptions being higher than 50 (NT 49, R 10, NT 27). These andesites are petrographically dominated by a hyalopilitic texture but differ somewhat from one to another volcanic complex. Typical lavas are those south of Ciudad Serdán. Another main type with large phenocrysts of pyroxene is forming in the lava field, from Jalapa down to Dos Ríos. In total these lavas which are of monogenetic origin do not contain hornblende, but olivine phenocrysts (1-10 vol.-%). On an average they contain higher Cr- and Ni-contents than the afore mentioned andesites.

In detail we have to realize the following distribution in time and space (Fig. 2, 3, 4, Tab. I 4).

Monogenetic cone andesites: Distribution in time and space

	Basin of Oriental	Cofre-Pico range	Naolinco-Jalapa
Holocene	U16, NT11, NT20		
Young			
Pleistocene	NT18, NT19, NT22,		
20 000	U15, NT21		
30 000			
35 000			
			U36, NT51, NT54, U44, NT55
Pleistocene		NH31, (R10),	
Middle		U42, R17, U41. 1/2	
Old			
Oldest		NT27	NT50, NH16, NT49

Samples NH 31 and R 10 belong to one Middle Pleistocene lava of Atlitzin (Fig. 2, 4a). U 41.1/2, U 42 belong to the Caldera Series and NT 27 to the Oldest Pleistocene rocks of Microondas.

All other rocks are distributed in the Basin of Oriental and E of the Cofre-Pico range and were erupted during the Pleistocene (Fig. 2, 3, 4a, b).

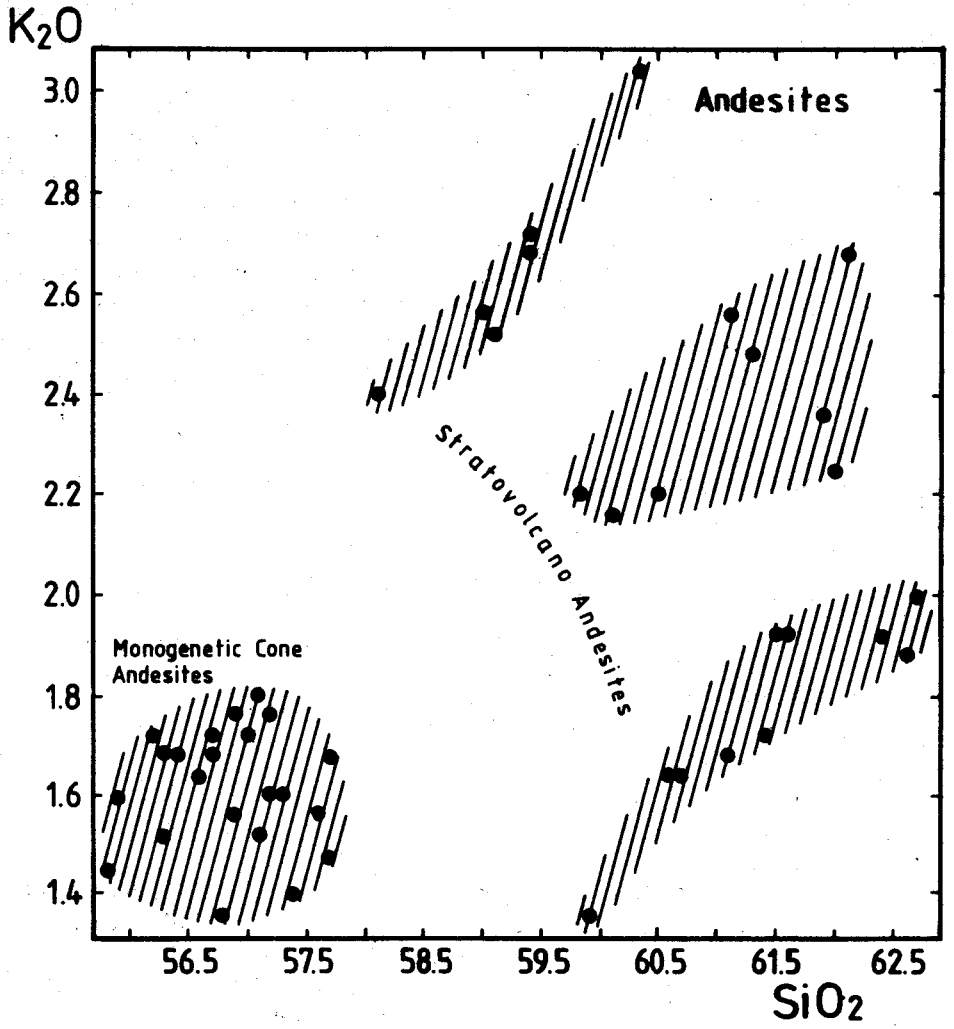

Fig. 7a. K_2O/SiO_2- diagram for the two andesite groups (with High-, Middle and Low-K stratovolcano andesites).

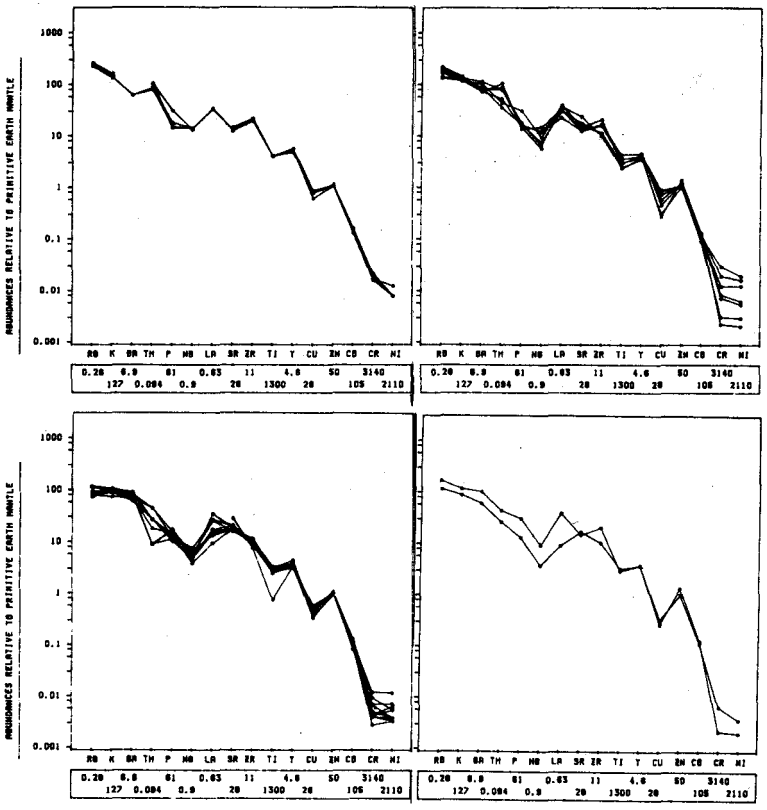

Fig. 7b. Mean values of highly incompatible through compatible elements of andesites normalized against primitive mantle. Mantle values used for normalization are given below the abscissa (Jagoutz *et al.*, 1979).

7b1: High-K-stratovolcano andesites
7b2: Middle-K-stratovolcano andesites
7b3: Low-K-stratovolcano andesites
7b4: Stratovolcano andesites of Basin of Oriental

The spiderdiagrams (Fig. 7b6 - 7b8) were drawn for the area Basin of Oriental, Cofre-Pico range and Naolinco-Jalapa. All three trace element distribution patterns are comparable and congruent, hence we cannot observe regional differences in the evolution of these rocks.

From Ciudad Serdán to Jalapa the same monogenetic rocks were produced during the Pleistocene. Robin (1981) has used these monogenetic cone andesites from Ciudad Serdán with a "Caracter Primaire" (Robin, 1981, p. 205 ff., p. 392 ff.) to evolve a conclusive model of magma generation and magma mixing for the young volcanic

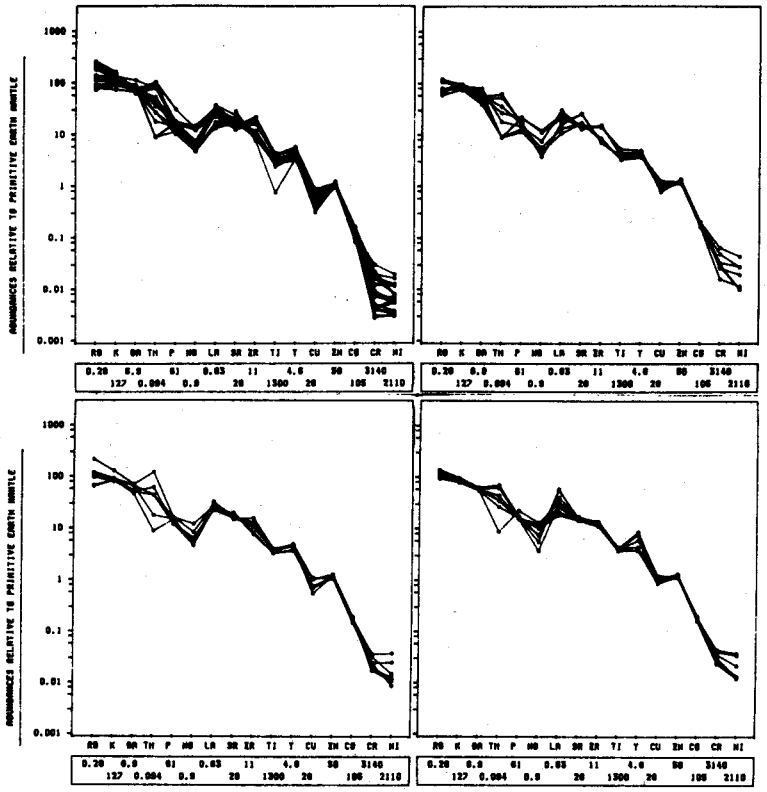

7b5: Stratovolcano andesites of Cofre-Pico range
7b6: Monogenetic cone andesites of Basin of Oriental
7b7: Monogenetic cone andesites of Cofre-Pico range
7b8: Monogenetic cone andesites of Naolinco-Jalapa

phase of Pico de Orizaba (Robin and Cantagrel, 1982).

Our results support these ideas having low differentiated lavas in these monogenetic cone andesites in comparison with the highly differentiated stratovolcano andesites.

The third cluster, not so well established as the first two, lies within the basaltic andesite field (Tab. I 5).

Petrographically these rocks look like the previously described andesites; they have the same phenocrysts and a hyalopilitic-pilotaxitic texture.

Regionally these basaltic andesites are distributed not only in the Altiplano area but also in the Massif de Palma Sola associated with eruption centers of monogenetic cones with lava streams. Oxide variations MgO vs. TiO_2, P_2O_5, Na_2O, K_2O, CaO, SiO_2 for all andesites are given in Fig. 8. In each diagram we can suggest always two trends with increasing MgO, so for SiO_2 vs. MgO, K_2O vs. MgO, TiO_2 vs. MgO.

The enrichment of TiO_2 appears to correspond to an increase in K_2O, irregular P_2O_5 increase, low SiO_2-contents and a decrease in MgO-contents.

Basaltic andesites: Distribution in time and space

	Basin of Oriental	Cofre-Pico range	Naolinco-Jalapa	Palma Sola
Holocene	NT12, NT17			
Young	NT15, NT14, NT30		NT57	
Pleistocene	NH4, NH5, NH28, NH29, NH30		U29, U37, NT63, U39, U31, NT61, U30, U38	
20 000	NH6			
30 000				
35 000			NT62	
	NH32			
Middle				+NT41
Old				
Oldest			+U45	
Pleistocene				+U55
Pliocene			+NT47	U71

+ trachyandesitic character

This distribution pattern in time and space shows that these types have been erupted in the Basin of Oriental and in the area Naolinco-Jalapa and Palma Sola during Pleistocene times with the exceptions of NT 47 and U 55 being of Pliocene age.

If we take in consideration Fig. 8 and especially SiO_2 vs. MgO we can trace our three andesite groups. The stratovolcano andesites bear ~2 - 4 wt.-% MgO, the monogenetic cone andesites ~4 - ~6 wt.-% MgO and the basaltic andesites show a high scatter in MgO-contents.

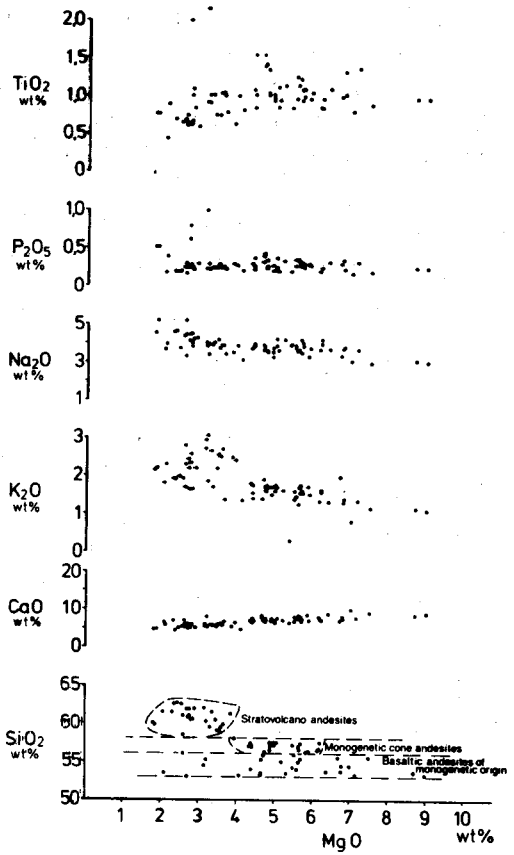

Fig. 8. Oxides/MgO- plots for all andesites.

The low MgO-contents of these rocks (~2 - 3 wt.-% MgO) are characteristic for basaltic andesites with trachyandesitic affinity, distributed in the Jalapa and Palma Sola area. High MgO-content of around 6 - 7,5 wt.-% MgO is typical for lavas of volcano Cerro Malpaís and E Aljojuca. The highest values (8 - 9 wt.-% MgO) are found in the volcano Atzizintla (NH 4, NH 5) southeast of Ciudad Serdán, having in respect to the low Al_2O_3-contents (15,7 wt.-%) "Boninite" affinities (Dietrich *et al.*, 1978; Bailey, 1981).

The rocks especially those from Cerro Malpaís and surroundings were incorporated by Robin (1981) in his evolutionary model of the volcanism. The acid (stratovolcano) andesites have Co-contents between 10 - 12 ppm, the basic (mono-

genetic cone) andesites between 18 - 25 ppm and the basaltic andesites between 23 and 36 ppm.

Using the diagram K_2O/SiO_2 (Fig. 7 a) it is obvious that our two andesite groups (stratovolcano and monogenetic cone andesites) are well discriminated but a further distinction is possible within the stratovolcano andesite group. They plot in three separate fields with a High-, Middle- and Low-potassium content. (High-K trend, samples U 40.1, U 40.2, R 15, 16, 18, Middle-K trend, samples U 18, R 8, NT 29, CP 3, OM 2, NT 23, 24 and Low-K trend samples C1SP, NT 7, NH 1, 2, U 17, NH 25, 26, R 7 and C2SP.)

This pattern finds even its expression in the distribution of Th and Rb/Sr to SiO_2 and in the spiderdiagrams (Fig. 7 b). This Figure indicates clearly the evolution from High-K (Fig. 7 b1) over Middle-K (Fig. 7 b2) to Low-K trend in correlation with the thorium-scatter from a positive anomaly (High-K) over a medium scatter to mainly negative Th-anomalies (Low-K).

Additionally this pattern is oriented regionally because the High-potassium trend is distributed mainly in the northern part (Cofre de Perote) of the Cofre-Pico range whereas the Low-potassium trend of these stratovolcano-andesites is situated in the south (Pico de Orizaba).

A similar refinement of geochemical trends is given in the K_2O/SiO_2-diagram (Fig. 9a) of the basaltic andesites. A High-, a main Middle- and a Low-potassium trend are visible.

The High-potassium rocks are of trachyandesitic character in respect to their Na_2O+K_2O-contents and are distributed in the Palma Sola and Jalapa area (compare low MgO-contents). The Low-K trend is distributed in the Basin of Oriental.

All other rocks are characterized as mean K-basaltic andesites. If we consider the Fig. 9 b 1, 2, 3 we can observe two diagrams with completely congruent trace element distribution patterns. These are the basaltic andesites from the Basin of Oriental (Fig. 9 b1) and the basaltic andesites from Naolinco-Jalapa (Fig. 9 b2).

Fig. 9 b3 gives the spiderdiagram for the basaltic andesites of the trachyandesitic character, with high K_2O-, low MgO-contents and enriched in incompatible trace elements in comparison with the Fig. 9 b1, b2. These rocks are of Pliocene age with

the exceptions of U 45 (Old-Pleistocene) and NT 41 (Pleistocene "Old El Abra Series").

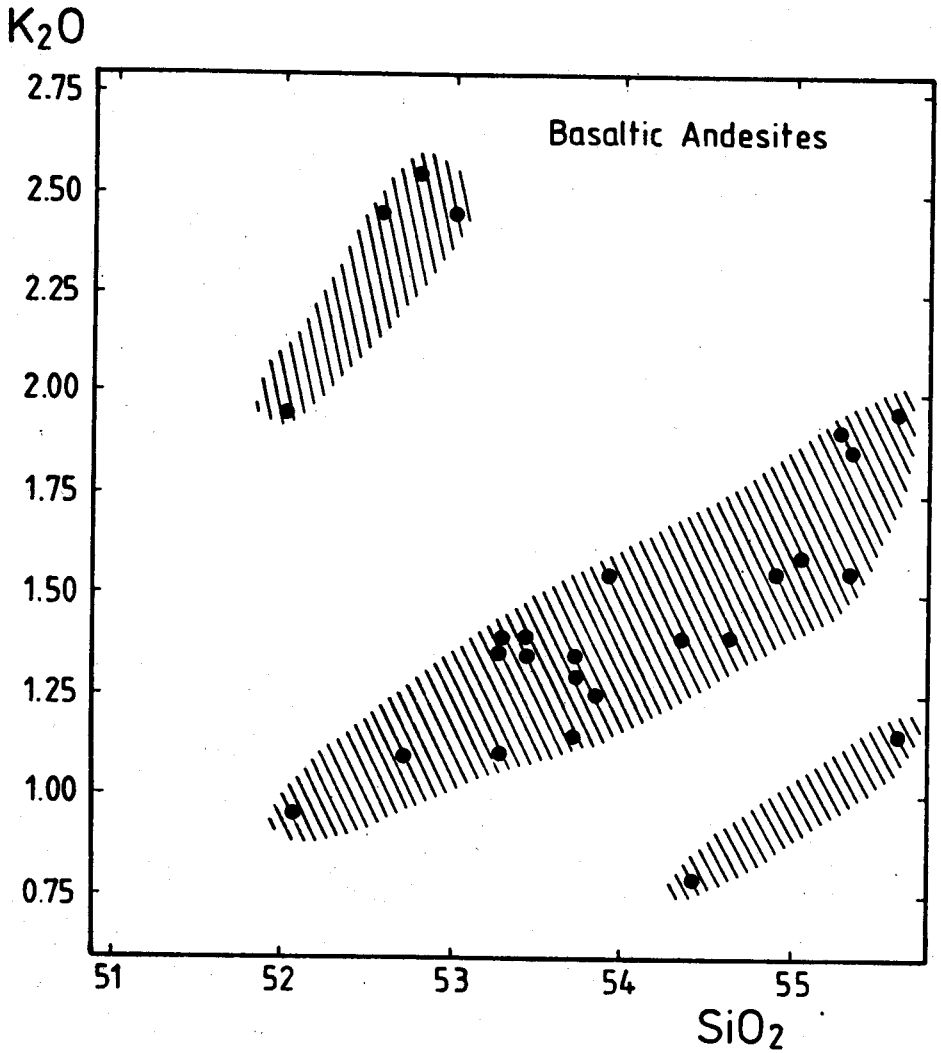

Fig. 9a: K_2O/SiO_2- diagram for basaltic andesites.

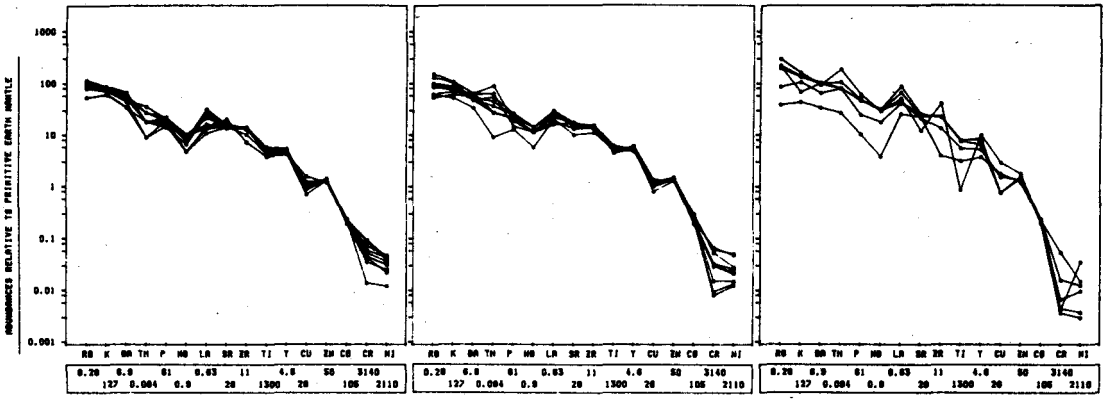

9b: Mean values of highly incompatible through compatible elements of basaltic andesites normalized against primitive mantle. Mantle values used for normalization are given below the abscissa (Jagoutz *et al.*, 1979).

9b1: Basaltic andesites (Mean-K) of Basin of Oriental

9b2: Basaltic andesites (Mean-K) of Naolinco-Jalapa

9b3: Basaltic andesites (High-K and one Low-K). The Low-K-rock is NH 32 of Basin of Oriental. The High-K-rocks are distributed in the region Naolinco-Jalapa and Palma Sola (for further information see text)

4. Basalt-clan

This group of rocks with SiO_2-contents smaller than 53 wt.-% was discriminated into *basalts* (olivine-basalts), *alkali basalts, hawaiites, tholeiites* and 5 *differentiates* (Tab. I 6-10). In some rocks an absarokitic-shoshonitic trend can be observed, $K_2O/Na_2O \cong 1$ or > 1, especially within the group of differentiates characterized by very low MgO-contents (Tab. I 10).

Basalts (Tab. I 6)

The basalts are characterized by SiO_2 wt.-% between 46.3 and 51.9. The range of Al_2O_3 is 15.9 to 18.1 wt.-%, that of CaO is 9.24 - 13.1 wt.-%. These rocks are distributed in Miocene and Pliocene in the Massif de Palma Sola, during Pleistocene-Holocene times in the area Naolinco-Jalapa. The time-space distributions for these rocks are as follows:

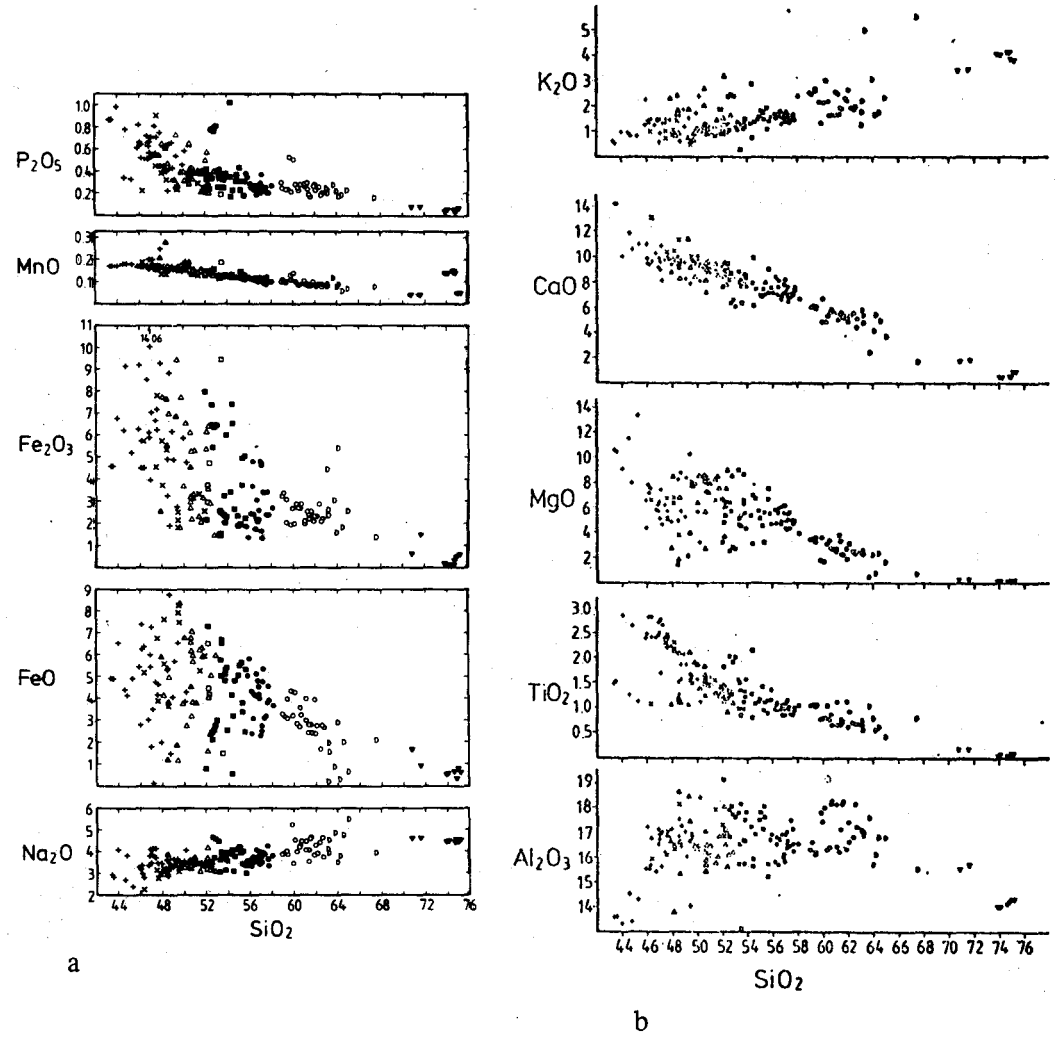

Fig. 10. a./b. Harker plot of all rock samples: (crosses) nepheline-normative alkali basalts, (diagonal crosses) olivine basalts, (open triangle, apex up) hawaiites, (triangles apex up) "differentiates", (open squares) tholeiites, (squares) basaltic andesites, (circles) monogenetic cone andesites, (open circles) stratovolcano andesites, (half circle open) dacites, (triangle, apex down) rhyolites.

86 70

Basalts: Distribution in time and space

	Basin of Oriental	Cofre-Pico range	Naolinco-Jalapa	Palma Sola
Holocene			NH18, U22, NH19	
Young Pleistocene			U31b	
Middle Old Oldest Pleistocene				
Pliocene				U5.1(1/2), U53
Miocene				U8, NT32, U7, U6 (Gabbro)

If we consider Fig. 11 a 1, 2, 3, we can observe the distribution of the trace element pattern. *Even here we can observe the negative Nb- and Ti-anomaly, which is characteristic for all described andesite types.* During Pliocene times the Ti-anomaly in the Palma Sola area seems to disappear.

Alkali basalts

These rocks bear normative nepheline and are distributed in Miocene times exclusively in the Massif de Palma Sola followed by Pliocene rocks in the same region.

Rocks of the same character around Actopan belong to Pliocene series, which form in parts the basalt sequences of the lava field extending in the direction of Jalapa (Robin, 1981).

Only a few alkali basalts are distributed in the western area. NT 64 is a small volcanic cone SW of Perote in the Basin of Oriental, NT 25 from the cone and lava field S of Las Vigas and U 24, 25 from the lava field SW of Vista Hermosa (Fig. 2, 4 a, b). These rocks erupted during Young Pleistocene-Holocene times as one example in the Massif de Palma Sola (U 52, Fig. 3, 4 b).

Alkali basalts: Distribution in time and space

	Basin of Oriental	Cofre-Pico range	Naolinco-Jalapa	Actopan	Palma Sola
Holocene			NT25		U52
Young Pleistocene 20 000 30 000 35 000	NT64		U24, U25		
Middle Old Oldest Pleistocene				NH21,NH15, NT48,NT43, NT44,NT44R	
Pliocene				U48,NT45 U35	U50,U51,U4,NT40, U49,U56,U57, NT35,U63
Miocene					U72,U10,U74,U75, U67,U76,NT33, U9,U7b

A consideration of Fig. 11 a 4, 5, 6, 7, gives an overview over the trace element distributions of all analysed rocks of the Young Pleistocene volcanism from the Basin of Oriental down to the Massif de Palma Sola represented by only 5 analyses. The rocks of the Basin of Oriental (NT64) and Las Vigas (NT 25) show strong decrease of incompatible elements (e.g. Rb) in comparison with the other rocks.

Fig. 11 a 9 presents the spiderdiagram of the lavas of Old Pleistocene (Pliocene) times on the eastern edge of the lava field of Jalapa around Actopan.

The most basic rock NT 44, 44R, characterized by the highest La-values, has olivine and titanoferous augites as phenocrysts and contains apatite, titanomagnetite and plagioclase in the groundmass. Because of its modal nepheline distributed in the matrix, it is of basanitic character. In parts the rock bears augite agglomerates. Its spiderdiagram approximates diagrams without negative Nb- and Ti-anomalies, but is different from typical alkaline lavas of intraplate (or graben-like) regions, which show a distinct positive Nb- and Ti-anomaly (e.g. Fig. 11 a 12 (Eifel-region)) or as it was published by Hawkesworth *et al.* (1979) for Patagonian intraplate lavas.

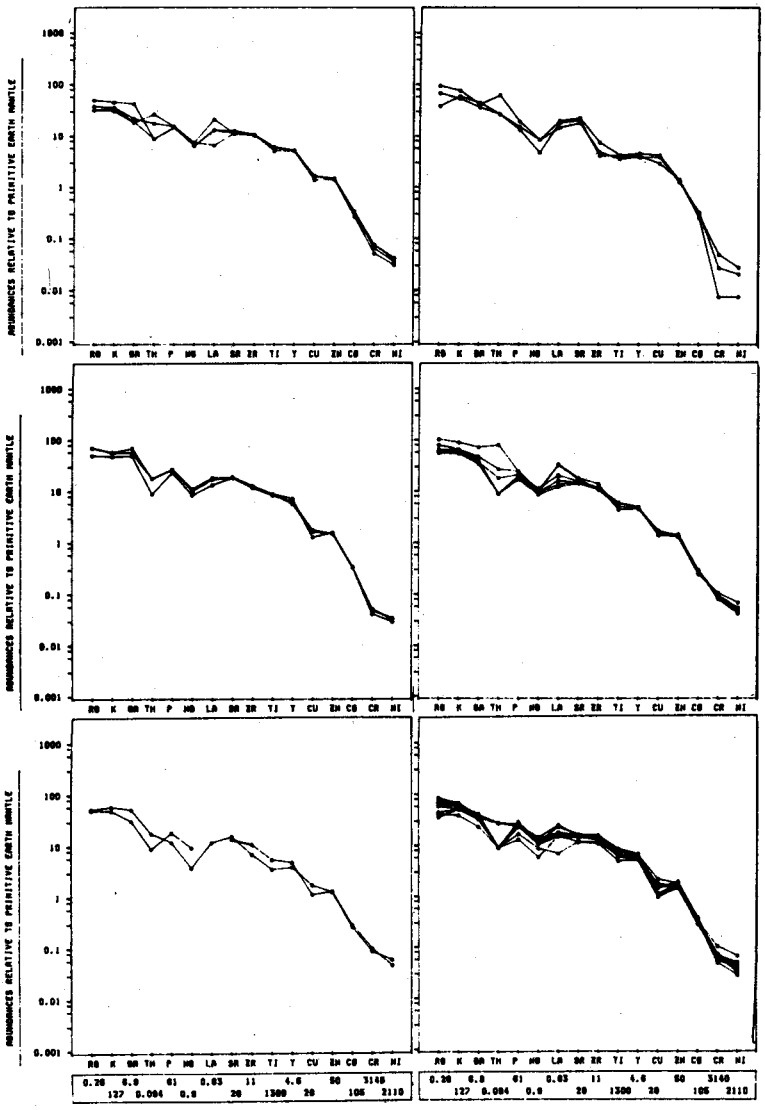

Fig. 11a: Mean values of highly incompatible through compatible elements of basalts, hawaiites, alkali basalts normalized against primitive mantle (s. Fig. 7b, 9b).

11a1: Basalts of Naolinco-Jalapa (Pleistocene-Holocene)

11a2: Basalts of Palma Sola (Miocene)

11a3: Basalts of Palma Sola (Pliocene)

11a4: Hawaiites of Basin of Oriental (Pleistocene)

11a5: Hawaiites of Cofre-Pico range (Pleistocene)

11a6: Hawaiites of Naolinco-Jalapa (Pleistocene-Holocene)

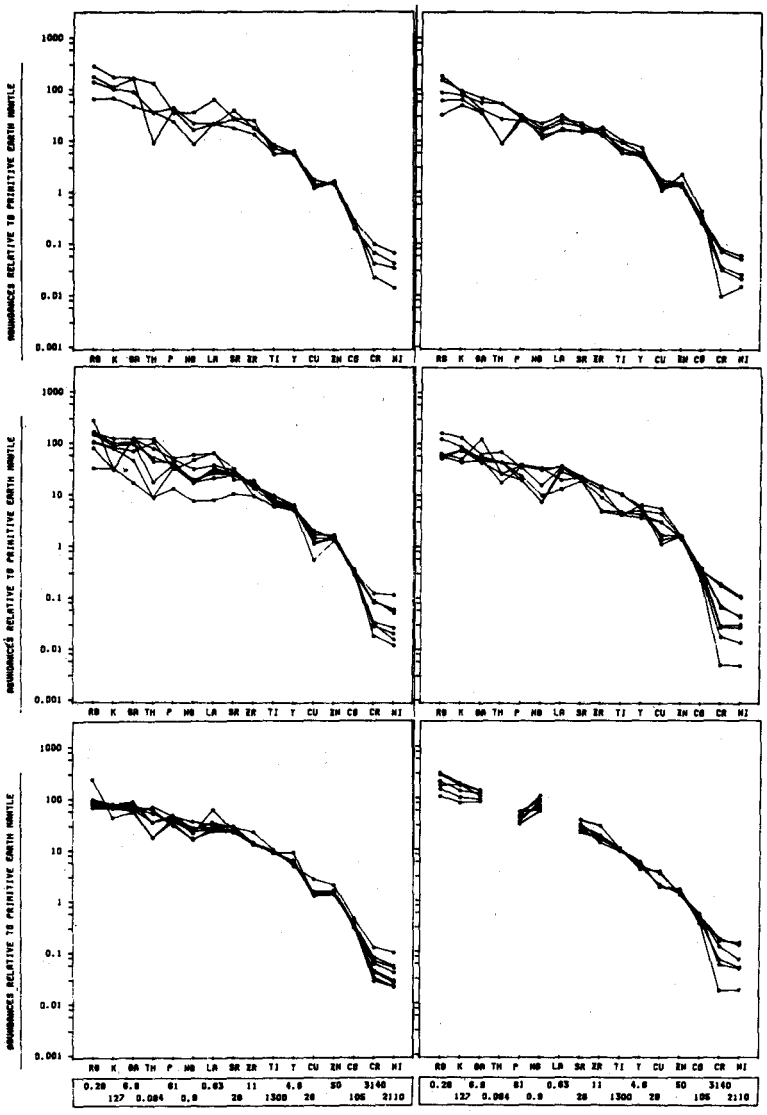

11a7: Hawaiites of Actopan (Pliocene/Pleistocene)
11a8: Alkali basalts of Basin of Oriental to Naolinco-Jalapa (Pleistocene)
11a9: Alkali basalts of Actopan (Pliocene/Pleistocene)
11a10: Alkali basalts of Palma Sola (Miocene)
11a11: Alkali basalts of Palma Sola (Pliocene)
11a12: Alkali basalts, nephelinites, basanites of the Eifelregion (Intraplate alkaline volcanism) (Schmincke *et al.*, 1983) for comparison with positive Nb-Ti-anomalies.

All other rocks of this sequence show negative anomalies of Nb and Ti as it was described for the different andesite types of our study area. This observation is also valid for the alkali basalts of Miocene and Pliocene times of the Massif de Palma Sola (Fig. 11 a 2, 3).

"Hawaiites"

Another group of these basalts were classified as "Hawaiites" in respect to their normative andesine contents (Ab/An-ratio). Hawaiites after the chemical classification using the sum of Na_2O+K_2O normally have contents higher than ~6 wt.-% Na_2O+K_2O.

Our rocks have the following characteristics:

SiO_2: 48.6 - 52.8 wt.-%; Al_2O_3: 15.4 - 18 wt.-%; CaO: 7.8 - 9.78 wt.-%.

It is a transitional group of rocks having a more subalkaline character (Kuno, 1959, 1966).

"Hawaiites" (Tab. I 8) and "Tholeiites" (Yoder and Tilley, 1962): Distribution in time and space

	Basin of Oriental	Cofre-Pico range	Naolinco-Jalapa	Actopan	Palma Sola
Holocene			NT28,NH22,NT60, U46		(NT31,U13) ("Tholeiites")
		R19,NH3	NH17,U33,NT58		
Young Pleistocene	NH10,NH11, NH12,NH14, U19,NT65, NT13		U23		
20 000					
30 000					
35 000					
			NT52		
Middle					
Old				NT53?	
Oldest Pleistocene					
Pliocene				NT46,NT42, NH20	
Miocene					U78

The trace element distribution was plotted in the same way as it was done before as abundances to primitive earth mantle (values from Jagoutz *et al.*, 1979) for Basin of Oriental, Cofre-Pico range, Naolinco-Jalapa and the Palma Sola, here only the tholeiites, which erupted during Young Pleistocene and Holocene times. Another group summarizes the hawaiites of Pliocene/Oldest Pleistocene times around Actopan. Fig. 11 a 4, 5, 6, 7 indicate the pattern, which is congruent for Young Pleistocene-Holocene lavas of Basin of Oriental (Fig. 11 a 4), Cofre-Pico range (Fig. 11 a 5), Naolinco-Jalapa (Fig. 11 a 6) and the tholeiites of Palma Sola (Fig. 11 b 1, Tab. I 9, NT 31, U 13). All are characterized by the negative Nb- and Ti-anomalies. The contents of incompatible elements are slightly lower than those of the andesites.

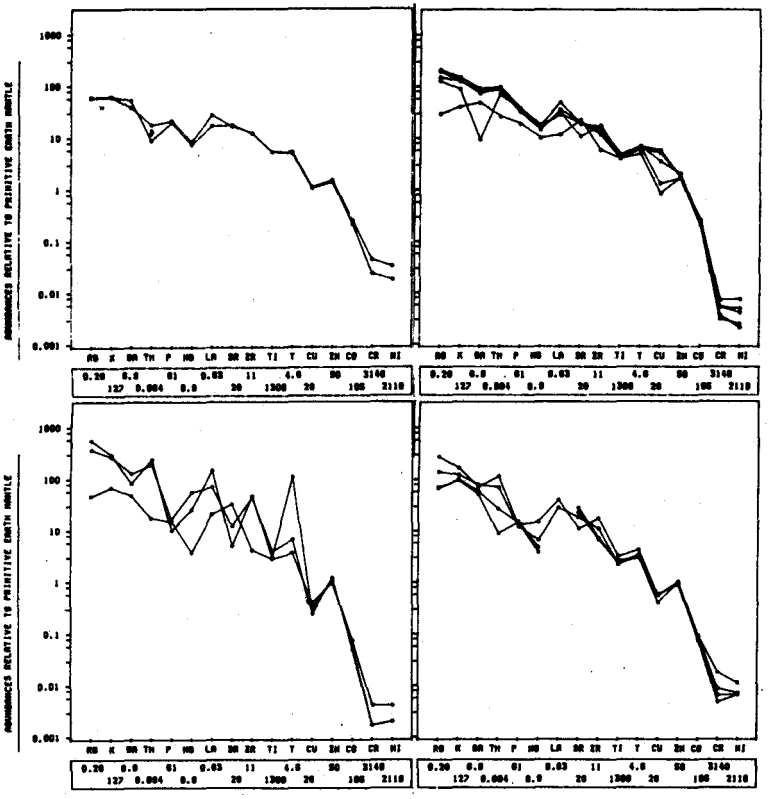

11b: Spiderdiagrams of tholeiites, differentiates, dacites and rhyolites.
11b1: Tholeiites of Palma Sola (Holocene)
11b2: "Differentiates" (Dykes etc.) of Punta Delgada, Palma Sola (Miocene)
11b3: Dacites of Basin of Oriental (two with "shoshonitic" trend, one normal dacite) (Pleistocene)
11b4: Dacites of Cofre-Pico range (Pleistocene)

The Pliocene-Pleistocene lavas around Actopan show incompatible trace element enrichment but also the negative anomalies of Nb and Ti.

Remarkable is the fact that the occurrences of these basalts (normative "hawaiites") are distributed not only in the Basin of Oriental and Naolinco-Jalapa area but also in the Cofre-Pico range. NH 3 is a dyke in the SE flank of stratovolcano Atlitzin, R 19 is a monogenetic volcano in the N-Caldera S of Cofre de Perote complex.

In the Basin of Oriental NT 65 (SE of Zacatepec) is a sample from a small monogenetic cone S of Cerro Derrumbadas, NH 10-14, U 19 are samples from the lavas around Guadalupe Victoria and NT 13 is from the complex SE of El Limón. These rocks of the area Guadalupe Victoria have been indicated by Robin and Tournon (1978) and Robin (1981) as transitional basalt types.

Thus we can state that the alkali basalts (ne-normative) have been erupted during Miocene and Pliocene times in the Massif de Palma Sola and around Actopan during Pliocene/Pleistocene times, being parts of the Cofre-Pico base after Robin (1981).

During Young Pleistocene-Holocene times only a few alkali basalts occur in Basin of Oriental (NT 64) and in the Naolinco-Jalapa area.

This picture is similar for the basalts (Miocene and Pliocene in the Massif de Palma Sola) whereas in the region Naolinco-Jalapa the basalts erupted during Pleistocene-Holocene times.

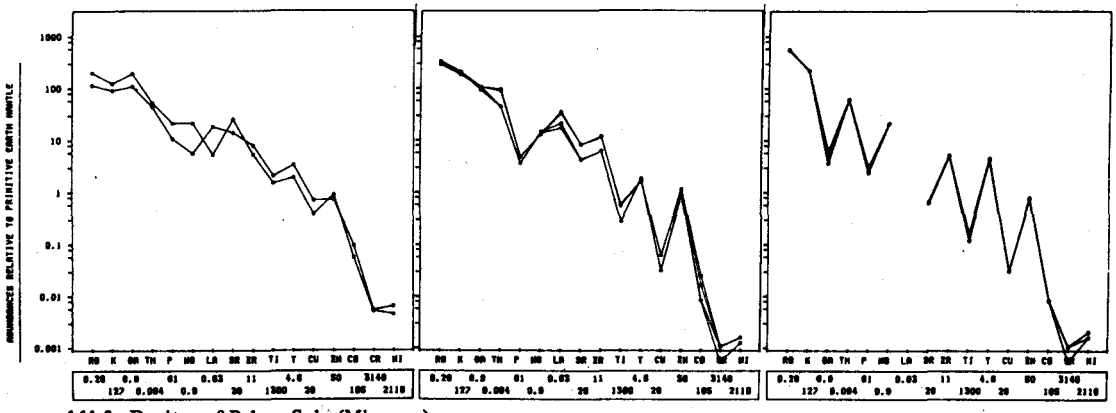

11b5: Dacites of Palma Sola (Miocene)
11b6: Rhyolites of Cerro Derrumbadas (Pleistocene)
11b7: Rhyolites of Cerro Pinto (Pleistocene)

However, our "hawaiites", being subalkaline, are distributed during the Pleistocene-Holocene times from the Basin of Oriental over the Cofre-Pico range down to Naolinco-Jalapa. Tholeiites occur only during Pleistocene-Holocene times in the Massif de Palma Sola.

This distribution pattern overlaps the eruptions of basaltic andesites during Young Pleistocene-Holocene times occurring in the Basin of Oriental and in the region Naolinco-Jalapa with one example in the Massif de Palma Sola (NT 41, Lower El Abra Series). In Pliocene times we also have only a few occurrences in the eastern part (NT 47, S of Actopan, U 55, Massif de Palma Sola).

Monogenetic cone andesites are distributed during Young Pleistocene-Holocene times in Basin of Oriental, Cofre-Pico range and the area Naolinco-Jalapa and not in the more eastern parts. Stratovolcano andesites are restricted to the Cofre-Pico range with two exceptions in the Basin of Oriental.

5. Exotic, superacid rocks (= Silexite, Miller, 1919).

The detailed geological map of the Massif de Palma Sola reveals the situation of the three complexes of anomalous rocks. Cerro El Corral, Cerro Azul and Cerro El Oro seem to be volcanic ruins with a central caldera at the top of El Corral. Several small domes in all complexes are formed by these superacid rocks. In other areas of these complexes these rocks are widespread and seem to form autoclastic block-lava-fields.

In general, these complexes are built up by andesites, rhyolites and diorites which seem to be hydrothermally altered (NT 39).

The geological situation suggests the interpretation as rhyolitic to andesitic volcanic complexes, in which domes of diorites and superacid rocks intruded altering the rocks hydrothermally. Field studies do not exclude the possibility of acid tuffs altered by metasomatic processes.

The geochemistry is tabulated in Tab. II (Banzer-Bussmann, 1981). The average SiO_2-contents is 96.16 wt.-% (91.34-97.67 SiO_2 wt.-%) and they bear anomalous high TiO_2-contents (0.78-2.15 wt.-%). The rare earth element distribution is similar in Cerro El Oro and Cerro Azul "Silexites" and seems to correspond - with the exceptional La/Ce-ratio - to the distribution pattern of granitic "residual differentiates".

Petrographically these rocks are gray, very fine grained quartz rocks, bearing rutile and in several cases hematite and alkali feldspars.

Schwab (1972) gives an example of similar rocks as products of metasomatic processes in andesite-dacite-rhyodacite complexes in Argentina. In contrast to this interpretation, our results (e.g. rare earth distribution pattern, high TiO_2-contents) may also support the hypothesis that these superacid rocks may be products of a "silicate liquid immiscibility" (Roedder, 1979) and hence be igneous rocks.

Geochemical and petrogenetical aspects

Our considerations upon petrogenetical processes report preliminary results and general outlines because our detailed petrographic-microprobe studies are not finished and therefore we cannot trace exactly the history of each rock. It has to be mentioned that besides fractional crystallization, mixing seems to be another important process as it was reported by Robin (1981), Robin *et al.* (1983) for the youngest history of Pico de Orizaba. Krawczyk (1984) has investigated several rocks of monogenetic origin with strange mineral assemblages asking for an explanation of mixing processes.

On the other hand, it is complicated to create a model of one volcanic complex, without having complete information by lacking sequences of the older parts of stratovolcanoes, or by having not analysed all available rocks around one complex, e.g. the rhyolite complex of Cerro Derrumbadas and Cerro Pinto.

Which rocks have we to incorporate in our model? Around the Middle Pleistocene dome structures, we have found Young Pleistocene-Holocene volcanic cones and maars. The sequence of eruptions has been basaltic andesite cone E of Cerro Pinto (NH 32), maars S of Cerro Derrumbadas, dacite cone SW of Cerro Pinto (NT 1), a hawaiite cone SW of Cerro Derrumbadas (NT 65) contemporaneous with stratovolcano andesite cone E of Cerro Derrumbadas (U 18) and the eruption of the maars Laguna Alchichica, Laguna Preciosa, and Atexcac. During this time interval the young lahars, pyroclastic flows, etc. of Cerro Derrumbadas formed.

One Holocene-Recent lava erupted E of Cerro Derrumbadas, representing a stratovolcano andesite too (NT 7), but of monogenetic origin, forming with the volcano SE of it (U 18) the two exceptions not fitting into our classification of monogenetic cone andesites.

The sequence is:
rhyolite - basaltic andesite - dacite - hawaiite/stratovolcano andesites. This is rather contradicting and therefore it seems to be better to be cautious incorporating these rocks into one sequence. This is our impression considering stratovolcanoes and surrounding monogenetic cones.

Possibly the afore described distribution pattern has to be interpreted in respect to different residence times during the ascent of the magma in mantle and crust (O' Hara, 1984).

On the other hand, the sequence of lavas of one stratovolcano of middle to upper part of Cofre de Perote is andesite (CP 3, SiO_2 61.9 wt.-%, K_2O 2.34 wt.-%), andesite (NT 24, SiO_2 62.1 wt.-%, K_2O 2.68 wt.-%), andesite (NT 23, SiO_2 61.1 wt.-%, K_2O 2.57 wt.-%) dacite (CP2, SiO_2 64 wt.-%, K_2O 3.08 wt.-%). This line demonstrates a change from High-K-stratovolcano andesites to dacite and shows a similar situation as it was observed in three stratovolcanoes in the Sierra de las Cruces west of "Valle de México" (Negendank *et al.*, 1981).

It is not without signification but has to be explained, that during the Young Pleistocene to Holocene stratovolcanoes produce stratovolcano andesites and more differentiated rocks like dacites, etc., whereas monogenetic cones are formed overwhelmingly by tholeiites, alkali basalts, basalts, hawaiites, basaltic andesites and monogenetic cone andesites. A further explanation has to be given for rhyolite domes. The geochemistry and mineralogy of monogenetic cone andesites has led us to the conclusion that these rocks form a close group of less differentiated rocks.

However, in general, during older Pleistocene times the formation of stratovolcano andesites prevails over the other volcanic rocks by volume whereas in Young Pleistocene to Holocene times all products were erupted contemporaneously but without limitation in defined areas. The calcalkaline tendency decreases in volume of eruption from west to east as the subalkaline and alkaline trends increase.

Robin (1981) concluded that the volcanism started in Pleistocene times in this region with basalts being partial melting products of the hydrated upper mantle (dehydration of amphibolites of the downgoing lithosphere). Later on basaltic and andesitic primary magma erupted, the andesitic magma being a product of reaction of dacitic liquids from the subducted oceanic crust exhibiting eclogitic petrology with mantle peridotites.

This hypothesis internally is consistent but it is contradictory to the described time relationships of the volcanism e.g. of Cofre de Perote, interpretating the basaltic volcanism as the initial stage.

All samples have been analysed for major and selected trace elements. Harker diagrams (Fig. 10) show the broad range of compositional variation from nepheline-normative alkali basalts through basalts, basic and acid andesites to dacites and rhyolites, mostly as roughly linear or curved trends.

The investigated rock-types and some important characteristics as SiO_2, Al_2O_3, TiO_2, MgO, CaO and K_2O with a few trace elements Rb, Sr, Zr, Ba, Ce, K/Rb, K/Sr, Rb/Sr were summarized in Table III(1-9) to define these igneous rocks by calculating averages (ranges) of the oxides and trace elements. It was the intention to demonstrate the average composition of these rocks in respect to their spatial and temporal distribution as it was described in detail in the previous chapters.

Since the basalts, andesites, dacites, and rhyolites collectively show smooth scatter in a high number of element/element diagrams, these plots can be interpreted as representing an apparent liquid line-of-descent. We should realize that only data of phenocryst-poor or aphyric volcanic rocks will give a true indication of this line. In contradiction, a substantial percentage of our samples does contain phenocrysts, the percentage of plagioclase being highest in dacites, while the amounts of phenocrystal olivine and pyroxene are decreasing with increasing SiO_2-content. In some andesites phenocrystal hornblende and magnetite were observed.

Keeping these restrictions in mind, chemical data are used to critically assess several models proposed to account for the origin of andesites and related rocks of the eastern TMVB. These include (e.g. Gill, 1981) *a)* partial melting of garnet peridotite of the mantle wedge at high P_{H_2O}, *b)* partial melting of subducted oceanic lithosphere, metamorphosed to amphibolite or quartz eclogite, or crystal fractionation of basaltic magma controlled by eclogite, *c)* crystal fractionation of basaltic magma controlled by low-silica amphibole at 80-100 km, *d)* crystal fractionation of basaltic magma at crustal level, controlled by olivine, pyroxene, plagioclase and magnetite, and *e)* crustally contaminated primary partial melts of the mantle wedge.

In Fig. 11 concentrations of highly incompatible through compatible elements in the different rocks grouped according to petrology, regional and temporal distribu-

tion are normalized against the primitive mantle (Jagoutz *et al.*, 1979). The element patterns show remarkably consistency and conformity between each other, suggesting a comagmatic genesis of the whole range of rocks. The basalts and andesites are definitely more LIL-element enriched than MORB samples (Sun *et al.*, 1979) and oceanic andesites (Maaløe and Petersen, 1981).

All spiderdiagrams reveal a depletion of Nb and Ti, being typical for calcalkaline suites (Gill, 1981). This is in contrast to typical alkaline volcanism of the Patagonian Plateau (Hawkesworth *et al.*, 1979) or the Eifel region (Schmincke *et al.*, 1983), which definitely show no relative depletion of these two elements.

Variation diagrams of trace elements are very capable of testing hypotheses on both the source and the differentiation of magmas. To illustrate by an example the behaviour of highly compatible elements, in Fig. 12 a log Ni- vs. log Cr- diagram is presented covering all samples of the range of rocks studied. All rocks with SiO_2-contents <63 wt.-%, thus excluding dacites and rhyolites, are characterized by a Cr/Ni-ratio of 2.26 ± 0.12. This ratio is 1.69 and 1.00 for dacites and rhyolites, respectively.

Altogether, the data define a straight belt with a steep slope depicting nepheline-normative alkali basalts and hawaiites at the upper, dacites and rhyolites at the lower end of the plot. The Cr- and Ni-contents of primary melts of mantle peridotite and hydrous condition when D_{Ni}/D_{Cr} are 30/1, 2/10, and 3/10 for olivine, orthopyroxene, and augite, respectively, are 300 ppm resp. 100 ppm (Gill, 1981), thus plotting in the range of slightly undersaturated and slightly oversaturated basalts of our suite of volcanics.

Since fractional crystallization is the only differentiation process which causes trace elements to follow a Rayleigh distillation pattern, this log Ni- vs. log Cr- diagram indicates that all sampled volcanics are fractionates of potentially primitive basalts which plot at the uppermost end of this diagram being themselves partial melt products of the mantle peridotite overlying the downgoing oceanic lithosphere. Since partial melts of subducted amphibolitic or eclogitic MORB should have Cr/Ni- ratios <1 (Gill, 1981, p. 145), they are not the candidates for primitive melts of our rock suite. This seems to be the reason why Robin (1981) proposes a reaction of primary magmas of the lithosphere with peridotite of the overlying mantle peridotite.

The Cr- and Ni-contents sharply and continuously drop from the group of basaltic

rocks via basaltic andesites, monogenetic cone andesites, stratovolcano andesites to dacites and rhyolites. The monogenetic cone andesites definitely are less differentiated by crystal fractionation than the stratovolcano andesites.

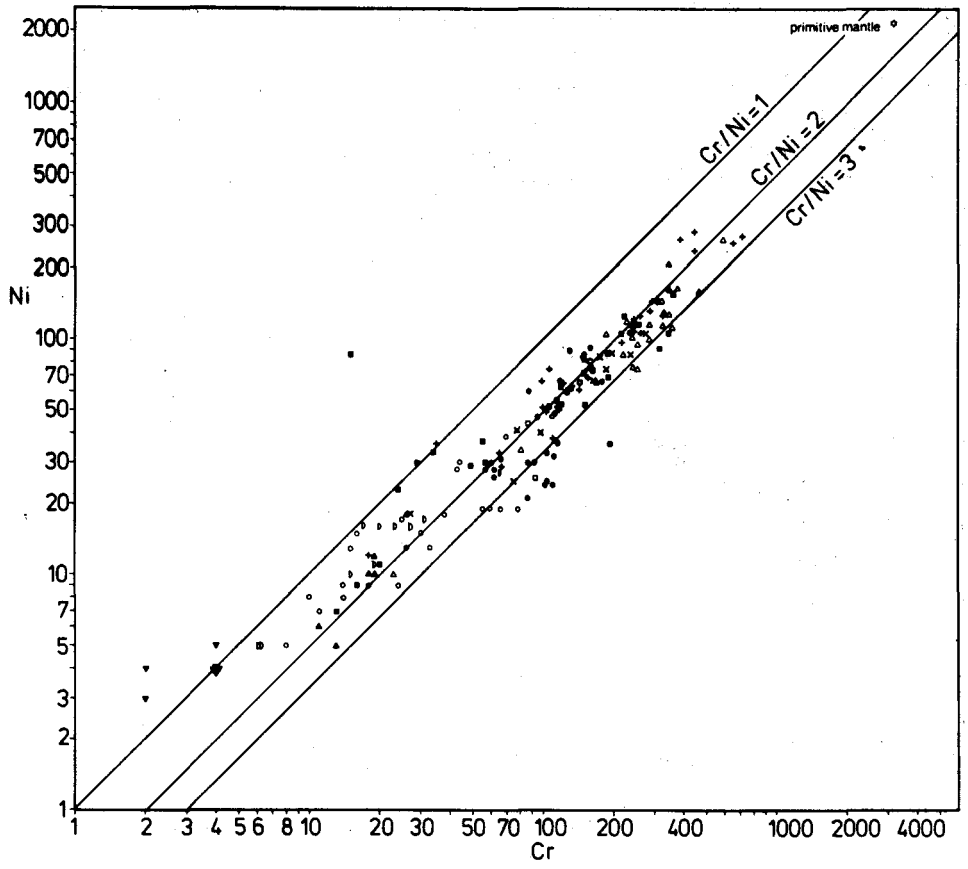

Fig. 12. Log Ni- vs. log Cr- diagram. (open star) primitive mantle (Jagoutz *et al.*, 1979), all other symbols as in Fig. 10.

This apparent liquid line-of-descent is also shown by log-log plots of Co and Ni, and - with negative slope - of the highly incompatible elements Rb and K.

The log-log plots of the compatible elements suggest for the derivation of the different volcanics that olivine, Cr-spinell, orthopyroxene, and augite fractionated eventually already within the mantle. It can be speculated that during this differentiation and the ongoing ascent, the viscosity of the liquid increases and the density con-

trast to its surrounding decreases, resulting in a subsidiary reservoir at the base or within the crust. Differentiation continues within the reservoir whereby calcic plagioclase and magnetite fractionation probably is the principal cause of a rapid increase in silica content of the derivative liquids (POAM model, Gill, loc. cit.).

Log-log plots of Rb vs. Rb/Sr and Sr/Ca s. Ba/Ca (Fig. 13 and Fig. 14; Onuma *et al.*, 1983) clearly indicate the fractionation of plagioclase giving rise to sharp increases of total Rb and the three ratios in the suite of rocks.

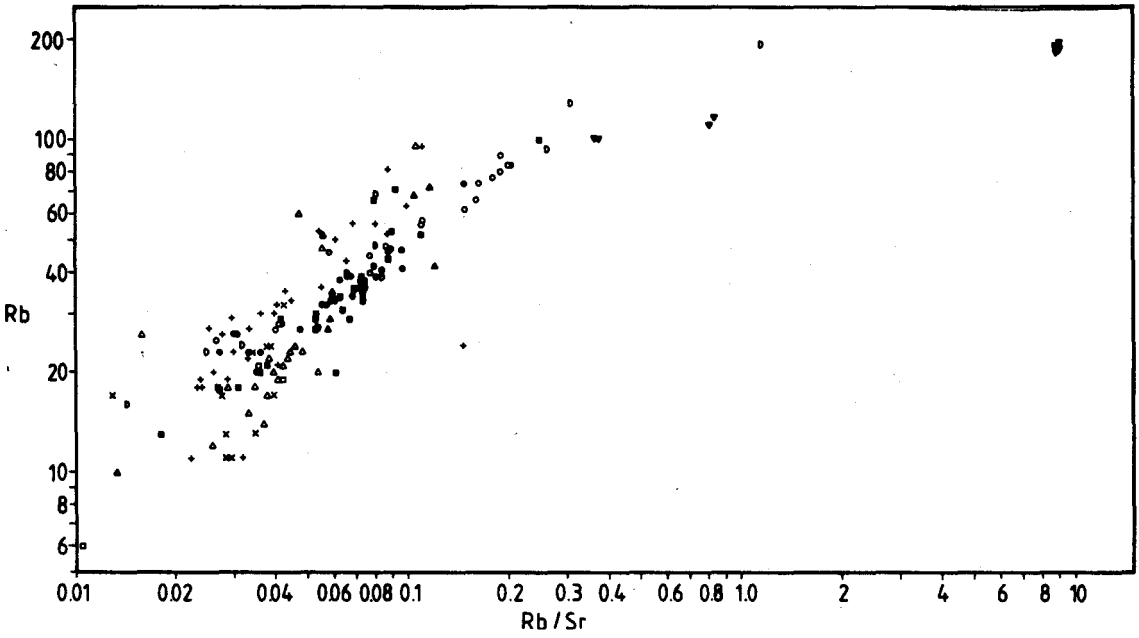

Fig. 13. Systematics of all rock samples in log Rb- vs. log Rb/Sr- diagram. Symbols as in Fig. 10.

In the laboratory of A. W. Hofmann, Max-Planck-Institut für Chemie, Abteilung Geochemie, Mainz, FRG, $^{87}Sr/^{86}Sr$- and $^{143}Nd/^{144}Nd$- ratios for 2 monogenetic cone andesites (NT 11 (Cerro Malpaís), NT 54 (Jalapa)), 2 stratovolcano andesites (NT 24 (Cofre de Perote), NH 26 (Pico de Orizaba, Middle Pleistocene)), and 1 tholeiite (NT 31 (El Abra)) have been determined. Because the analysed samples are all geologically very young (<1 m.y.), the isotope ratios are used as initial ratios. The range of $^{87}Sr/^{86}Sr$- ratios is 0.70421 (NT 24) to 0.70494 (NH 26), for $^{143}Nd/^{144}Nd$ from 0.51257 (NH 26) to 0.51269 (NT 54).

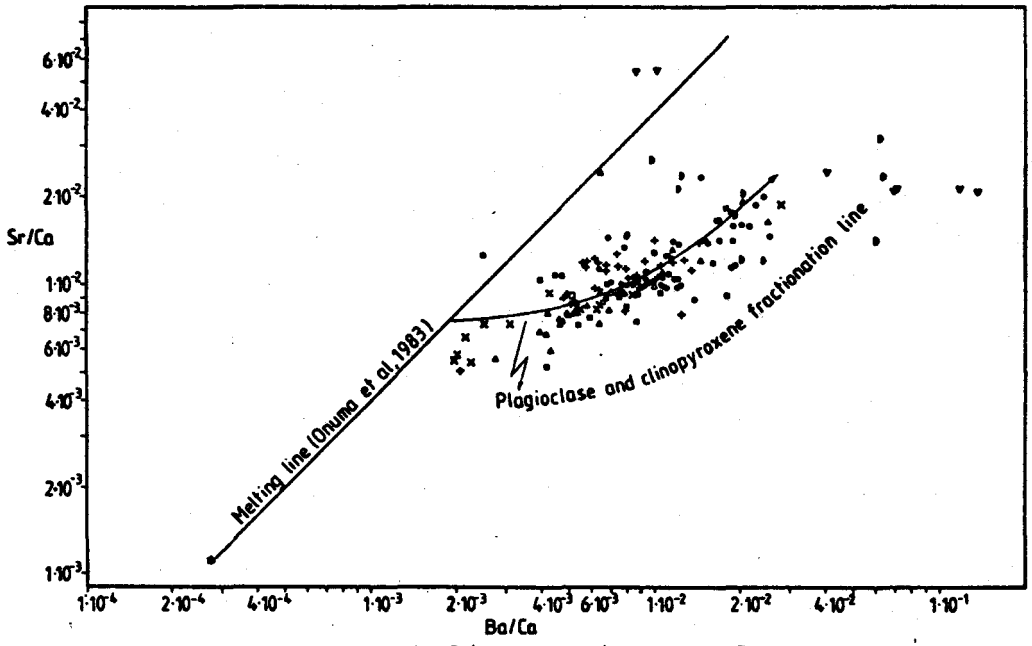

Fig. 14. Systematics of all rock samples in log Sr/Ca- vs. log Ba/Ca- diagram. Symbols as in Fig. 10.

In an ϵ^{o}_{Sr} vs. ϵ^{o}_{Nd} plot (Fig. 15) the data cluster very close to bulk REE values. Thus, the data cannot be explained by direct derivation of the volcanics from the oceanic lithosphere. The source of the primary magmas whose derivatives form the calcalkaline suite of rocks has suffered no time-integrated light REE depletion.

The Rb/Sr and Sm/Nd isotopic systems can also be used to test the possibility of interaction of the calcalkaline magmas with the overlying lithosphere. Briqueu and Lancelot (1977) and Lancelot *et al.* (1978) demonstrated that in calcalkaline lavas from active margins where the overlying plate consists of intermediate or oceanic crust, the $^{87}Sr/^{86}Sr$- ratio ranges from 0.7032 to 0.7043 with an average of 0.7036. This indicates a significant Sr isotopic homogeneity of calcalkaline magmas for this kind of active margins (Briqueu and Lancelot, 1979). On the other hand, the Sr isotopic composition of calcalkaline lavas exhibits a significant range when continental crust occurs in the active margin. E.g., $^{87}Sr/^{86}Sr$ ratios for South American active margins range from 0.7038 to 0.7090 (Francis *et al.*, 1977; James *et al.*, 1976; DePaolo and Wasserburg, 1977) suggesting the addition of radiogenic Sr from continental crust to the Sr of mantle-derived calcalkaline magmas.

In Fig. 15, $^{87}Sr/^{86}Sr$ ratios for samples of the stratovolcano andesite Cofre de Perote (NT 24), the tholeiite of El Abra (NT 31), the Jalapa monogenetic cone andesite (NT 54), the Cerro Malpaís cone andesite (NT 11), and the Pico de Orizaba stratovolcano andesite (NH 26) are plotted versus their $^{143}Nd/^{144}Nd$- ratios and SiO_2-, Rb-, Sr-, and Ba-concentrations. It demonstrates that $^{143}Nd/^{144}Nd$- ratios decrease and $^{87}Sr/^{86}Sr$- ratios increase in the course of fractional crystallization from tholeiitic to andesitic composition. This is taken as a hint on a contamination of the primary magma during the fractionation process by radiogenic Sr from the crust.

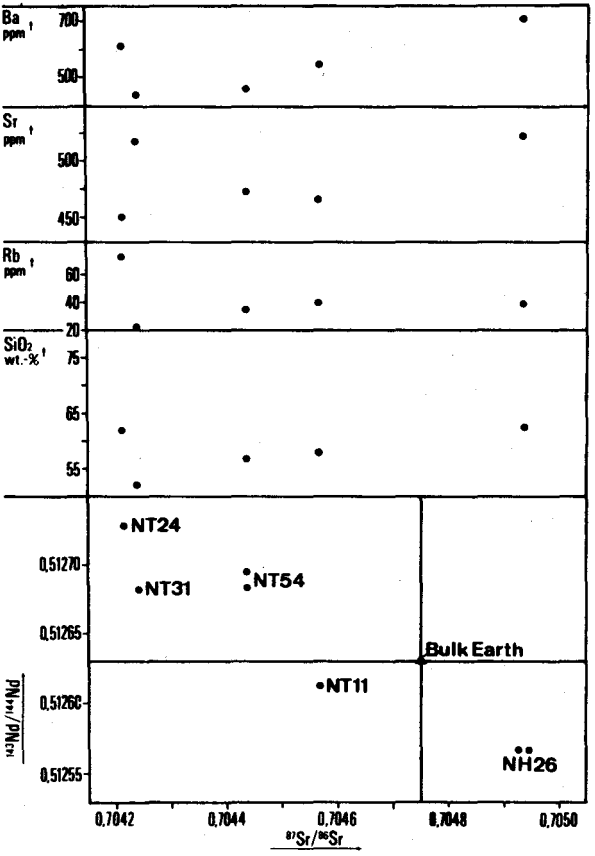

Fig. 15. $^{87}Sr/^{86}Sr$- ratios vs. $^{143}Nd/^{144}Nd$- ratios and concentrations of SiO_2, Rb, Sr, and Ba for 5 samples characterized in the text. Concentrations for Rb, Sr, and Ba are given in ppm, for SiO_2 in wt.-%.

Altogether the $^{87}Sr/^{86}Sr$- ratios are slightly higher than those reported by Moorbath *et al.* (1978), Whitford and Bloomfield (1975), Robin (1981) and Verma

(1983) for the TMVB. Since the continental crust underlying the eastern TMVB has a thickness of about 45-50 km below the Cofre-Pico range and decreases sharply eastwards to 40-28 km (Urrutia-Fucugauchi, 1984), the low values seem to suggest that a sialic contribution to this rock suite is minor.

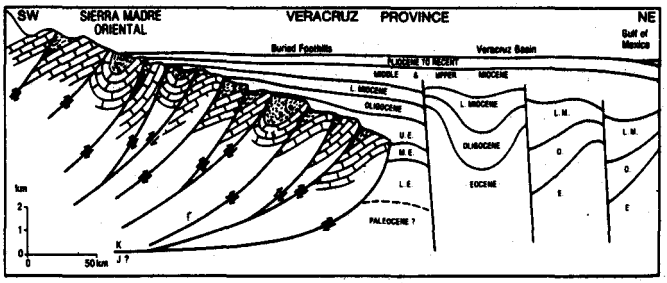

Fig. 16. Geological cross-section Sierra Madre Oriental-Gulf of Mexico after Viniegra (1965).

CONCLUSIONS

Regional and temporal variations of the volcanism of the study area

The study area lies in the crossing of two volcanic provinces defined by Robin (1976, 1981), Robin and Nicolas (1978), Robin and Tournon (1978) and Cantagrel and Robin (1979).

The model of Robin (1981) distinguishes 6 stages for the evolution of the volcanism which was caused by the eastward dipping Palaeopacific plate, later on since Miocene times triggered by the Cocos plate in NE direction. Between 30-15 m.y. the volcanism started with calcalkaline products in the west, in the east a graben evolved with the alkaline volcanism of the eastern part. During 15-9 m.y. the volcanism migrated from north to south and both provinces crossed each other between 9 and 6 m.y. Later on in the time of 6-3 m.y. the alkaline volcanism in the eastern province extended to the Palma Sola area with basalts and ignimbrites of the fracture zone to the west.

Since 3-2 m.y. the Trans Mexican Volcanic Belt hit the alkaline province in the study area and between 2-0 m.y. the evolution to the mature stage is postulated by Robin (1981). This hypothesis was evolved by his detailed studies of the different volcanic provinces and the idea to correlate this volcanism with the observable subduction zones.

We have investigated a selected sector comprehending the Trans Mexican Volcanic Belt in its eastern part and incorporating the crossing area of the two provinces down to Massif de Palma Sola.

Our intention has been to find a clear relation between compressional and tensional tectonics and their related volcanic products. However, our results produced another working hypothesis, which considers this investigated cross-section as related to the subduction zone.

Therefore, we believe that the study area can be interpreted as a cross-section through the Trans Mexican Volcanic Belt in its eastern extension. From the Cretaceous limestone belt SW of Ciudad Serdán to Jalapa it is a distance of around 100 km, from Jalapa down to the coast (Massif de Palma Sola) additional 60 km, in summary 160 km. This SW-NE profile is approximately perpendicular to the SW lying downdipping Cocos plate.

In general, the Pleistocene volcanism in the study area (Basin of Oriental and Cofre-Pico range) is characterized by the suite of calcalkaline rocks including alkaline products (Fig. 2, 3). As we mentioned in the previous chapters, the overwhelming majority of the rock-volume is however of calcalkaline character, especially caused by the Cofre-Pico stratovolcano range.

But if we consider the cluster of subalkaline to alkaline volcanoes (hawaiites, alkali basalts, etc.) we can observe its distribution over the whole study area from Basin of Oriental over Cofre-Pico range, Naolinco-Jalapa down to Palma Sola, the most SW lying volcano (NT 65 Volcano SE of Zacatepec) having only a distance of ~20 - 30 km from the southern border of the TMVB.

Including the uncertainties concerning the age relations by a few radiometric dates (Cantagrel and Robin, 1979), age estimations by geological and palaeomagnetic methods in such a large area of several hundreds of volcanoes it is possible to give a first outline of the evolution of volcanism, which is in most parts in agreement with Robin (1981).

One plutonic rock (syenite) was radiometrically dated by Yáñez García and García Durán (1982) as 31.0 ± 3.7 m.y., that is of Oligocene age. During the following

Miocene we do not have testimonies of volcanism in our study area of the Altiplano, excluding the volcanism of the TMVB in the northern part described by Robin (1981), Cantagrel and Robin (1979).

However, during this time (Fig. 4 b) the volcanism in the Massif de Palma Sola evolves.

The so-called "Old Formation" is dated by two radiometric dates on the microdiorite (17.0 ± 0.6 Laguna Verde microdiorite, Cantagrel and Robin, 1979, and 12.3 - 12.9 Candelaria diorite, Mooser and Soto, 1980). Besides these diorites, gabbros, alkali basalts and basalts are widespread. A hawaiite (U 78) was dated with 8.94 ± 0.54 belonging to the Espinazo volcanics (Fig. 4 b).

The Quiahuixtlan dacite was dated 6.5 ± 0.2 m.y. (Cerro Cantera dacite) by Cantagrel and Robin (1979) and being 7.2 ± 0.2 m.y. after Mooser and Soto (1980). This is a second calcalkaline product within this alkaline province. Their origin is explained by Robin (1981) with the calcalkaline province reaching down to the Palma Sola Massif during stage 1 and 3 of his proposed evolutionary sequence. Stage 2 has produced the alkaline products. This is a conclusive model, however the above mentioned contradictions in the time sequences seem to restrict this interpretation.

During *Pliocene times* the volcanism in the Palma Sola Massif is of alkaline character and well documented (Chiconquiaco and Laguna Verde lavas), however, the 4.31 ± 0.8 m.y. La Lumbre - Los Venados lavas (Mooser and Soto, 1980) contain basaltic andesites (U 71) with calcalkaline character. It seems to be correct here to incorporate the "El Oro Rhyolite"-Formation with the strange exotic rocks.

During Pliocene times (with exception of the youngest part), we did not find volcanic products in the western study area (Basin of Oriental, Cofre-Pico range), although in Los Humeros caldera the old lavas were dated 3.6 m.y. by Ferriz and Mahood (1984).

At the change from *Pliocene to Pleistocene* times the volcanism is widespread in the study area (Fig. 4 a, b). Cantagrel and Robin (1979) have dated the lavas S of Actopan with 1.9 ± 0.06 m.y. being alkali basalts.

If we rely on the date of Yáñez García and García Durán (1982) even the volcanism of the basal part of the Cofre de Perote complex starts with 1.9 (1.7) m.y.

Therefore we can state an *Oldest, Old-Middle Pleistocene* volcanism in the whole area from the Basin of Oriental (Domes of Cerro Derrumbadas and Cerro Pinto) over the Cofre-Pico range (stratovolcanoes) to the region of Jalapa (Fig. 4 a, b).

"Hawaiites" we find in the area S and SW of Actopan, alkali basalts in the same region and in the direction Naolinco-Jalapa, a few basaltic andesites in the Massif de Palma Sola and SE of Jalapa, monogenetic cone andesites in the region Naolinco-Jalapa and Cofre-Pico range and the stratovolcano andesites and dacites mainly in the Cofre-Pico range. This represents a continuous change from calcalkaline to alkaline products into the eastern direction.

The same evolutionary picture we can see considering the time sequences of Fig. 4 c for the *Young Pleistocene-Holocene times.*

This chain of several hundred young volcanoes, inclusive the young edifice of Pico de Orizaba which has not been studied by us, but was reported in detail by Robin (1981), erupted during the Young Pleistocene and Holocene and forms a band from the Altiplano down to Palma Sola (Fig. 5).

If we consider the alkaline (subalkaline) and calcalkaline character of the volcanoes then we can realize that the alkaline (alkali basalts) and subalkaline ("hawaiites") migrated to the west, as it can be observed in Fig. 2, 3, 4, in comparison to the older Pleistocene times. SW of Perote we could analyse alkali basalts in two small cones (NT 64). These alkali basalts are rare in comparison with the "hawaiites" and only three cones in the Naolinco-Jalapa region and one in the Palma Sola area were analysed.

The "hawaiites", transitional basalts after Robin and Tournon (1978) and Robin (1981) and of subalkaline character are widespread in the Basin of Oriental (the most southern cone is located SE of Zacatepec, NT 65 S of Cerro Derrumbadas) and extends down to the region Naolinco-Jalapa. In the Massif de Palma Sola tholeiites of the Upper El Abra Series erupted.

Basalts we found in the Naolinco-Jalapa area and basaltic andesites show the same distribution pattern as the "hawaiites" (Basin of Oriental, Naolinco-Jalapa), which is congruent with the distribution of the monogenetic cone andesites.

Two small volcanoes in the Basin of Oriental show the characteristics of stratovolcano andesites.

One small cone W of Cerro Derrumbadas represents a dacite (NT 1).

If we summarize the volcanism of *Recent* to *Subrecent* (Young Pleistocene-Holocene) times we can recognize a majority of calcalkaline and subalkaline products in comparison with only a few alkaline products in respect to our data material. A few tholeiites erupted in the Massif de Palma Sola.

During the *Oldest-Middle Pleistocene* times the transitional "hawaiites" seem to disappear and the extreme calcalkaline and alkaline character is emphasized and more restricted regionally.

This result for the 2 eruption timespans (Oldest-Middle Pleistocene and Young Pleistocene-Holocene) during the Pleistocene has led us to the interpretation to consider this area besides the other mentioned reasons as one "volcanic belt", more and more immediately influenced by the subducted Cocos plate producing trenchward calcalkaline, then subalkaline and alkaline volcanism. It has to be taken in consideration that from the Altiplano area down to Palma Sola we have a change in crustal thickness from around 50 to 28 km.

Tectonics and volcanism in the investigated area

Considering the TMVB in its eastern extension along the investigated cross-section we did not observe features that can be interpreted as graben-ectonics (Fig. 5), in the sense of continental rifting in such huge dimensions which are necessary to explain the postulated eastern alkaline-graben-province of intraplate character after Robin (1981). Therefore we prefer the following interpretation.

The volcanics of the TMVB bury folded and overthrusted limestones etc. of the Sierra Madre Oriental, overthrusting even in parts old-Tertiary sediments (Fig. 16). This compression has influenced tectonically sediments even in the Actopan area up to end-Miocene times. Younger than final Aquitanian phases are absent, which can be read in Fig. 16 (Viniegra, 1965). Local graben-like structures are of Miocene times as a result of the mentioned compression. This does not exclude a pre Lower Miocene and Oligocene tension, which produced the graben-structures in Fig. 16, ac-

companied by the alkaline volcanism of this province (Robin, 1981; Robin and Tournon, 1978). The Miocene volcanic complex of the Massif de Palma Sola is a result of this tectonic mainly as alkaline province following the flysch and molasse states of geosynclinal folding.

This evolution can be interpretated as result of the subduction of the Palaeopacific plate (Robin, 1976; Clark *et al.*, 1982; Urrutia-Fucugauchi, 1984), having caused additional calcalkaline volcanism in the western part of Mexico underlying even parts of the TMVB. The observed migration of the volcanism in the eastern alkaline province from N to S from Oligocene to Miocene times (Robin, 1981) traces the temporal change of tectonic compression and tension from north to south.

During Pleistocene-Holocene times the alkaline volcanism is incorporated into the calcalkaline volcanism of the trenchward part and seems to form a structure like the Japan arc.

For us, the TMVB therefore extends to the Gulf coast, probably is caused or induced by the subducting Cocos plate and comprehends the volcanism in this eastern section from late Pliocene times on. This is in accordance with our geochemical results. The volcanism of the easternmost extension of the TMVB contains calcalkaline, subalkaline and alkaline products.*

Shurbet and Cebull (1984) added a new hypothesis concerning the volcanotectonic association in southern Mexico, illuminating old considerations (Mooser *et al.*, 1974; Stewart, 1971; Le Pichon and Fox, 1971; Gastil and Jensky, 1973) in a microplate version.

* A recently published surface heat flow profile perpendicular to the trench (Ziagos *et al.*, 1985) suggests that the "angle of subduction is low and that convective heat transfer in the back arc region is probable". The TMVB coincides with the high heat flow zone between 200 and 400 km N of the trench Acapulco-Pachuca and gives hints to the heat induced tensional features within the TMVB. This asks for a more detailed tectonic model to explain the tectonic features in the trenchward or back arc region respectively within the upper mantle and crustal levels. The simple volcano-tectonic model (compression/tension - calcalkaline/alkaline) is obsolete.

ACKNOWLEDGMENTS

This work was supported by the Deutsche Forschungsgemeinschaft (DFG) grants Ne 154/7/10.

Thanks is given to Mrs. Granados (Mainz) and E. Krings (Trier) for drawing the figures.

BIBLIOGRAPHY

BAILEY, J. C., 1981. Geochemical criteria for a refined tectonic discrimination of orogenic andesites. *Chem. Geol., 32,* 139-154.

BANZER-BUSSMANN, G., 1981. Zur Geochemie und Petrographie der Silexite des Palma Sola Massivs (Mexiko). Unpubl. M. A. Thesis, Mainz, Federal Republic of Germany.

BLOOMFIELD, K., 1973. A late Quaternary monogenetic volcanic field in central Mexico *Geol. Rundsch., 64,* 476-497.

BÖHNEL, H., 1985. Paläomagnetische Untersuchungen an jurassischen-quartären Gesteinen Zentral- und Südmexikos. Unpubl. Doctor Thesis, Münster, Federal Republic of Germany.

BÖHNEL, H. and J. F. W. NEGENDANK, 1981. Preliminary results of palaeomagnetic measurements of Tertiary-Quaternary igneous rocks from the eastern part of the Trans Mexican Volcanic Belt. *Geof. Int., 20,* 3, 235-248.

BOWEN, N. L., 1928. The Evolution of the Igneous Rocks. Princeton University Press, Princeton, New Jersey.

BRIQUEU, L. and J. R. LANCELOT, 1977. Nouvelles données analytiques et essai d'interprétations des compositions isotopiques en Sr des laves calc-alcalines plio-quaternaires du Pérou. *Bull. Soc. Géol. Fr., 19,* 6, 1223-1232.

BRIQUEU, L. and J. R. LANCELOT, 1979. Rb-Sr-systematics and crustal contamination models for calc-alkaline igneous rocks. *Earth Planet. Sci. Lett., 43,* 385-396.

CANTAGREL, J. M. and C. ROBIN, 1979. K-Ar dating on eastern Mexican volcanic rocks - relations between the andesitic and the alkaline provinces. *J. Volcanol. Geotherm. Res., 5,* 99-114.

CLARK, K. F., C. T. FOSTER and P. E. DAMON, 1982. Cenozoic mineral deposits and subduction related magmatic arcs in Mexico. *Geol. Soc. Am. Bull., 93,* 533-544.

DEMANT, A., 1978. Características del Eje Neovolcánico Transmexicano y sus problemas de interpretación. Univ. Nal. Autón. México, *Inst. Geol. Rev., 2,* 172-187.

DEMANT, A., 1981. L'Axe Néo-Volcanique Transmexicain: Etude Volcanologique et Pétrographique, Signification Géodynamique. Unpubl. Doctor Thesis, Aix-Marseille, France.

DePAOLO, D. J. and G. J. WASSERBURG, 1977. The source of island arcs as indicated by Nd and Sr isotopic studies. *Geophys. Res. Lett., 4,* 465-468.

DIETRICH, V., R. EMMERMANN, R. OBERHANSLI and H. PUCHELT, 1978. Geochemistry of basaltic and gabbroic rocks from the west Mariana basin and the Mariana trench. *Earth Planet. Sci. Lett., 39,* 127-144.

EMANI, M. H. and R. MICHEL, 1982. Les volcans domeens du Neogene de la region de Qom (Iran Central). Essai de classification de l'activité volcanique domeenne. *Bull. Volcanol., 45,* 317-332.

FERRIZ, H. and G. A. MAHOOD, 1984. Volcanismo riolítico en el Eje Neovolcánico Mexicano. *Geof. Int.,* in press.

FRANCIS, P. W., S. MOORBATH and R. S. THORPE, 1977. Strontium isotope data for recent andesites in Ecuador and North Chile. *Earth Planet. Sci. Lett., 37,* 197-202.

GASTIL, R. G. and W. JENSKY, 1973. Evidence for strikeslip displacement beneath the Trans-Mexican volcanic belt. Stanford Univ. Publ., *Geol. Sci., 13,* 171-180.

GILL, J. B., 1981. Orogenic Andesites and Plate Tectonics. Springer Verlag, Berlin-Heidelberg-New York.

HAWKESWORTH, C. J., M. J. NORRY, J. C. RODDICK, P. E. BAKER, P. W. FRANCIS and R. S. THORPE, 1979. $^{143}Nd/^{144}Nd$, $^{87}Sr/^{86}Sr$ and incompatible element variations in calc-alkaline andesites and plateau lavas from South America. *Earth Planet. Sci. Lett., 42,* 45-57.

IRION, G. and J. F. W. NEGENDANK, 1984. Das Meerfelder Maar - Untersuchungen zur Entwicklungsgeschichte eines Eifelmaares. *Cour. Forsch. Inst. Senckenberg, 65,* 101 p.

ISACHSEN, Y. W., R. H. FAKUNDINY and S. W. FOSTER, 1973. Evaluation of ERTS-1 imagery for geological sensing over the diverse geological terranes of New York State. NASA SP-327, 1, 223-230.

JAGOUTZ, E., H. PALME, E. BADDENHAUSEN, K. BLUM, M. CENDALES, G. DREIBUS, B. SPETTEL, V. LORENZ and H. WANKE, 1979. The abundances of major, minor and trace elements in the earth's mantle as derived from primitive ultramafic nodules. Proc. Lunar Planet. Sci. Conf. 10th, 2031-2050.

JAMES, D. E., C. BROOKS and A. CUYUBAMBA, 1976. Andean Cenozoic volcanism, magma genesis in the light of strontium composition and trace element geochemistry. *Geol. Soc. Am. Bull., 87,* 592-600.

KRAWCZYK, R., 1984. Petrographische und geochemische Zonierung des Pliozän-quartären Transmexikanischen Vulkangürtels: Ein Beitrag zur Erklärung der Genese kalkalkaliner und ne-normativer Gesteine und ihrer Differentiate an aktiven Kontinentalrändern. Unpubl. Doctor Thesis, Giessen, Federal Republic of Germany.

KUNO, H., 1959. Origin of Cenozoic petrographic provinces of Japan and surrounding areas. *Bull. Volcanol., 20,* 37-76.

KUNO, H., 1966. Lateral variation of basalt magma across continental margins and island arcs, *In:* W. H. Poole (Ed.), Continental margins and island arcs. *Can. Geol. Surv. Paper, 66-* 15, 317-36.

LANCELOT, J. R., L. BRIQUEU, B. WESTPHAL and M. TATSUMOTO, 1978. Sr and Pb isotopic data bearing on the origin of recent calc-alkaline lavas from Peru and New Hebrides active margins. 4th Int. Conf. Geochronol., Cosmochronol., Isotope Geol., Aspen, U. S. Geol. Surv. Open-file Rep., 78-701, 240-241.

LE PICHON, X. and P. J. FOX, 1971. Marginal offsets, fracture zones and the early opening of the North Atlantic. *J. Geophys. Res., 26,* 6294-6308.

LUHR, J. F. and I. S. E. CARMICHAEL, 1980. The Colima volcanic complex, Mexico. I. Post-caldera andesites from Volcan Colima. *Contrib. Mineral. Petrol., 71,* 343-372.

MAALØE, S. and T. S. PETERSEN, 1981. Petrogenesis of oceanic andesites. *J. Geophys. Res., 86,* 10273-10386.

MARTIN DEL POZZO, A. L., 1982. Monogenetic volcanism in Sierra Chichinautzin, Mexico. *Bull. Volcanol., 45,* 9-24.

MILLER, W. J., 1919. Pegmatite, Silexite and Aplite of Northern New York. *J. Geol., 27,* 28-54.

MOORBATH, S., R. S. THORPE and J. L. GIBSON, 1978. Strontium isotope evidence for petrogenesis of Mexican andesites. *Nature,* 271, 437-438.

MOOSER, F., A. E. M. NAIRN and J. F. W. NEGENDANK, 1974. Palaeomagnetic investigations of the Tertiary and Quaternary igneous rocks. VIII. A palaeomagnetic and petrologic study of volcanics of the Valley of Mexico. *Geol. Rundsch.,* 63, 451-483.

MOOSER, F. and S. SOTO, 1980. Geology of Laguna Verde, Vol. I-III. Comisión Federal de Electricidad, México, D. F.

MOSSMAN, R. W. and O. F. VINIEGRA, 1976. Complex fault structures in Veracruz Province. *AAPG Bull., 60,* 3, 379-388.

MÜLLER, W. Chr., 1979. Geologische Luftbildkarte der Umgebung von Laguna Verde (Palma Sola), Veracruz, Mexiko. Unpubl. Report, Mainz, Federal Republic of Germany.

96

NEGENDANK, J. F. W., R. EMMERMANN, F. MOOSER, U. SEIFFERT-KRAUS and H. J. TOBSCHALL, 1981. Evolution of some Tertiary and Quaternary Central Volcanoes of the TMVB and possible different positions of the Benioff-Zone. *Zbl. Geol. Paläont., 1,* 3/4, 183-194.

NEGENDANK, J. F. W., H. BÖHNEL, R. EMMERMANN, R. KRAWCZYK, F. MOOSER, S. SOTO-PINEDA and H. J. TOBSCHALL, 1982a. Der Ostteil des Transmexikanischen Vulkangürtels und seine Position im Gesamtgürtel. *Naturwiss.,* 69, 130-139.

NEGENDANK, J. F. W., G. IRION and J. LINDEN, 1982b. Ein eozänes Maar bei Eckfeld nordöstlich Manderscheid (SW-Eifel). *Mainzer geowiss. Mitt.,* 11, 157-172.

NIXON, G. T., 1982. The relationship between Quaternary volcanism in central Mexico and the seismicity and structure of subducted ocean Lithosphere. *Geol. Soc. Am. Bull.,* 93, 514-523.

NORRISH, K. and B. W. CHAPPELL, 1967. X-ray fluorescence spectrometry, *In:* J. Zussmann (Ed.)., Physical Methods in Determinative Mineralogy. Academic Press, London, 161-214.

O'HARA, N. J., Draft - June, 1984. Continuous partial melting regimes in the Upper Mantle, refilled-tapped-fractionated (RTF) magma chambers, and the evolution of chondrite or whole earth normalized trace element concentration patterns (Spidergrams) for igneous magmas and residuals. Submitted for Proc. of Taros-Conf. on open magma systems.

OHNGEMACH, D., 1973. Análisis polínico de los sedimentos del Pleistoceno Reciente y del Holoceno en la región Puebla-Tlaxcala. *Comunicaciones,* 7, 47-49.

OHNGEMACH, D. and H. STRAKA, 1983. Beiträge zur Vegetations- und Klimageschichte im Gebiet von Puebla-Tlaxcala: Pollenanalysen im Mexiko-Projekt, *In:* W. Lauer (Ed.), Das Mexiko-Projekt der Deutschen Forschungsgemeinschaft, 18, Wiesbaden.

OHNGEMACH, D. and H. STRAKA, 1983. Contribuciones para la Historia de la Vegetación y del Clima en la Región de Puebla-Tlaxcala: Análisis Polínicos en el Proyecto México, *In:* W. Lauer (Ed.), El Proyecto México de la Fundación Alemana para la Investigación Científica, 18, Wiesbaden.

O'LEARY, D. W., J. D. FRIEDMAN and H. A. POHN, 1976. Lineaments, linear, lineation: some proposed new standards for old terms. *Geol. Soc. Am. Bull., 87,* 10, 1463-1469.

ONUMA, N., M. HIRANO and N. ISSLUKI, 1983. Genesis of basalt magmas and their derivatives under the Izu Islands, Japan, inferred from Sr/Ca - Ba/Ca systematics, *J. Volcanol. Geotherm. Res.,* 18, 511-530.

PEARCE, J. A., 1982. Trace element characteristics of lavas from destructive plate boundaries, *In:* R. S. Thorpe (Ed.), Andesites: Orogenic Andesites and Related Rocks. John Wiley and Sons, 525-548.

PECCERILLO, A. and S. R. TAYLOR, 1976. Geochemistry of Eocene calcalkaline volcanic rocks from the Kastamonu area, Northern Turkey. *Contrib. Mineral Petrol.*, 58, 63-81.

PICHLER, H. and R. WEYL, 1976. Quaternary alkaline volcanic rocks in eastern Mexico and Central America. *Münster. Forsch. Geol. Paläont.*, 38/39, 159-178.

ROBIN, C., 1976. Présence simultanée de magmatismes de significations tectoniques opposées dans l'est du Mexique. *Bull. Soc. Géol. Fr., 18,* 1637-1645.

ROBIN, C., 1981. Relations Volcanologie - Magmatologie - Géodynamique: Application au passage entre volcanismes alcalin et andésitique dans le Sud Mexicain. (Axe trans-mexicain et Province alcaline Orientale). *Ann. Sci. de l'Univ. de Clermont-Ferrand II.*

ROBIN, C., 1982. Mexico, *In:* R. S. Thorpe (Ed.), Andesites: Orogenic Andesites and Related Rocks. John Wiley and Sons, 137-147.

ROBIN, C. and J. M. CANTAGREL, 1976. La zone orientale de L'Axe volcanique transmexicain: formations calco-alcalines et alcalines au Miocène et au Plio-Quaternaire. 4ème. Réun. Ann. Sci. Terre, Paris, 353, Soc. Géol. Fr. (Ed.).

ROBIN, C. and J. M. CANTAGREL, 1982. Le Pico de Orizaba (Mexique): Structure et évolution d'un grand volcan andésitique complexe. *Bull. Volcanol., 45,* 299-315.

ROBIN, C., J. M. CANTAGREL and P. VINCENT, 1983. Les nuées ardentes de type Saint-Vincent: épisodes remarquables de l'evolution récente du Pico de Orizaba (Mexique). *Bull. Soc. Géol. Fr., 25,* 727-736.

ROBIN, C. and E. NICOLAS, 1978. Particularités géochimiques des suites andésitiques de la zone orientale de l'axe transmexicain, dans leur contexte tectonique. *Bull. Soc. Géol. Fr., 20,* 193-202.

ROBIN, C. and J. TOURNON, 1978. Spatial relations of andesitic and alkaline provinces in Mexico and Central America. *Can. J. Earth Sci., 15,* 1633-1641.

ROEDDER, E., 1979. Silicate liquid immiscibility in magmas, *In:* H. S. Yoder (Ed.), The evolution of the igneous rocks. Princeton University Press, Princeton, New Jersey, 15-57.

SCHMINCKE, H.-U., V. LORENZ and H. A. SECK, 1983. The Quaternary Eifel Volcanic Fields, *In:* K. Fuchs *et al.* (Ed.), Plateau Uplift, 139-151.

SCHWAB, K., 1972. Cenozoic volcanism in the Argentine Puna and its relationship to tectonic movements. 24th JGC, Section 2, 211-221.

SHURBET, D. H. and S. E. CEBULL, 1984. Tectonic interpretation of the Trans-Mexican Volcanic Belt. *Tectonophysics, 101,* 159-165.

STEWART, J. H., 1971. Basin and Range structure: a system of horsts and grabens produced by deep-seated extension. *Geol. Soc. Am. Bull., 82,* 1019-1044.

SUN, S.-S., R. W. NESBITT and A. Y. SHARASKIN, 1979. Chemical characteristics of mid-oceanridge basalts. *Earth Planet. Sci. Lett., 44,* 119-138.

THORNTON, C. P. and O. F. TUTTLE, 1960. Chemistry of igneous rocks. I. Differentiation index. *Amer. J. Sci., 258,* 664-684.

THORPE, R. S., 1977. Tectonic significance of alkaline volcanism in eastern Mexico. *Tectonophysics, 40,* 19-26.

TOBSCHALL, H. J., 1975. Geochemical investigations on the composition and the depositional environment of Palaeozoic marine pelites: The contents of the major elements and the trace elements Ni, Cu, Zn, Rb, Sr, Y, Zr, Nb and Ba in the Steiger Slates (Vosges, France). *Chem. Erde, 34,* 105-167.

URRUTIA-FUCUGAUCHI, J., 1978. Cordilleran Benioff zones. *Nature, 275,* 464.

URRUTIA-FUCUGAUCHI, J., 1984. Late Mesozoic-Cenozoic Evolution of the northwestern Mexico magmatic arc zone. *Geof. Int.,* in press.

VERMA, S. P., 1983. Magmagenesis and chamber processes at Los Humeros caldera, Mexico - Nd and Sr isotope data. *Nature, 302,* 52-55.

VERMA, S. P. and M. LOPEZ, 1982. Geochemistry of los Humeros Caldera, Puebla, Mexico. *Bull. Volcanol., 45,* 1, 63-79.

VINIEGRA, F., 1965. Geología del Macizo de Teziutlán y la cuenca cenozoica de Veracruz. *Bol. Asoc. Mex. Geol. Petrol., 17,* 7, 101-163.

WERLE, D., 1984. The role of airphoto and satellite image interpretation in analysing volcanic landforms and structures in the eastern part of the Trans Mexican Volcanic Belt, Mexico. Unpubl. M. Sc. Thesis, Dept. of Geography, McGill Univ., Montreal, Canada.

WHITFORD, D. J. and K. BLOOMFIELD, 1975. Geochemistry of late Cenozoic volcanic rocks from the Nevado de Toluca area, Mexico. *Carnegie Instn. Wash. Yb., 76,* 207-213.

WILDBERG, H. G. H., 1984. Der Nicoya-Komplex, Costa Rica, Zentralamerika: Magmatismus und Genese eines polygenetischen Ophiolith-Komplexes. *Münster. Forsch. Geol. Paläont., 62,* 123 p.

YAÑEZ GARCIA, C. and S. GARCIA DURAN, 1982. Exploración de la Región geotérmica Los Humeros - Las Derrumbadas, Estados de Puebla y Veracruz. Comisión Federal de Electricidad, México, D. F.

YODER, H. S. and C. E. TILLEY, 1962. Origin of basalt magmas: an experimental study of natural and synthetic rock system. *J. Petrol., 3,* 342-532.

ZIAGOS, J. P., D. D. BLACKWELL and F. MOOSER, 1985. Heat flow in southern Mexico and the thermal effects of subduction. *J. Geophys. Res., 90,* 5410-5420.

(Received: June 14, 1984)
(Accepted: May 6, 1985)

It is recommended that reference to this paper be made as follows:

J. F. W. Negendank, R. Emmermann, R. Krawczyk, F. Mooser, H. Tobschall and D. Werle, 1985. Geological and geochemical investigations on the Eastern Trans-Mexican Volcanic Belt. *Geofis. Int.*, Special Volume on Mexican Volcanic Belt - Part 2 (Ed. S. P. Verma), *Vol. 24-4*, pp. 477-575.